Nonpoint Controls on the Quality of Shallow Groundwaters in Louisiana

1993

Jeffrey S. Hanor
Department of Geology and Geophysics
Louisiana State University
Baton Rouge, LA 70803

Project Completion Report

Louisiana Water Resources Research Institute
Louisiana State University
Baton Rouge, LA 70803

September 28, 1993

Louisiana Water Resources Research Institute
Project Completion Report

Project Number: 03
Project Initiation Date: 9/1/92
Project Ending Date: 8/31/93

Title: Nonpoint controls on the quality of shallow groundwaters in Louisiana

Investigator: Prof. Jeffrey S. Hanor, Department of Geology and Geophysics, Louisiana State University, Baton Rouge, Louisiana 70803

Acknowledgements

I would like to thank Gina Bagnetto-Waters, Paige Baldassaro, Young Chen, Lee Esch, and Shaobing Su for their technical help on this project. I would also like to thank George Cardwell of the Capital Area Groundwater Conservation Commission for making available an extensive collection of sediment cuttings which formerly belonged to the U.S. Geological Survey and Perry L. Brown for making available temporary space to store this collection.

Disclaimer

The research described in this report represents the results of the first year of a projected multi-year effort. Much of the research has been done by three graduate students and one undergraduate student as part of their respective thesis and dissertation research projects. Each student is currently in the midst of his or her project. The purpose of this report is to outline the long-term goals of this research and to document what has been completed to date, with the understanding that some of the results are preliminary in nature and some phases of the project will not be completed for another one to two years.

Abstract

Understanding the natural chemical and physical processes which control ground water quality is essential for predicting the effects of anthropogenic activities the composition of fluids in shallow aquifer systems and ground water discharge zones. These chemical and physical processes occur over broad areas within the regional aquifer systems of Louisiana and hence represent nonpoint controls on both subsurface and surface water quality. The specific area targeted for research is the Chicot aquifer system of southwestern Louisiana, which supplies nearly 610 Mgal/d of water for public supply, industry, rice irrigation, and aquaculture.

Research during the first year of this projected several-year project has focused on identifying specific geochemical reactions occuring along 100 km lateral regional flow paths and 10 to 100 m vertical paths of infiltration and recharge in the Chicot using a combination of thermodynamic modeling and mass balance techniques. Integration of this information with flow fluid rates will help to constrain the kinetics of these reactions. Experimental work has begun on the effects of variable salinity in driving changes in water quality though mineral hydrolysis reactions and on the role the production of organic acids plays in controlling water quality.

Purpose and Objectives

The ultimate objective of the research undertaken in this project is to develop a quantitative understanding of the controls on water quality in shallow aquifer systems in the Louisiana Gulf Coast. As we enhance our understanding of the ultimate controls on the composition of these waters, we will better be able to predict what effects anthopogenic modification of aquifer systems, such as the introduction of pollutants or increased pumping, will have on water quality. Such information will aid in the planning of appropriate steps to minimize or accomodate the impact of these activities. Relevant questions to be answered include: are the natural systems sufficiently buffered that they will control the behavior of a potential pollutant, or will the pollutant significantly modify the behavior of the natural system? What is the long term effect on water quality of the continuous recycling of water through pumping, irrigation, and vertical leakage back down into shallow aquifers?

This one-year project, funded in part by the U.S. Geological Survey through the Louisiana Water Resource Research Institute, is the first phase of a planned multi-year effort. The specific area targeted for initial research is the Chicot aquifer system of southwestern Louisiana. This aquifer system is an ideal candidate for the study of shallow subsurface geochemical processes for several reasons:

i. The Chicot regional aquifer system supplies nearly 610 Mgal/d of water for public supply, industry, rice irrigation, and aquaculture. In terms of the rate of total ground water withdrawal, this is the most important aquifer system in the State.

ii. There are several significant water quality problems associated with this aquifer system. These include the occurence of high levels of dissolved iron, contamination by saline ground water, the siting of numerous hazardous waste landfills immediately above the aquifer system, and the potential infiltration of agricultural wastes.

iii. Recent studies by the U.S. Geological Survey (Nyman, 1984, 1989; Pettijohn et al., 1992, and references therein) have defined both the hydrologic and geologic setting of the Chicot aquifer. In addition, a large body of water quality data exists for this system. These previous studies provide the initial hydrogeologic framework and geochemical data base for this research.

Related Research

The proposed research builds on and compliments the regional and local studies of the Chicot aquifer system conducted by the U.S. Geological Survey (Nyman, 1984; Nyman, 1989; Nyman et al., 1990; Pettijohn et al., 1992; Trudeau et al., in review). Although quantitative flow-path modeling of the geochemical evolution of waters in aquifer systems has been an increasingly important aspect of hydrogeologic research (e.g., Lee, 1988; Plummer et al., 1990; and Plummer et al., 1991, and references therein), the only such work that has been done in the northern Gulf Coast is the study by Lee (1985) and Hanor and McManus (1988) in the Mesozoic of Mississippi-Alabama. The proposed research thus represents a new and important direction for water resources research in Louisiana.

Methods and Procedures

Flow path studies

Although discussion of the controls on the composition of pore waters in aquifers is often presented as a strictly chemical problem, pore water compositions are a direct function of both chemical *and* physical factors. These factors include:

1. The composition of the water physically included in the pore spaces of the sediment at the time of sediment deposition.

2. The net effects of diagenetic exchange of components between the water and: a) the ambient solids which make up the matrix of the sediment and b) any other fluids, such as gases or organic liquids, which may be present.

3. The net physical transport of material into and out of the sediments by bulk flow and the mixing of waters.

All of the above can be accounted for in the following basic equation for the conservation of mass of a dissolved solute or isotopic species:

$$\frac{\partial C_i}{\partial t} = \Sigma R_{ij} + (-\mathbf{v}\cdot\nabla C_i) + (\nabla\cdot(D\,\nabla C_i)) \qquad (1)$$

where $(\partial C_i/\partial t)$ is the change in the aqueous concentration, C_i, of solute or isotope i with time. Porosity, ϕ, which often appears in such equations, has been assumed here to be constant with time and thus has been factored out. The first mass balance term on the right, ΣR_{ij}, describes the net effects of diagenetic reaction on the concentration of solute i. R_{ij} is the rate of the jth diagenetic reaction which results in the addition or removal of i from solution. The next term, $(-\mathbf{v}\cdot\nabla C_i)$, where $\mathbf{v}$ is the fluid velocity field, defines the net addition or removal of dissolved i as a function of time as a result of bulk fluid flow through the sediment. The last term on the right hand side of the equation, $(\nabla\cdot(D\,\nabla C_i)$, describes the net rate in change in composition due to diffusional and dispersive mixing. D is a dispersion tensor which describes the magnitude of mixing which occurs in response to a given concentration gradient and fluid velocity. The initial, or connate, composition of the fluid, $C_i(0)$, comes into play when we integrate equation (1) with respect to time.

There has been considerable progress in recent years in our understanding of the controls on water quality in aquifer systems by use of flow-path modeling (see discussion and extensive references in Plummer et al., 1991). One aspect of this technique consists of reconstructing the evolution of pore water quality by establishing the changes in water composition along ground water flow paths. Spatial variations in composition and rates of ground water flow put important contraints on interpreting how natural systems work.

There are two distinct types of ground water flow paths within the Chicot which are currently being studied as part of this research project. The first are pre-anthropogenic longitudinal flow paths, which provide insight into broad regional processes of chemical modification, and the second are the paths of nearly vertical leakage and recharge, which are required to evaluate the short-term response of industrial and agricultural waste waters to shallow subsurface conditions.

Available water analyses have been used to define the present two-dimensional variation in composition of key reactive components of the ground waters along the flow paths. These components include major cations and anions; dissolved silica; redox sensitive metals, such as Fe and Mn; and N and P species. Thermodynamic evaluation of water compositions have been made using SOLMIN88 (Kharaka et al., 1988) to evaluate the saturation state of the pore fluids with sedimentary mineral phases known from previous work to be present in the aquifer system. This will provide information on the extent to which the fluid compositions are being buffered by water-rock equilibria or determined by rate-controlled processes.

Changes in composition along the flow paths are related not only to chemical sources and sinks but to physical transport processes, such as hydrodynamic dispersion. By comparing the behavior of conservative components of the ground water system, such as chloride, with reactive components, such as silica, it will be possible through parametric analysis to differentiate between the effects of chemical reaction and physical mixing. Quantification of the effects of dispersion is of critical importance. Some existing mass balance codes, such as NETPATH (Plummer et al., 1991) neglect these effects, but they have been shown to be important in Gulf Coast systems, where complex intercalation of beds of differing permeablity induces significant lateral and vertical mixing (e.g., Hanor and McManus, 1988; Bray and Hanor, 1990).

The paired water quality and sediment diagenetic studies of Mesozoic aquifers in the northeast Gulf Coast (Lee, 1985; Hanor and McManus, 1988) have demonstrated the necessity of coupling changes in water chemistry and sediment mineralogy in quantifying controls on water quality. Principal Investigator Hanor had made available to him during the project year a former USGS collection of sediment cuttings from wells penetrating ground water aquifers throughout Louisiana, including the Chicot Aquifer. During the period January - May, 1993, Hanor and two Ph.D. students, Yong Chen and Lee Esch, extracted samples from approximately 500 boreholes from the Chicot study area and other parishes in Louisiana. This material is currently being catalogued and archived. A preliminary description has been made of cuttings from one of these boreholes (Appendix A), and a comprehensive suite of sediment samples from the Chicot study area will be subjected to petrographic, geoechmical, and x-ray diffraction analysis.

Experimental work

The second approach followed in this project is an attempt to reproduce reactions thought to occur in aquifer systems in the laboratory. On the assumption that reactions involving intercalated mudstones and siltstones in aquifer systems is one of the factors controlling fluid compositions in aquifer sands (c.f., McMahon et al., 1992), experiments have been started using natural, carbonate-free, clay-rich silts containing quartz, kaolinite, smectite, muscovite, albite, and K-feldspar. Future experiments will use silts with calcite and/or dolomite added. Two processes are

being investigated: first, the effects of of varying salinity on bulk fluid and sediment composition and second, the effects of addition of organic acids.

The basic experimental technique is straightforward. Fluids and sediments of a fixed water-rock ratio are reacted under controlled temperature conditions for varying lengths of time. The fluids are then analyzed chemically and the sediments analyzed using x-ray diffraction, scanning electron microscopy, and chemical techniques.

Principal Findings

Regional study of the Chicot aquifer

The Chicot aquifer system consists of a complex series of shallow, intercalated beds of gravels, sands, silt, and clay (Nyman et al., 1990). Prior to extensive development of this aquifer system, groundwater flow was primarily from recharge areas in Vernon, Rapides, Beauregard, Allen, and Evangeline parishes, where the aquifers outcrop in west central Louisiana, to the south toward the Gulf of Mexico and to the southeast into the Archafalaya River Basin. As documented by Nyman et al. (1990), approximately 76 of the total inflow into the aquifer system occured in its outcrop area under predevelopment conditions and 19 percent resulted from vertical leakage downward in areas to the south.

The regional groundwater flow pattern in the Chicot has been profoundly and pervasively altered as a result of extensive pumping. Although inflow into the aquifer system in its outcrop area has increased from 199 to 316 Mgal/d, vertical leakage over a broad area of southwestern Louisiana has increased by over an order of magnitude from 48 to 738 Mgal/d. Nyman et al. (1990) estimate that in 1981, only 28 percent of the total recharge into the aquifer took place in its outcrop area, and 76 percent was from from vertical leakage. A significant portion of the vertical leakage is presumably water pumped from aquifer for irrigation and thus is being recycled through the aquifer system by continuing pumpage, irrigation, and leakage.

It is known that significant variations in water quality exist both laterally and vertically within portions of the Chicot aquifer system. For example, Nyman (1989) has documented major increases in pH, hardness, and specific conductance downdip from the outcrop area over lateral distances of nearly 100 miles. The areal variation in dissolved Fe is much more complex. Total dissolved Fe is generally low in the outcrop area, then increases and then decreases downdip. The trends Nyman has illustrated represent complex regional gradients in pH, redox conditions, and salinity along the predevelopment flow paths of this aquifer system. Although Nyman did not investigate vertical variations in water quality within the Chicot, Trudeau, Hanor, and Olhoeft (in review) have documented the existence of significant pH and redox gradients from the surface to depths of less than 150 feet in shallow portions of the Chicot system at a site in Calcasieu Parish.

We have compiled a large number of existing data on ground water compositions and water levels for the Chicot Aquifer and underlying Evangeline Aquifer in southwestern Louisiana. This information is being used in conjunction with previous U.S.Geological Survey hydrologic modeling studies to identify regional flow paths along which controls on pore fluid compositions are being studied. A former USGS collection of sediment cuttings from wells penetrating ground water aquifers throughout Louisiana, including the Chicot Aquifer has been obtained. This material is currently being catalogued and archived. Cuttings from one core have been described, and the results are presented in Appendix A of this report.

Waters along a portion of a flow path in the 500-Foot Sand of the Chicot Aquifer and a portion of a flow path in the Evangeline Aquifer have been chosen by Mr. Yong Chen as a portion of his Ph.D. dissertation research for thermodynamic and mass-balance analysis (Chen, in prep.).

Preliminary results of this work are presented in Appendix A of this report. The study flow path in the Chicot can be divided into two zones based on the inferred geochemical reactions taking place within it. Preliminary calculations suggest that Zone 1, in the shallow upgradient portion of the aquifer, is characterized by the apparent dissolution of albite and K-feldspar, the precipitation of kaolinite, and the reduction and solubilization of iron oxide. Zone 2, in contrast, is characterized by the precipitation of kaolinite and K-feldspar, the dissolution of Na-smectite and albite, and the reduction of sulfate and precipitation of pyrite. Waters in the portion of the Evangeline flow path studied appear to be dissolving calcite, a fluoride-bearing phase, K-feldspar, and silica. The study of sediment samples from wells within or near these flow paths, which has just begun, will provide further constraints on the mineral-fluid reactions which are occuring. Field work is planned to sample key wells for analysis of redox-sensitive components. All of the above information when integrated with rates of fluid flow will provide important constraints on the rates of these reactions.

Shallow controls on ground water compositions in the Chicot aquifer

We have begun a study of the hydrogeochemistry of a hazardous waste landfill in Calcasieu Parish, which is the focus of M.S. thesis research being conducted by Ms. Shaobing Su (Su, in prep.). The site is of particular interest to the general project because of the existence of a suite of high-quality analyses of ground waters from an closely-spaced array of wells screened at different shallow depths in the Chicot aquifer. These analyses in conjunction with hydrologic information available at the site provide an unique opportunity to determine the nature and rates of geochemical reactions influencing water compositions during infiltration and shallow recharge. Although portions of the site have been contaminated by oil field brine and halogenated hydrocarbons, analyses of waters upstream and downstream from the contaminant plumes reflect more pristine conditions.

As described in Appendix B of this report, two detailed geologic cross sections through the site have been constructed from available geotechnical logs. The hydraulic head field has been remapped from available water level measurements to establish the general directions of ground water flow. Laboratory and field measurements of permeability are available, so it is possible to put some constraints on the rates of ground water flow. There is, however, a pervasive zone of secondary porosity in the form of joints and slickensides at depths of 1 to 3 m below mean sea level which may increase the effective vertical permeability of sediments at this site above those predicted by conventional laboratory and field techniques. A thermodynamic evaluation has been made of the saturation state of the groundwaters at the site with respect to sedimentary mineral phases known to be present. Future work will be devoted to characterizing redox reactions occuring at the site and in constraining rates of solute transport and reaction.

Effects of variable salinity in driving rock-fluid reactions

There has been considerable interest in the role that mixing of fluids of varying salinity plays in driving fluid-rock interaction and diagenesis in sedimentary basins. It has been observed, for example, that brines near halite diapirs are usually enriched in Na, K, Mg, Ca, and Sr, not just simply NaCl, and it is thus necessary to invoke silicate and carbonate mineral hydrolysis to account for the excess K, Mg, Ca, and Sr present in these waters (Hanor, in press). The details and rates of such reactions, however, are poorly known. The problem is of particular interest in terms of the overall goals of the present project because of the encroachment of saline waters into the Chicot Aquifer as the result of heavy withdrawal.

Ph.D. candidate Mr. Lee Esch has completed the first of a series of laboratory experiments in which NaCl solutions ranging in concentration from 1 mg/L to halite saturation (*ca.* 350,000 mg/L)

have been reacted with natural, carbonate-free, clay-rich silts containing quartz, kaolinite, smectite, muscovite, albite, and K-feldspar (Esch, in prep.). The silts are intended as proxies for mudstones common in Gulf Coast ground water systems, such as the Chicot. Significant changes in aqueous fluid chemistry occur as a function of both time and salinity, even at modest temperatures of 25 to 90°C and total reaction times of 90 days or less. The changes reflect extensive water-sediment mass transfer which affects many dissolved components and mineral phases simultaneously. Consistent with field observations of compositions of saline waters and thermodynamic predictions, there is a general increase in dissolved K, Mg, Ca, Sr, and Ba and a decrease in pH and alkalinity with increasing salinity. There is also significant release of silica into solution during the early stages of reaction, particularly in the most saline waters, and its reincorporation into new aluminosilicates with time. The mass transfer of silica involves pervasive corrosion of detrital quartz, the intensity of which increases with increasing salinity. Of potential interest to problems of metal mobilization is the solubilization of Pb and Zn. The concentrations of both metals systematically increase with increasing chloride concentrations above *ca.* 20,000 mg/L to maxima of 77 and 2 mg/L for Pb and Zn, respectively. Work is underway to characterize the solid reaction products. The initial results of this study are described in Appendix C of this report and in Esch and Hanor (1993).

Organic acids as diagenetic agents

Subsurface production of acids by microbial processes plays an important role in driving the mineral hydrolysis reactions which strongly influence the composition of ground waters (McMahon et al., 1992; Sugimoto and Wada, 1993). Chief among these acids in shallow coastal plain aquifers, such as the Chicot Aquifer, is carbonic acid. Recent work has shown, however, that acetic acid may also be important. Mrs. Gina Bagnetto-Waters has begun an experimental study, as part of a B.S. honors thesis, in which acetic acid solutions ranging in concentration from 10 to 10,000 mg/L have been reacted with natural, clay-rich silts containing quartz, kaolinite, smectite, muscovite, albite, and K-feldspar at 25°C (Bagnetto-Waters, in prep.). The silts are intended as proxies for mudstones common in Gulf Coast ground water sequences such as the Chicot. Experiments both with and without calcite have been run. The fluids are cuurently being analyzed for their acetate and bicarbonate alkalinity and will be analyzed in 1993-94 for major cations and heavy metals.

Conclusions

Understanding the natural chemical and physical processes which control ground water quality is essential for predicting the effects of anthropogenic activities on the composition of fluids in shallow aquifer systems and ground water discharge zones. These chemical and physical processes occur over broad areas within the regional aquifer systems of Louisiana and hence represent nonpoint controls on both subsurface and surface water quality.

Research during the first year of this projected several-year project has focused on identifying specific geochemical reactions occuring along 100 km lateral regional flow paths and 10 to 100 m vertical paths of infiltration and recharge in the Chicot aquifer using a combination of thermodynamic modeling and mass balance techniques. Integration of this information with flow fluid rates will help to constrain the kinetics of these reactions. Experimental work has begun on the effects of variable salinity in driving changes in water quality though mineral hydrolysis reactions and on the role the production of organic acids plays in controlling water quality. The final product will be an integrated solute transport - diagenetic reaction model for the Chicot system which can be used as a predictive management tool.

References

Bagnetto-Waters, G., in preparation, Role of organic acids in silicate-carbonate hydrolysis: B.S. Honors Thesis, Department of Geology and Geophysics, Louisiana State University.

Chen, Y., in preparation, Nonpoint controls on the quality of shallow groundwaters in the Chicot Aquifer, southwestern Louisiana: Ph.D. Dissertation, Department of Geology and Geophysics, Louisiana State University.

Esch, L., in preparation, Salinity as a variable in sediment diagenesis: Ph.D. Dissertation, Department of Geology and Geophysics, Louisiana State University.

Esch, L., and Hanor, J.S., 1993, Reaction of NaCl brines with siliciclastic sediments: an experimental study: Geological Society of America 1993 Annual Meeting, Program with Abstracts.

Hanor, J.S., and McManus, 1988, Sediment alteration and clay mineral diagenesis in a regional ground water flow system, Mississippi Gulf Coastal Plain: Trans. Gulf Coast Assoc. Geol. Soc., v. 38, p. 495-502.

Hanor, J.S., in press, Origin of saline fluids in sedimentary basins: Special Publication, Geological Society of London.

Lee, R.W., 1985, Geochemistry of groundwater in Cretaceous sediments of the southeastern coastal plain of eastern Mississippi and western Alabama: Water Resouces Res., v. 21, p. 1545-1556.

Lee, R.W., and Strickland, D.J., 1988, Geochemistry of groundwater in Tertiary and Cretaceous sediments of the southeastern coastal plain in eastern Georgia, South Carolina, and southeastern North Carolina: Water Resources Res., v.24, 291-303.

McMahon, P.B., Chapelle, F.H., Falls, W.F., and Bradley, P.M., 1992, Role of microbial processes in liking sandstone diagenesis with organic-rich clays: Journal of Sedimentary Petrology, v. 62, p. 1-10.

Nyman, D.J., 1984, The occurrence of high concentrations of chloride in the Chicot aquifer system of southwestern Louisiana: LA Dept. Trans and Devel. Water Resources Technical Rept. 33, 51 p.

Nyman, D.J., 1989, Quality of water in freshwater aquifers in southwestern Louisiana: LA Dept. Trans. and Devel. Water Resources Technical Rept. 42, 22 p.

Nyman, D.J., Halford, K.J., and Martin, A., Jr., 1990, Geohydrology and simulation of flow in the Chicot aquifer system of southwesatrn Louisiana: LA Dept. Trans. and Devel. Water Resources Technical Rept. 50, 58 p.

Pettijohn, R.A., Busby, J.F., and Beckman, J.D., 1992, Properties and chemical constituents in ground water from the Mississippi River Alluvial Aquifer and Permeable Zone A (Holocene-Upper Pleistocene deposits), south-central United States: U.S. Geological Survey Water-Resources Investigations Report 91-4149.

Plummer, L.N., Busby, J.F., Lee, R.W., and Hanshaw, B.B., 1990, Geochemical modeling of the Madison aquifer in parts of Montana, Wyoming, and South Dakota: Water Resources Res., v. 26, 1981-2014.

Plummer, L.N., Prestemon, E.C., and Parkhurst, D.L., 1991, An interactive code (NETPATH) for modeling net geochemical reactions along a flow path: U.S. Geological Survey Water-Res. Invest. Rept. 91-4078, 227 p.

Su, S., in preparation, Hydrogeochemistry of a hazardous waste landfill, southwestern Louisiana Gulf Coast: M.S. Thesis, Department of Geology and Geophysics, Louisiana State University.

Sugimoto, A., and Wada, W., 1993, Carbon isotopic composition of bacterial methane in a soil incubation experiment: contributions of acetate and CO_2/H_2: Geochimica et Cosmochimica Acta, v. 57, p. 4015-4027.

Trudeau, D.A., Hanor, J.S., and Olhoeft, G, in review, Hydrogeology, occurrence, and movement of oil-filed brine and organic priority pollutant contamination at a waste site in Calcasieu Parish, Louisiana: U.S. Geological Survey Water Supply Paper.

von Gunten, U., and Zobrist, J., 1993, Biogeochemical changes in groundwater infiltration systems: column studies: Geochimica et Cosmochimica Acta, v. 57, p. 3895-3906.

APPENDIX A

Nonpoint controls on the quality of shallow groundwaters in the Chicot Aquifer, southwestern Louisiana

Yong Chen
Department of Geology and Geophysics
Louisiana State University
Baton Rouge, Louisiana 70803

Note: The research described in this appendix represents the results of the first year of a Ph.D. dissertation research project being conducted by Mr. Chen. The purpose of this appendix is to outline the long-term goals of this research and to document what has been completed during the 1992-93 period of funding by the Department of the Interior, U.S. Geological Survey, through the Louisiana Water Resources Research Institute. It should be understood that portions of the text, figures, and tables which follow are preliminary in nature and subject to revision and that some phases of the project will not be completed for another year or more.

Nonpoint controls of the quality of shallow groundwaters in the Chicot Aquifer, Southwestern Louisiana

Yong Chen

1. Introduction

The chemical composition of groundwater in aquifer systems is mainly the result of natural chemical and physical modifications on source water. Human activities, such as industry, agriculture and urban disposal, can greatly influence the quality of both surface and subsurface waters. To understand the quality of groundwater in aquifer systems and to predict effects of anthropogenic activities on the modification of water quality in aquifer systems, we have to understand the natural processes which control the quality of groundwater chemically and physically.

In this study, such an effort has been made on the Chicot aquifer, one of several major freshwater aquifers in southwestern Louisiana. Because the Chicot aquifer interacts with the underlying Evangeline aquifer, the Evangeline aquifer is also been studied.

1.1 Occurrence of Shallow Groundwater in Southwestern Louisiana

Southwestern Louisiana as defined in this study includes the 14 parishes which are shown in Figure 1.1. Fresh groundwater in southwestern Louisiana occurs mainly in four unconsolidated sand aquifers, the Atchafalaya aquifer, the Chicot aquifer, the Evangeline aquifer and the Jasper aquifer. The Chicot aquifer, the Evangeline aquifer and the Jasper aquifer are the three major water-supply aquifers in this area. These three aquifers are generally separated by relatively impermeable beds of clay. They are also underlain and overlain by beds of clays (Figure 1.2). The depth of freshwater in this region can reach as deep as 3100 ft (945 m) (Jones, et al., 1956). The water in all three aquifers is under hydrostatic pressure.

1.2 Anthropogenic stress

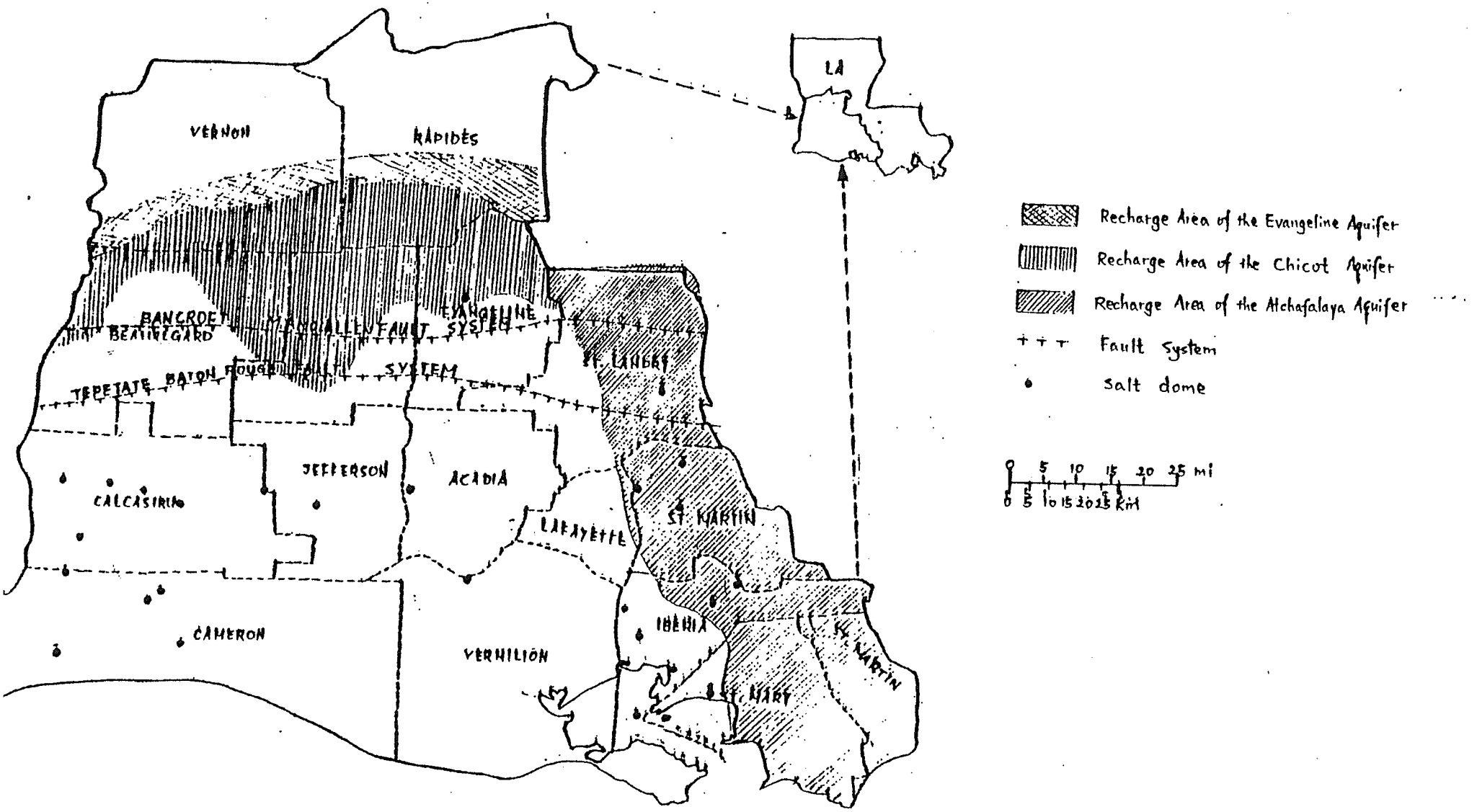

Figure 1.1 Regional Map of Southwestern Louisiana (Modified from Nyman, 1989; Whitfield, 1975; and Jones, and others, 1956)

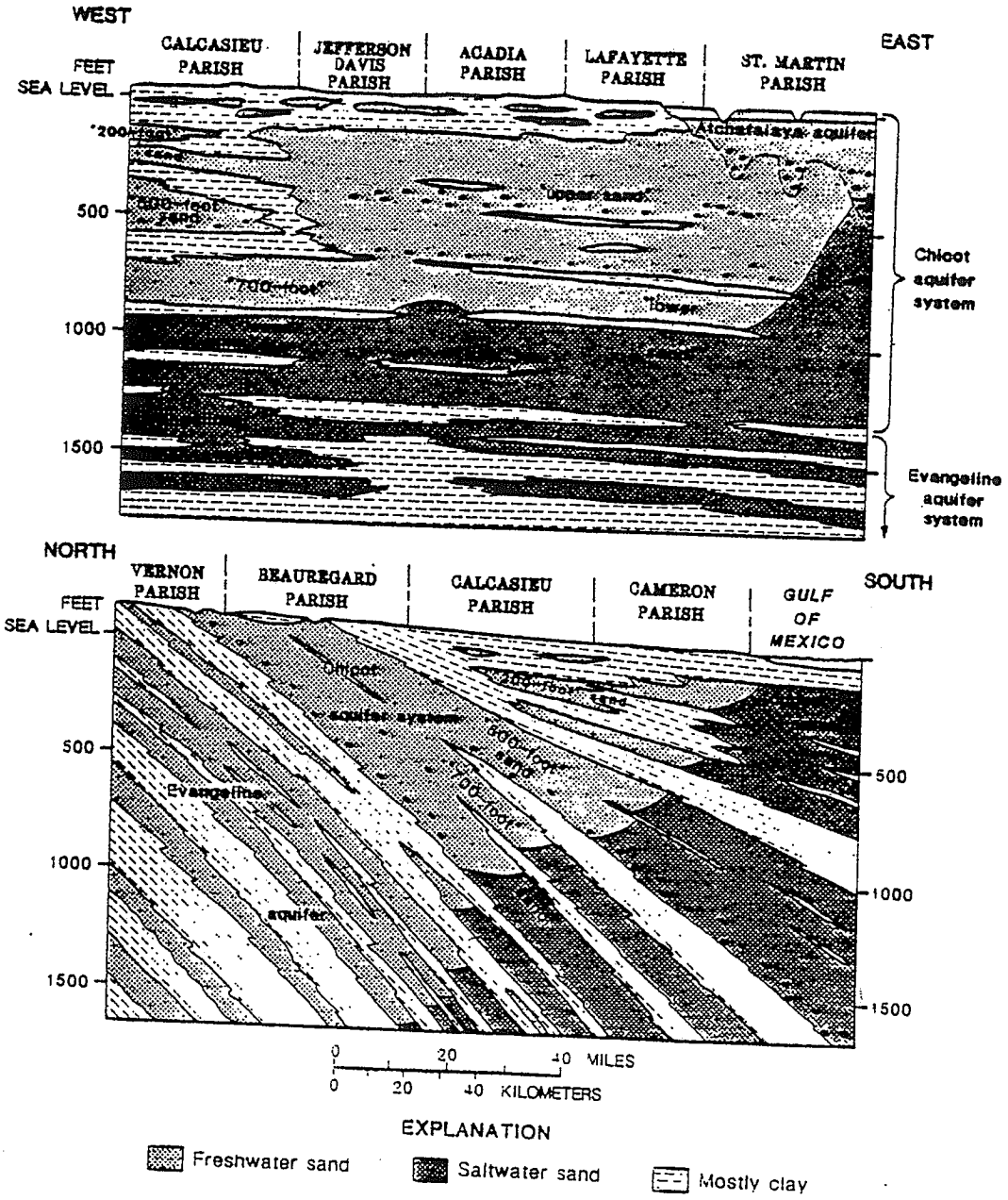

Figure 1.2. Generalized Cross-section of the region. (From Nyman, 1989).

Anthropogenic activities in southwestern Louisiana have had significant impacts on the groundwater systems in this region as will be discussed later. The groundwater usage in southwestern Louisiana is mainly for rice farming, petroleum industries, and public supply. Heavy groundwater withdrawals have occurred in Jefferson Davis, Acadia, and Vermilion Parishes for irrigation, and around the Lake Charles area for industries. The groundwater withdrawals for rice irrigation are the largest usage, which accounted for nearly 90% of the groundwater pumped in southwestern Louisiana during 1980 (Nyman and others, 1990) . They are from the "upper-sand" of the Chicot aquifer system (Figure 1.2). The groundwater withdrawals for industries are from "500-foot" and "700-foot" sands (Nyman, 1989).

These heavy groundwater withdrawals have greatly changed the natural groundwater flow systems in this area. The hydraulic head of the Chicot aquifer has continuously declined since the time when significant amount of groundwater was pumped out from the aquifer. From 1900 to 1981, the water levels in wells declined, on average, about 1 ft/yr (0.3 m/yr) in the Lake Charles and rice-growing areas (Nyman and others, 1990). Two draw-down cones have been formed in the area (Figure 3.2).

The decline of hydraulic heads of groundwater in the Chicot aquifer system has greatly changed fluid flow paths. This will be discussed later. The changes of flow path of the ground-water in the Chicot aquifer system may induce stresses on the quality of groundwater in this aquifer. Decline of hydraulic head in the aquifer could cause recharge of surface water through the overlying confining clay layers, in addition to natural water recharges from outcrop areas. This is especially likely around draw-down cone areas, where the head in the upper part of the Chicot aquifer is much lower than that of surface. Surface waters have been altered by agricultural contamination, such as pesticides, industrial waste, municipal sewerage, and contaminants from the atmosphere. There are many hazardous waste disposal fields state wide. These toxic contaminants could also be carried by surface water (such as rain water) entering the aquifer system where heads in the aquifer is lower than that of surface water.

The decline of hydraulic head of groundwater in the Chicot aquifer system, especially around

depression cone areas, have also changed groundwater flow rates within the aquifer system. This increased flow rate has reduced contact time between groundwater and sediments in the aquifer, thus reducing reaction time between the two. Because the reactions between groundwater water and sediments largely modify the chemical composition of groundwater, the water quality of the Chicot aquifer system may be affected by changes in flow rate of groundwater.

Finally, heavy pumpage of groundwater from the Chicot aquifer can cause salt water intrusion problems. As hydraulic head declines, original down-stream salt water and deep salt water will move toward low head areas in pumping centers. Such problems may already occurred in southwestern Louisiana. (Jones, et al., 1956; Nyman 1989)

1.3 Previous work

Geochemical evolution of groundwater in shallow sandstone aquifer systems has been subjects for many studies (Such as, Lee, 1985; Hanor and others, 1988; Lee and Strickland, 1988). These studies have investigated chemical reactions which are responsible for composition changes of groundwater as it migrate in an aquifer system. These reactions include mineral dissolution and precipitation, and alteration of clay minerals. Although biologically mediated redox reactions were discussed, no detailed studies have been done.

In southwestern Louisiana, the geologicalframe work was published as early as late 19th century. A summary of the geology, hydrology and general occurrence of groundwater can be found in Jones, et al. (1956). Some reports on geology, hydrology and water chemistry for individual aquifers and/or single parishs also exist, such as, Harder (1960), Whitfield (1975). Two recent studies by Nyman and coworkers address for the Chicot aquifer system (Nyman, 1989; Nyman and others, 1990).

Nyman (1989) has discussed the quality of water in freshwater aquifers in southwestern Louisiana, including the Chicot aquifer. Areal variations in chemical compositions of groundwater in the Chicot aquifer system were contoured in this region for individual units of the system. However, Nyman did not discuss what natural physical and chemical processes were responsible

for chemical composition variations of the groundwater in this aquifer.

Heavy groundwater withdrawals from aquifers in southwestern Louisiana have caused water levels to decline continuously, except for years when water pumpage was reduced. The impacts of such pumpage on water head changes in the future has been studied by numerial simulation by Nyman and others (1990). One interesting conclusion from their simulated results is that under 1981 conditions, vertical leakage was the largest component of recharge.

1.4 Remaining problems

As discussed above, there has been some study of geology and hydrology of groundwater aquifers in southwestern Louisiana. General occurrence of groundwater and its general chemical compositions have also been documented. However, no efforts have been made in this region to identify specific processes which modify groundwater compositions as groundwater moves through the aquifers. These modification processes include both natural and anthropogenic processes. Understanding natural controls on the evolution of groundwater is essential in understanding any anthropogenic impacts on the water quality.

1.5 Purpose of this study

The major purpose of this study is focused on natural chemical processes which modify the groundwater composition when groundwater moves from its recharge area to its discharge area. These processes include mineral dissolution and precipitation, clay mineral alteration, ion exchange, and biologically-mediated redox reactions.

Physical processes of advection and dispersion can also significantly modify water chemistry in aquifer systems. These processes will also be investigated in later phase of this study.

2. Regional Geology

(In preparation)

2.1 Regional geologic setting

(In preparation)

2.2 Regional deposition history and Stratigraphy

(In preparation)

2.3 Summary

(In preparation)

3. Regional Hydrology of Chicot Aquifer and Adjacent Units

The Chicot aquifer is the largest water supply aquifer in southwestern Louisiana. Walter (1982) reported that the total groundwater pumping rate averaged more than 1,000 Mgal/day (3,785 m^3/day) from the 13-parish area of southwestern Louisiana during 1980. However, an average of 990 Mgal/day (3,747 m^3/day) was pumped from the Chicot aquifer system and the Atchafalaya aquifer. Only 15 Mgal/day (57 m^3/day) was pumped from the Evangeline aquifer, and 25 Mgal/day (95 m^3/day) from the Jasper aquifer.

Many reports have been published on the Chicot and other aquifers in this area (e.g., Jones, et al., 1956; Harder, 1960; Whitfield, 1975; Nyman, 1989; Nyman, et al., 1990). The following is the summary of the regional hydrology of the Chicot aquifer and adjacent units as derived from these reports.

3.1 Hydraulic units of the Chicot aquifer and adjacent units

The general stratigraphic relation among these aquifers can be seen from Table 3.1. From the top to the bottom, these fresh groundwater bearing aquifers are Alluvium aquifer (including the Atchafalaya aquifer), the Chicot aquifer, the Evangeline aquifer, and the Jasper aquifer. All of the major fresh water bearing aquifers are composed of deltaic and near-shore marine sediments ranging from Holocene to Miocene in age (Nyman, 1989). These aquifers are generally separated by beds of clay (Jones, et al., 1956).

The Chicot aquifer system has been divided into several units. According to Nyman (1984), it is divided into four major units in Lake Charles area: the Alluviul aquifer, 200-foot sand, 500-foot sand, and 700-foot sand; and three units in east of Lake Charles area: the Atchafalaya aquifer, Upper sand, and Lower sand. A similar division was also given by Harder (1960). The Alluviul aquifer in Lake Charles area has been included in the 200-foot sand in Nyman's 1989 report. The upper part of the Chicot system usually consists of a single massive sand unit (Figure 1.2). The names of the units of the Chicot aquifer system in this report are the same as those used by Nyman (1989).

Table 3.1 Correlation Between the Geological Units and the Geohydrological Unit (modified from Nyman, et al., 1990):

System	Series	Harder (1960)		Harder and Others (1967)	Nyman (1984)		
		Formation	Hydrologic Unit		Lake Charles Area		East of Lake Charles Area
Quaternary	Holocene				Chicot Aquifer System	Alluvium	Alluvium, Atchafalaya Aquifer, and Abbeville Unit
	Pleistocene	Prairie	Chicot Shallow	Shallow Sand			
		Mont-gomery	"200-foot" Sand	"Upper Sand Unit"		"200-foot" Sand	"Upper Sand"
		Bentley	"500-foot" Sand	Undiffer-entiated Sand		"500-foot" Sand	Undifferentiated "Lower Sand"
		William	a "700-foot" Sand			"700-foot" Sand	
Tertiary	Pliocene and Miocene	Foley	Evangeline Aquifer	Evangeline Aquifer	Evangeline Aquifer		Evangeline Aquifer

The Chicot aquifer and the Atchafalaya aquifer are primarily of continental origin and contain mostly coarse sand with interbedded layers of gravel. The Evangeline aquifer and the Jasper aquifer are of marine origin and contain finer sediments and thicker clays. The Atchafalaya aquifer is connected hydraulically with upper part of the Chicot aquifer in the east part of the study area (Nyman, 1989). The Chicot aquifer and the underlying Evangeline aquifer are generally separated from each other by a thin clay layer. However, this clay layer is missing in some places (Withfield, 1975). This may cause some hydraulic interaction between these two aquifers.

Within the Chicot aquifer system, the 200-foot sand and the Upper sand are hydraulically connected with each other. So are the 700-foot sand and the Lower sand. The 500-foot sand is relatively well confined on both east side and west side (Nyman, 1989). The general stratigrapgic relations between the different aquifers and different units within the Chicot aquifer system have been shown on Plate 2 of Nyman (1989). This plate shows two idealized geologic sections across the study area from west to the east and from the north to the south. This aquifer system thickens and dips to the south at the rate of about 30 ft/mile (5.7 m/km) (Nyman, et al., 1990).

3.2 Hydraulic heads

As mentioned above, the Chicot aquifer system is a heavily pumped aquifer in southwestern Louisiana. This continuously heavy pumpage on the aquifer has changed its potentiometric surface. Figure 3.1 is a simulated predevelopment potentiometric surface of upper Chicot aquifer by Nyman and his co-workers (1990). This map shows that the potentiometric surface of the upper Chicot aquifer is highest at the outcrop area of the aquifer, and generally declines toward the gulf of Mexico.

Figure 3.2 is a potentiometric surface map in the spring of 1981 made by Nyman (1981). The most significant difference between this map and the predevelopment map is that the potentiometric surface of groundwater in this aquifer no longer decresses all the way to the coastal shoreline. Instead, there are two pronouced draw down cones in this area. These two cones coincide with the two regional pumping centers, one in Lake Charles area, the other in the Acadia area. These two

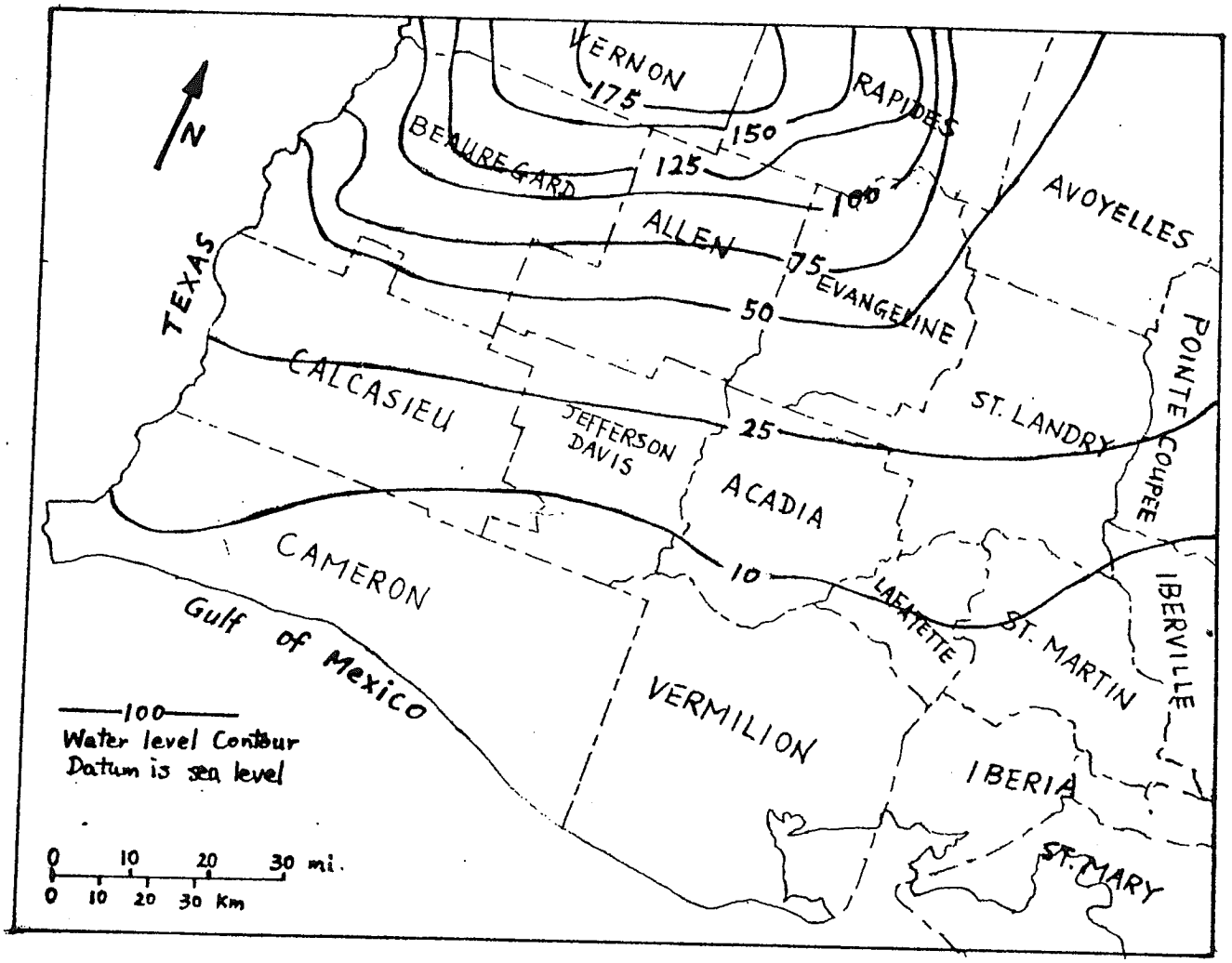

Figure 3.1 Computer-simulated Predevelopment Potentiometric Surface Map of the Upper Chicot Aquifer (Modified from Nyman and Others, 1990)

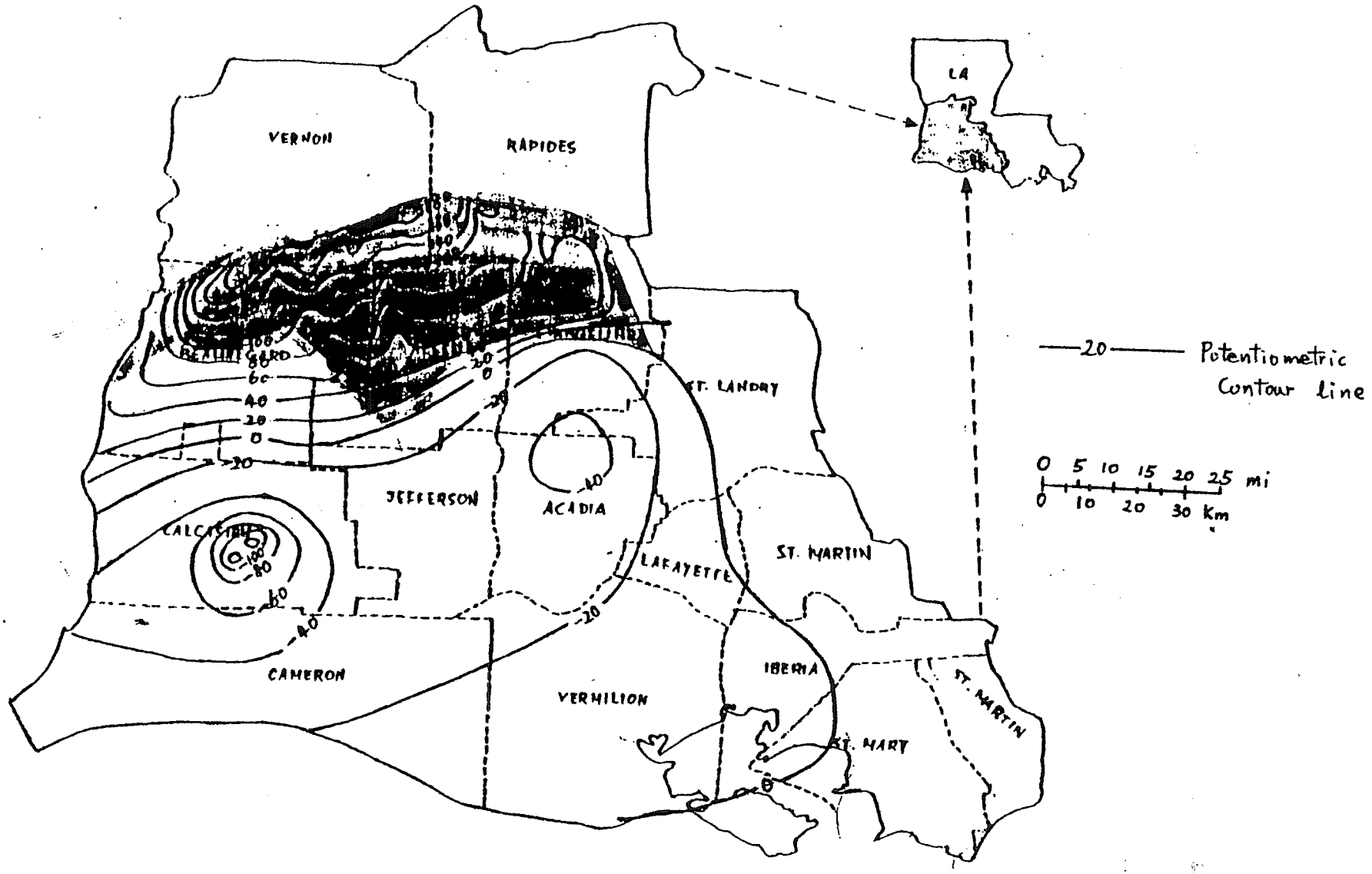

Figure 3.2 Potentiometric Surface Map of the Chicot Aquifer in Southwestern Louisiana in 1981 (From Nyman, 1989)

cones are obviously caused by the heavy groundwater withdrawal from these two areas.

The general flow direction of the groundwater in the Evangeline aquifer is also from north to south (Plate 2, Whitfield, 1975). Water withdrawals from this aquifer for both municipal and industrial uses have lowered water levels in this aquifer at an average rate of less than 1 foot (0.3 m) per year since 1967 except near pumping centers, where rates are higher (Whitfield, 1975). Several local depression cones have developed at pumping centers near De Ridder, Merryville, Elizabeth, Oakdale, Oberlin, Kinder, Ville Platte, Mamou, Melville, and Krotz Springs (Whitfield, 1975). However, only one significant cone which may change the flow path locally is one near Ville Platte (Plate 2, Whitfield, 1975).

3.3 Flow paths

The Chicot aquifer system crops out in Louisiana in southern Vernon and Rapides parishes and in northern Beauregard, Allen, and Evangeline parishes (Jones, et al., 1956; Nyman, et al. 1990). According to Jones, et al.(1956), this area accounts for about 2000 square miles (5180 km^2). The outcrop area of the Chicot aquifer is the major recharge area. Small amount of groundwater in the Chicot aquifer system may comes from the underlying Evangeline aquifer through the thin confining clay layer where the hydraulic head in the Evangeline aquifer is higher than that in the Chicot aquifer (Whitfield, 1975).

A computer simulation study conducted by Nyman, et al. (1990) concluded that prior to groundwater development, water flowed from recharge area where the aquifer crops out southward to a discharge area along the coast and eastward to the Atchafalaya River basin. Discharge took place upward through overlying clay beds in the coastal-wetland areas and in the Atchafalaya River basin. However, after heavy pumpage of groundwater from the aquifer was established, the flow pattern changed. From the present potentiometric surface map of the Chicot aquifer (Figure 3.2), one can easily find that the groundwater now flows toward two pumping centers, but not the coastal area and the Atchafalaya River basin as it did before. The Atchafalaya River basin has become recharge area instead of discharge area as it used to be.

3.4 Hydraulic conductivity

The average hydraulic conductivity for 200-foot sand and upper-sand is 62.5 m/day. The 700-foot sand and lower-sand has an average hydraulic conductivity of 42.7 to 91.4 m/day. The average hydraulic conductivity of the middle 500-foot sand is 48.8 m/day. All these numbers are converted from Nyman (1989).

3.5 Fluid mass balance

According to a computer-simulated results (Nyman and others, 1990), under 1981 conditions, approximately 1,113 Mgal/day (4210 m^2/day) of water recharges into the Chicot aquifer. This is more than 4 times the recharges prior to development. More than 90 percent of the recharged water discharges out the aquifer through pumpage. In their model, the Chicot aquifer system has been divided into two parts, upper part and lower part. They estimate that 55 percent of water entering the upper Chicot aquifer in 1981 was discharged to the surface or by pumpage without moving into the lower part of the aquifer system. In 1981, 65 percent of the water pumped from the rice-growing area was supplied by recharge from the surface. Less than 1 percent of the water entering the aquifer system came from storage. Detailed dscussion explanation can be found in the report (Nyman, et al., 1990).

3.6 Saline waters

(In preparation)

3.7 Summary

(In preparation)

4. Areas Selected for Detailed Studies

4.1 Introduction

The major purpose of this study is focused on the natural chemical and physical processes on the evolution of groundwater quality. Therefore, it is better to chose an area where anthropogenic impacts on the groundwater have been at minimum. For this reason, an area has been chosen for detailed study which includes Vernon, Beauregard, and Calcasieu parishes and covers the most part of a flow path from the recharge area to a previous discharge area (Figure 4.1).

The Chicot aquifer system in this area is well confined on the top by a thick clay layer. It can be demonstrated that the volume of surface water or shallow groundwater, which are the waters most likely to be affected by surface anthropogenic activities, being vertically recharged into the Chicot aquifer is small compared with the total volume of water within the aquifer. The thickness of overlying clay bed is 1 to 200 feet (0.3 to 60 meters) from the outcrop area to the coast (Jones, et al., 1956). Nyman et al. (1990) gave the vertical hydraulic conductivity values of clay within the Chicot aquifer, which were based on laboratory studies of clay cores from the Lake Charles area, as an average of 2.33×10^{-3} ft/day (7.10×10^{-4} m/day). The hydraulic head of groundwater in the Chicot aquifer is normally only several tens of feet below land surface on most part of the selected area, therefore, the hydraulic head of surface or shallow subsurface water should be slightly higher, if not lower, than that of groundwater in the Chicot aquifer. Assume that the hydraulic head of the surface and/or shallow subsurface water is the same as the land surface. The head difference between surface or shallow subsurface water and the water in the Chicot aquifer is nearly zero in the outcrop area, where clay layers is the thinnest, and the head difference increases downdip while the thickness of the confining clay layer also increases. As a result, the vertical hydraulic gradient may not be large except for heavily pumped area, where the hydraulic head drops rapidly toward the pumping center.

Consider as an example, a 50-feet head difference over a 50-feet thick clay. The hydraulic gradient from this should be larger than that in most of the places of the selected area. Harder

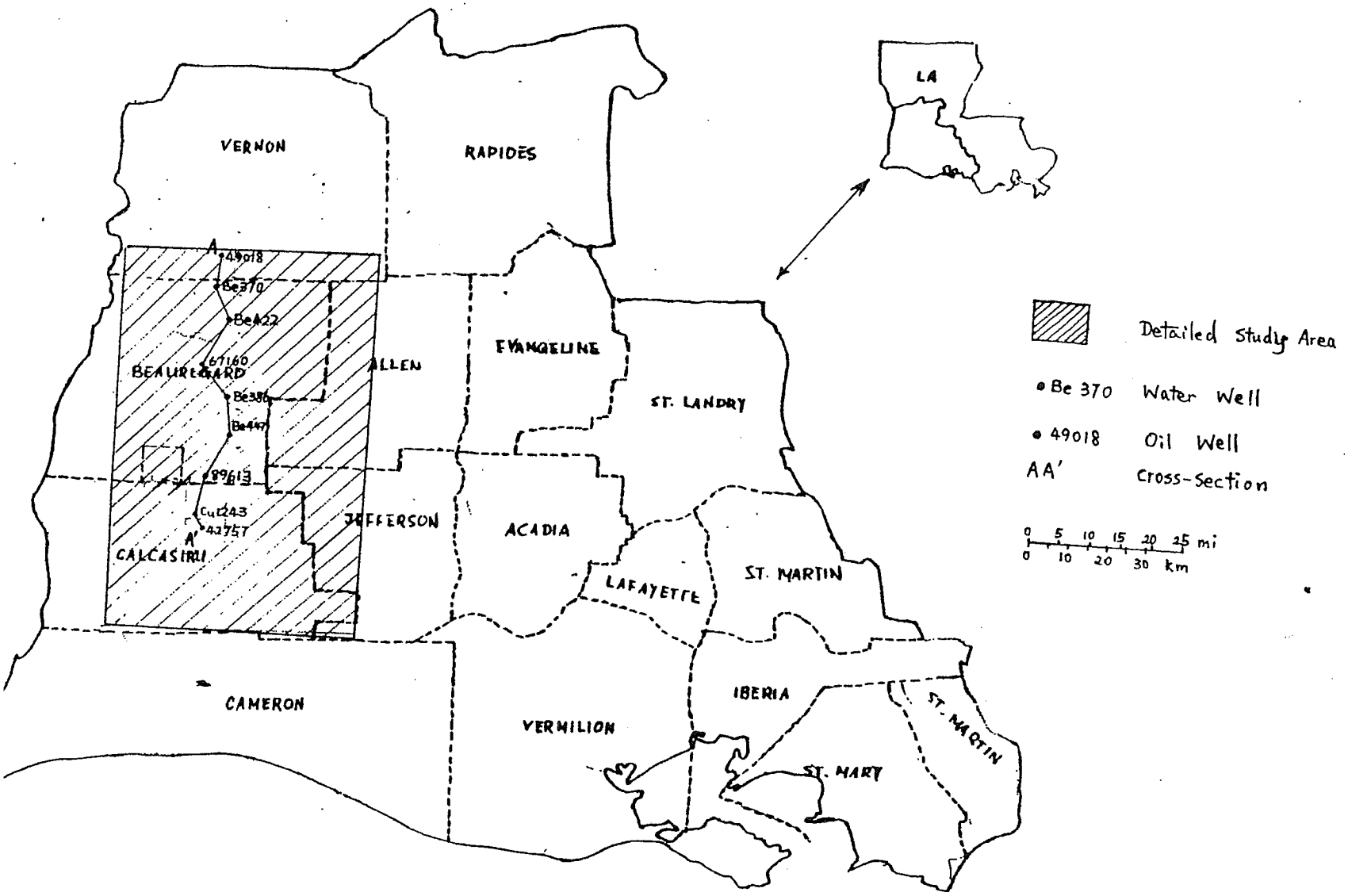

Figure 4.1 Selected Study Area and Cross-Section AA'

(1960) reported that the thickness of clay layer on top of the Chicot aquifer is up to 75 feet in many places of Beauregard Parish where head of the Chicot groundwater is generally less than 50 feet. In Calcasieu Parish, the top of the 200-foot sand for all wells in Harder's report (1960) is deeper than 165 feet except for one well at eastern edge of the parish, where it is 85 feet. A simple calculation shows that the amount of water recharge into the Chicot aquifer through the clay layer will be 0.25 gal/day for every square mile (3.6×10^{-4} m^3/day for every square kilometer). This is not a significant amount of water compared with the amount of water stored in the aquifer in 1 square mile area, which is about 1.2×10^{10} gal (4.7×10^7 m^3) if we use 150 ft as the aquifer average thickness and 0.40, which is within the range of values given by Freeze and Cheery (1980) for unconsolidated sand, as aquifer porosity.

In this selected study area, a stratigraphic profile has been constructed across the area from the north to the south. Several wells have been chosen along two flow paths, one in the Chicot aquifer, the other in the Evangeline aquifer, based on their present potentiometric surface map. These two flow paths were used in this study for demonstrating possible geochemical evolution processes, which will be discussed in Chapter 7 and 8.

4.2 Geology

Figure 4.2 is a stratigraphic profile along section AA' (Figure 4.1). This profile was constructed based on an interpretation of electric logs for selected wells along the section AA'. It shows that the Chicot aquifer exists as a single massive sand bed in most part of Beauregard Parish and the south part of Vernon Parish, but as three separate units, the 200-foot sand, 500-foot sand, and 700-foot sand, in Calcasieu Parish. The thickness of the aquifer along this cross section is 80 to 400 feet (25 to 120 m) for the massive sand, less than 50 feet (15 m) for 200-foot sand, around 145 feet (45 m) for 500-foot and 700-foot sand.

Underlying the Chicot aquifer is the Evangeline aquifer, which is composed of a series of separate beds of sand. These beds of sand are relatively thin, generally less than 50 feet (15 m) thick (as coverted from Whitfield, 1975), and are separated by clay beds, which are generally discontinuous (Whitfield, 1975). Hydrologically, these sand beds can be treated as a single aquifer

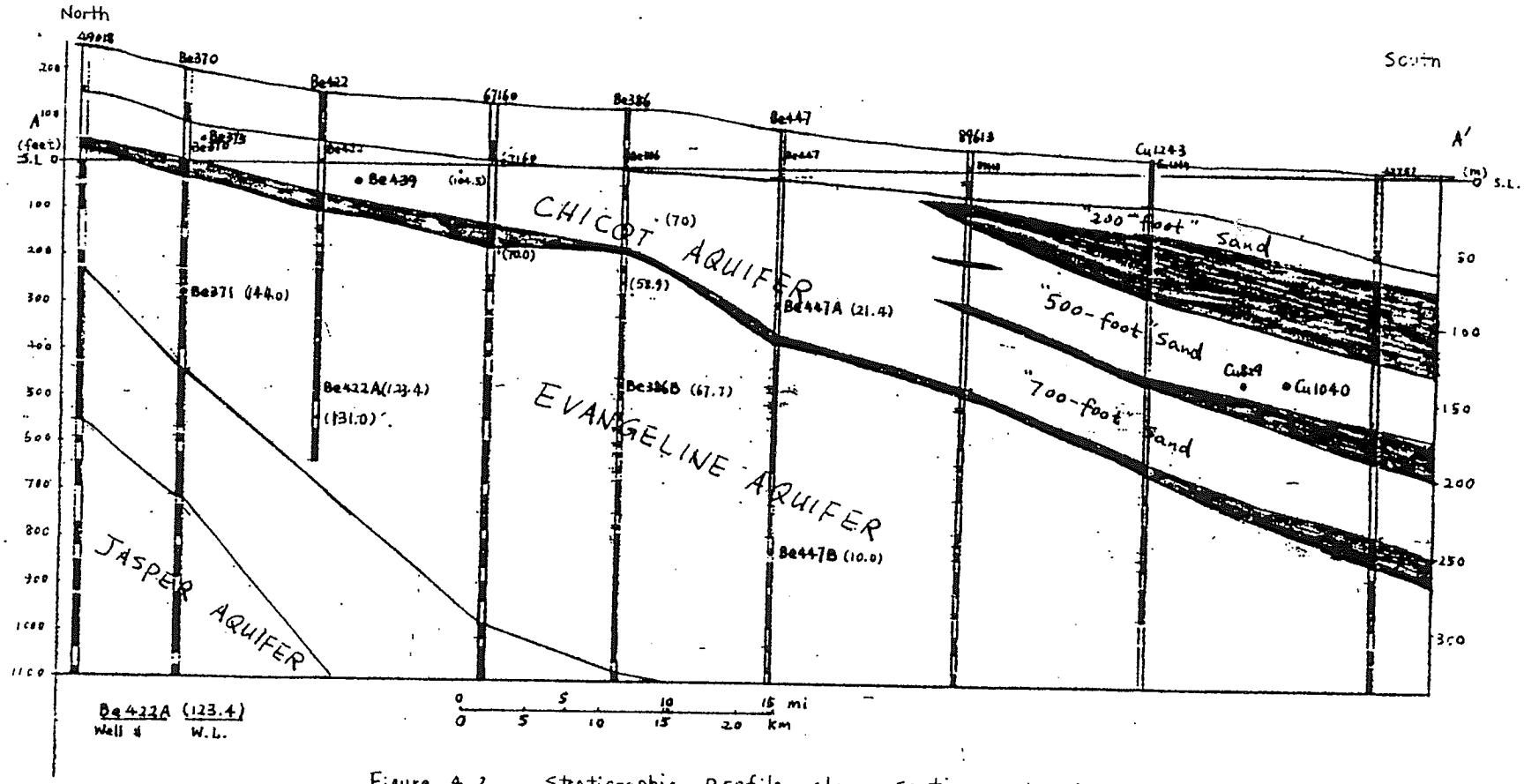

Figure 4.2 Stratigraphic profile along section AA'. It shows relative positions of wells for selected Flow Paths. It also shows water levels for some wells. Black areas are clays.

system.

There is a thin clay bed existing between the Chicot aquifer and the Evangeline aquifer. The thickness of the bed, based on these logs, ranges from less than 15 feet (5 m) to 65 feet (20 m). There is no evidence that the confining clay bed between these two aquifers is missing anywhere along this cross section. However, in places the clay bed is very thin, for example, less than 15 feet (5 m) at well Be386. This may permit some leakage of groundwater from the Evangeline aquifer into the Chicot aquifer, as discussed by Jones et al. (1956) and Whitfield (1975), because the hydraulic head in the Evangeline aquifer may be higher than that in the Chicot aquifer. As a matter of fact, the hydraulic head in the Evangeline aquifer is generally slightly lower, not higher, than that in the Chicot along the cross section AA' (figure 4.2), therefore, the water leakage may occur not from the Evangeline aquifer to the Chicot aquifer, but the reverse direction.

4.3 Hydrology

The Chicot aquifer, as discussed previously, receives recharging water mainly from its outcrops in northern part of the selected area. Just based on the constructed cross section, the major recharge area probably extends even farther north of the cross section. Minor recharge could also come from the water which leaks through the clay beds on top of the Chicot aquifer in most part of the selected area. Unlike suggested by Whitfield (1975), the Chicot aquifer discharges small amount of water into the underlying Evangeline aquifer as discussed previously. However, Whitfield (1975) reported that most natural discharge water of the underlying Evangeline aquifer goes upward into the Chicot aquifer in southern part of the southwestern Louisiana, Calcasieu Parish. Because such major recharging water from the Evangeline aquifer occurs at far north of the selected area, it may not seriously affect our later thermodynamic analysis and mass-balance calculation, especially for the upper part of the segment of flow path chosen in this study.

Groundwater of uniform density flows from areas of higher head to areas of lower head. The ground-water in the Chicot aquifer flows downdip the aquifer system toward south, which can be seen on figure 4.3. Figure 4.3 is a potentiometric contour map of the selected area, constructed

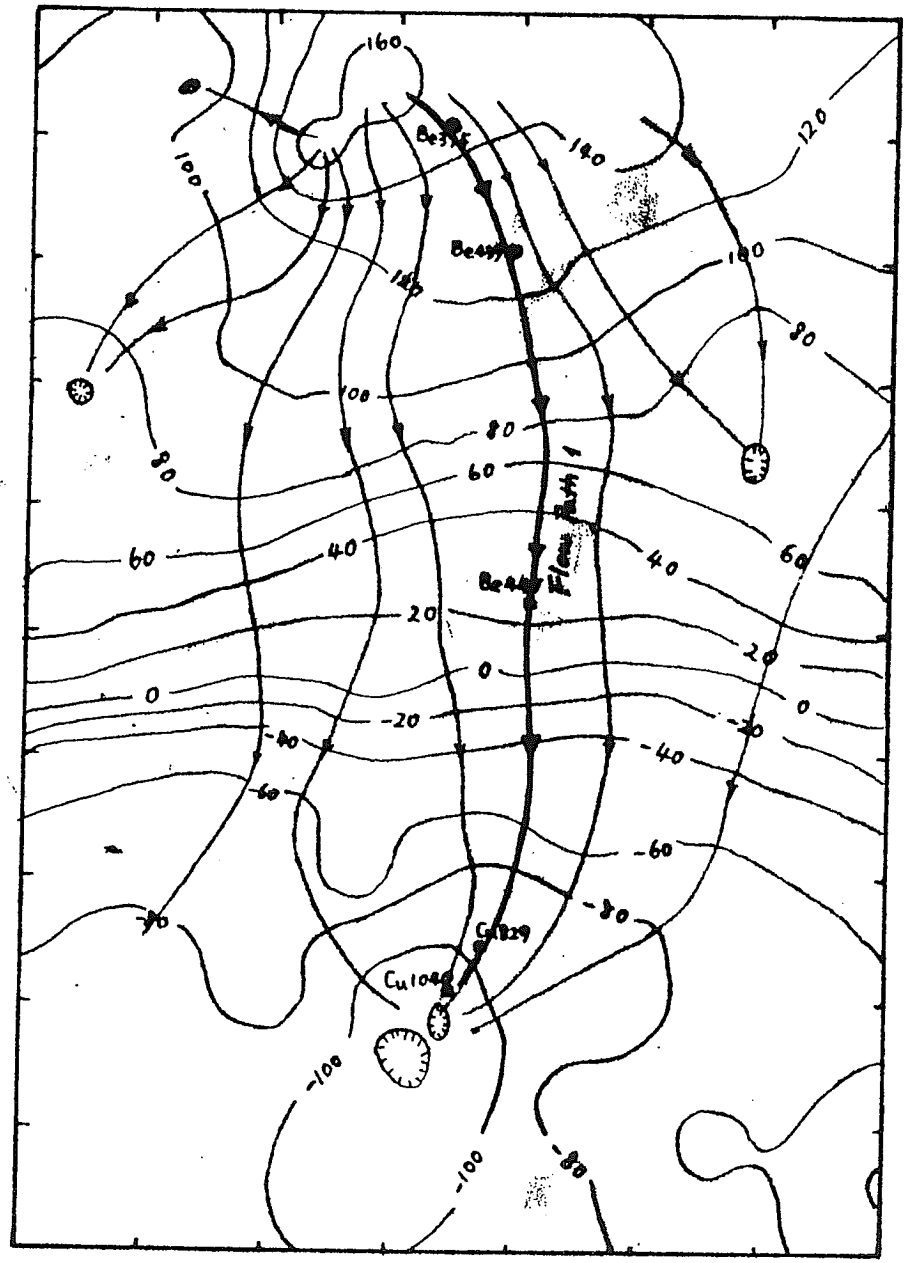

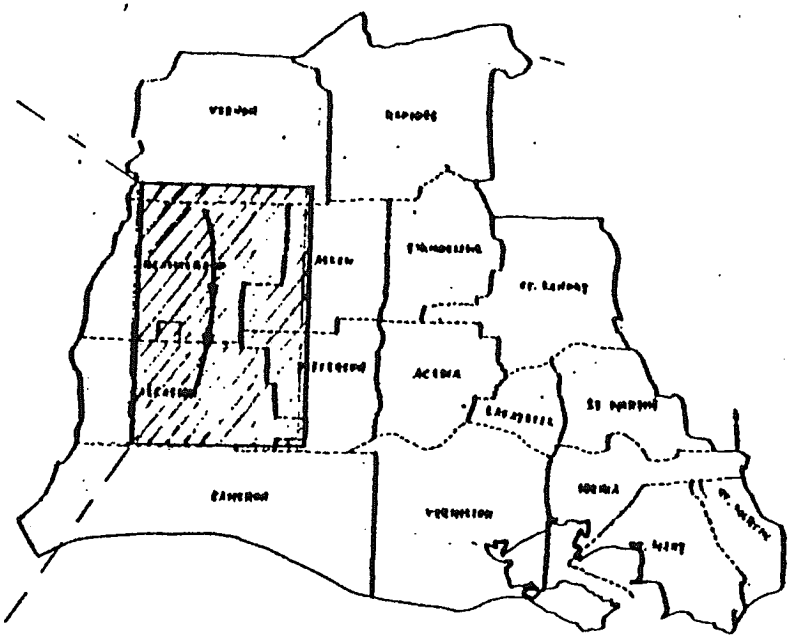

Flow line

80 Potentiometric line

• Be375 Water Well

Figure 4.3 Potentiometric Surface Map for the Study Area in 1974. A Flow Path has been Defined Based on Contour Lines.

from the USGS unpublished data of 1974.

The natural discharge before heavy pumpage of groundwater began in this selected area is to the coast area of gulf of Mexico (Nyman, et al., 1990). Now, most discharge of groundwater from the Chicot aquifer in this area is the water withdrawals by pumping in Lake Charles area as indicated by the potentiometric maps(figure 3.2 and figure 4.3).

The hydraulic conductivity of the Chicot aquifer sand through pumping test has been reported by many people (Jones, et al., 1956; Harder, 1960; Whitfield, 1975). The hydraulic conductivity values for the massive single sand of the Chicot aquifer range from 1500 to 2520 gpd/ft^2, with an average value of 1810 gpd/ft^2 for four wells, JD-242, Ev-1, Ve-134 and Ve236 (Jones, et al., 1956). They range from 660 to 1520 gpd/ft^2 for 200-foot sand, with an average of 1275 gpd/ft^2 for 6 testing wells, from 930 to 1950 gpd/ft^2 for 500-foot sand, with an average of 1165 gpd/ft^2 for 20 testing wells, and from 1070 to 1360 gpd/ft^2 for 700-foot sand, with an average of 1240 gpd/ft^2 for 6 testing wells. (Harder, 1960).

The groundwater in the Evangeline aquifer generally flows downdip toward the south. This can be seen from the potentiometric surface map of Whitfield (1975, plate 2). As discussed previously, there are many interbedded clay beds in the Evangeline aquifer. They impede the vertical movement of water and impart a predominantly lateral direction of movement to the water as it moves downgradient (Whitfield, 1975) even through vertical head differences exist. The hydraulic head increases with depth throughout the study area (Whitfield, 1975) as observed at well Be386 and Be422 (Figure 4.2). This head difference causes the water in the Evangeline aquifer to follows a generally upward stairstep path across beds of sand, silt and clay toward areas of natural discharge into the overlying Chicot aquifer in southern Calcasieu Parish as reported by Whitfield (1975), even through the Evangeline aquifer may receive water input from the Chicot aquifer in most part of the area as indicated by the cross section (Figure 4.2).

4.3 Defining Flow Paths

For this preliminary study, two flow paths, one for the Chicot aquifer and the other for the

Evangeline aquifer, have been defined for further studies described in chapters 6, 7, and 8. Flow paths of groundwater can be determined by potentiometric contour lines. Groundwater flows in the direction which is perpendicular to potentiometric lines. Flow path 1, Be375 --> Be439 --> Be447 --> Cu829 --> Cu1040, is shown on Figure 4.3, which is a potentiometric surface map, constructed with data in 1974, for the selected area. Flow path 2, which was based on the potentiometric surface map (Plate 2, Whitfield, 1974), Be371 --> Be422A --> Be386B --> Be447B is chosen similarly to path 1 from the Evangeline aquifer.

The screened positions of wells along the flow paths have been put on the stratigraphic profile (Figure 4.2).

5. Sediment Mineralogy

5.1 Introduction

The chemical composition of groundwater is controlled in large part by chemical reactions occuring between source water and minerals in the aquifer. In order to understand chemical evolution processes of groundwater, we must know the mineral composition of the sediments. We also need to know if there are any dissolution and/or precipitation features occurring on sediment surfaces. These can help us constrain thermodynamic calculations and mass balance calculations.

5.2 Sources of Samples

An extensive collection of cuttings from boreholes penetrating freshwter aquifer systems in Louisiana was made available to the project by G.C. Cardwell, formally of the U.S.G.S.
(Rest of this section in preparation)

5.3 Techniques

Based on the nature of the available sediment samples, a variety of analytical techniques will be used in this study.

5.3.1 Binocular microscope observation. Because most of the sediments are sand size, it is useful to go through some samples using binocular microscope. It can help me to establish some stratigraphic profiles, identify some existing minerals, look for any fossils and any other features, and pre-check if the sample is suitable for other analyses.

5.3.2 SEM analysis. Scanning electron microscope will be used in this study. The purposes of using this method are: (1) looking for dissolution and precipitation features on the sand grain and clay surfaces; (2) semi-qualitatively determining what minerals have been dissolved or precipitated by using EDS.

5.3.3 X-ray diffraction analysis. X-ray diffraction method will be used for bulk sediment and clay mineral analysis. It can be used to determine mineral compositions of clays. Clay minerals play very important roles in modifying groundwater compositions.

5.4 Results

Mineral compositions of the sediments have not been yet analyzed, however, such analyses should be done in the future in order to better understand the natural geochemical controls on the groundwater compositions. As an example of the type of information which can be extracted from examination of the sediments, however, Figure 5.1 is a preliminary stratigraphic profile constructed by binocular microscope analysis for well Cu789. Its detailed description is given in table 5.1. Both figure 5.1 and table 5.1 show that the individual sand beds in the Chicot aquifer coarsen upward.

Jones, et al. (1956) give somewhat more detailed example for well Al157 in Allen Parish. Their study on the well indicated (Jones et al., 1956, table 4) that the mineral composition of Pleistocene sediments is composed of quartz, feldspar, mica minerals, some dark minerals, and some iron minerals, e.g. magnetite, siderite, marcasite and pyrite. The mineral assemblage at different depth seems to be different with some preference. For example, with depth increases, iron minerals seem to change their composition in the sequence of magnetite-siderite-marcasite-pyrite.

5.5 Discussion

(In preparation)

5.6 Summary

(In preparation)

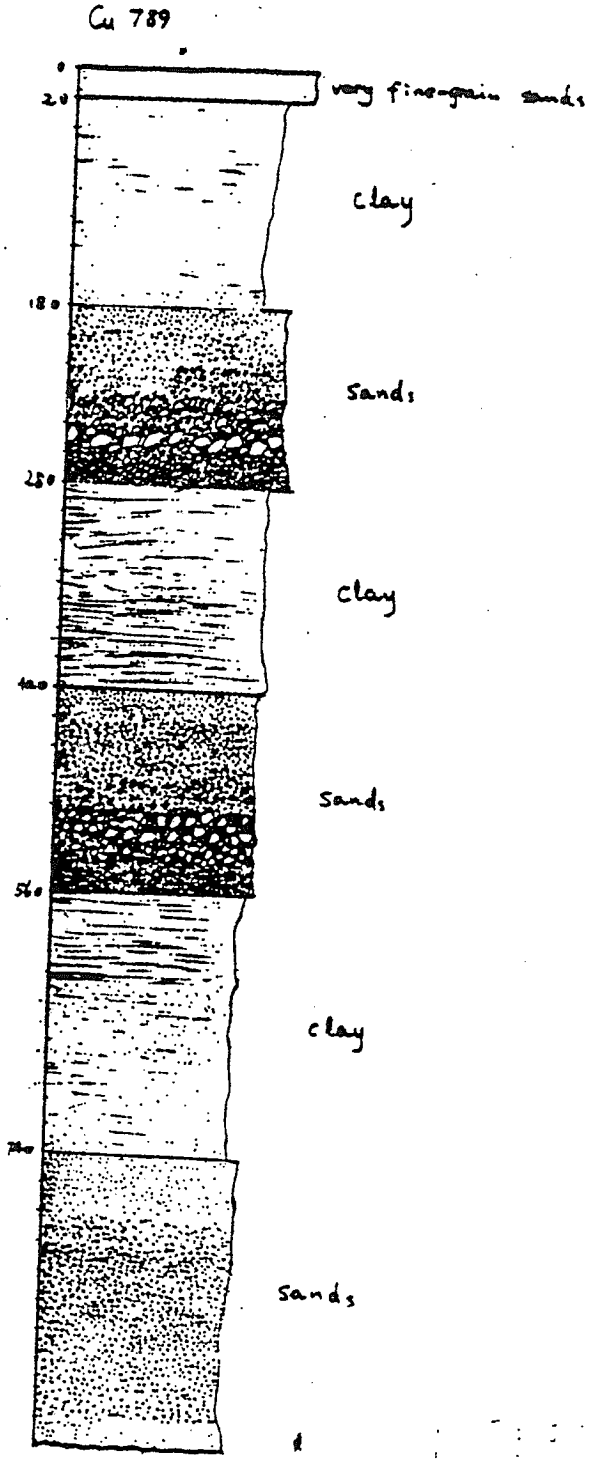

Figure 5.1 Stratigraphic Column for Well Cu-789. It shows the relative grain size.

Table 5.1 **Lithologic Description of sediments of the well Cu-789 in Calcasieu parish:**

Depth (ft)	Description
0 - 20	Very fine-grain sand ($\phi \sim 0.5$mm). Most are clear quartz (> 90%). Some quartz grains were stained to brown. Some dark minerals and a few hemitite grains. no fossils have been found. Some cemented grain cluster.
20 - 40	Gray color clay.
40 - 60	Gray color clay. some black organic materials.
60 - 80	Light color clay with some fine-grain sand. no organics materials.
80 - 100	Same as the above interval but more sand. Color become yellowish.
100 - 120	Light color clay with sand. some fossilized plant roots.
120 - 140	Same as the above interval.
140 - 160	Gray color clay with sand.
160 - 180	Well sorted rounded clear sand ($\phi \sim 1$ mm). most quartz. few stained grains. some dark minerals and redish grains. Some cemented grain cluster.
180 - 200	Similar to the above interval, but sizes of grains are large ($\phi \sim 2$ mm). most are clear quartz. some dark minerals. Almost all grain are well rounded and have smooth surfaces.
200 - 220	Similar to the above interval but less well sorted. Sizes are even larger ($\phi \sim 1.5$ - 2.5 mm). Some new formed minerals on surfaces of large grains.
220 - 240	Similar to the above interval but larger grain sizes. ($\phi = 1$ - 4 mm). Well rounded.
240 - 260	Poorly sorted coarse-size sands ($\phi = 1$ - 10 mm). There are some new formed minerals on the surfaces.
260 - 280	Poorly sorted sands with clay ($\phi = 0.1$ - 3 mm) , rounded. most quartz. some dark minerals. Some quartz grains were stained to brownish. Some cemented grain clusters.
280 - 300	Light color clay with some sands.
300 - 320	Same as the above interval.
320 - 340	Gray color clay. less sandy than the above interval.
340 - 360	Gray color clay.
360 - 380	Gray color clay. Some fossilized plant roots. more sandy than the above intervals.
380 - 400	Same as the above interval
400 - 420	Same as the above interval.
420 - 440	Well-sorted rounded fine-grain sands ($\phi < 0.5$ mm) with some clay. most are quartz. Some quartz grains were stained to brownish. Some dark minerals. A couple of biotite grains. Some cemented grain clusters. No fossils have been founded.
440 - 460	The same as the above interval, but sizes of grains are larger ($\phi = 0.5$ - 1 mm).
460 - 480	Same as the above interval. some redish clear and greenish minerals.
480 - 500	Most grain sizes are around 1 mm, but a few are larger than 3 mm. Most are quartz, but some dark minerals. Some fossils plant remains. Very smooth grain surfaces. Some cemented grain clusters.

(Table 5.1 Continued)

500 - 520	Coarse size poorly sorted sands (f = 3 - 10 mm), rounded. Some surface show new formed minerals.
520 - 540	Poorly sorted sands (f = 1 - 10 mm), rounded. Grain sizes are generally smaller than those of the above interval.
540 - 560	Poorly sorted sands (ϕ = 2 - 5 mm) and clays. Some plant fossils.
560 - 580	Light color clay with sands. Some plant fossils.
580 - 600	Same as the above interval.
600 - 620	Same as the above interval.
620 - 640	Most clay, some very fine sands. More sandy than the above interval.
640 - 660	Most clay, some sands. Some plant fossils (grass roots).
660 - 680	Gray clay. Some sands. Some plant fossils.
680 - 700	Gray clay. More plant fossils than the above interval. Some other fossils remains (bones or shells).
770 - 720	Same as the above interval.
720 - 740	Light color clay. More sandy than the above interval. Some plant and shell fossils.
740 - 760	Very fine sands (ϕ < 0.5 mm). Some clay. Sands are well sorted and rounded. Most sands are quartz. Some dark minerals. No fossils. Some cemented grain clusters.
760 - 780	same as the above.
780 - 800	Fine-grain sands (ϕ = 0.5 - 1 mm). Well sorted. few stained quartz. Some dark monerals. Some cemented grain clusters.
800 - 820	Well sorted fine-grain sands (ϕ~ 1mm). Most quartz but some dark minerals. There are some hemetite grains existing. Some stained quartz grains. No fossils.
820 - 840	Well sorted sands (ϕ ~ 1mm). Most clear quartz, some dark minerals. Hemetite has not been founded. Few quartz grains were stained. Some cemented gram clusters.
840 - 860	same as the above interval, but grain sizes are larger and sands are moree clear than the above interval.
860 - 880	Well sorted fine-grain sands (ϕ ~ 0.5mm). Most are quartz, but some dark minerals. A few quartz grains were stained. Some cemented gram clusters. No fossils.
880 - 900	Same as the above interval, but one piece of fossil shell has been found.
990 - 920	Sorted fine-grain rounded sands (ϕ = 0.5 - 1 mm) with some clays. Most quartz, but some dark minerals. Some fossilized plant remains.
920 - 940	Fine-grain sands. Most quartz, some dark minerals, biotite. A few stained quartz grains. No fossils. Several pieces of clay.

Some Comments on the Sediment Samples:

1. It is difficult to observe any authigenic minerals through binocular microscope.
2. There are some clay samples.
3. There are some cemented grain clusters, which may be useful for SEM analysis.
4. On grain surfaces, there are some new-formed minerals or evidences of dissolution, which could be observed by SEM.

6. Water Chemistry

6.1 Introduction

The general water quality of the Chicot aquifer and the underlying Evangeline aquifer has been studied by many researchers (Jones, et al., 1956; Harder, 1960; Whitfield, 1975; Nyman, 1989). No studies have been done to date on the isotopic composition of the groundwater. There are no studies which have compared the water chemistry of the Chicot aquifer and the Evangeline aquifer with each other, even though the different chemical characteristics of the water in these two aquifer were observed. Although the present study is mainly focused on the Chicot aquifer, the Evangeline aquifer will be included also because the Chicot aquifer may receive water recharge from the underlying Evangeline aquifer (Jones, et al. (1956); Whitfield, 1975).

6.2 Sources of data

The water quality data used in the first phase of this study are unpublished data from the U.S. Geological Survey. These data cover a period of time from 1940 to 1989 in age and all four seasons of the year.

There is little information on the chemical variations of groundwater within a single well with time. One available well, Be378, does show significant variations of the groundwater composition with time (Table 6.1). The sources of these variations are not yet known but may include differences in flow rate and reaction time between water and sediments as a result of hydraulic head changes because of pumping, seasonal variations of natural water recharge, and sea level rising. Surface water pollution, which may be caused by waste disposal and agricultural usage of pesticide, could also change the quality of shallow groundwater. Changes in analytical methods and their accuracy over time can also affect the consistancy of water quality data.

Future data will come from samples which will be taken in the field as part of this project.

6.3 Previous studies

A description of the chemical composition of fresh groundwater from the Chicot aquifer and adjacent aquifers has been reported by Nyman (1989), Jones, et al. (1956), Harder (1960), Whitfield (1975). The groundwater in the Chicot aquifer changes from an acid, low-solute, corrosive water to a slightly alkaline, calcium-bicarbonate type (Nyman, 1989). Further downdip in the aquifer, the Ca-HCO_3 type water is changed to a Na-HCO_3 type water. No studies on the vertical variation of groundwater composition have been done. Nyman (1989) considered such variation in the Chicot aquifer is small.

6.4 Present field study

6.4.1 Purpose. A field study has been planned for 1993-1994 in September, 1993. (Rest of section in preparation)

6.4.2 Techniques. Water samples will be taken in the field from well heads because it is impossible to sample water directly from wells at depth in the screened interval. The following procedures will be followed:

---Fill up two 1000 ml plastic bottles with water. All procedures below will use the water from these bottles.

---Fill up a 100 ml plastic bottle to half with water from one of the big bottles, then use Pt combination electrode to measure the Eh of the water. Similarly, use pH meter to measure the pH and temperature of the water. NH3 should also be measured in the similar way with a NH3 electrode.

---Fill up a 125 ml plastic bottle fully with unfiltered water; then cap the bottle tightly without any bubbles in it. Label it and store the bottle in a cooler for alkalinity measurement with HCl titration back to the lab in the same day.

---Fill up a 250 ml plastic bottle with unfiltered water, put in 20 ml 1 N ZnCl2 for preservation of sulfide. Cap the bottle tightly, label it, and store in the cooler for the same day lab titration for

6.1

Table 1. The chemical composition of water sample Be-378 of different time:

Year	pH	Alk.	Ca	Mg	Na	K	Cl	SO4	SiO2	Fe	Fe	F
							(mg/l)					
1984	6.7	61	11	4.0	43	2.4	28	0.4	33	2.6	0.1	0.3
1985	6.6	54	14	6.5	35	2.0	36	4.6	53	2.4	0.3	0.3
1986	6.2	54	15	6.1	35	1.5	39	15.0	61	3.3	0.2	0.3
1988	6.2	56	14	6.5	39	1.9	38	9.5	33	3.1	0.2	<0.2
1990	7.5	71	15	5.0	41	2.3	30	<0.2			0.1	0.2

6.2

Table 2. Chemical compositions of samples for the selected flow pathin the Chicot Aquifer:

Well#	Distance	pH	Alk.	Ca	Mg	Na	K	Cl	SO4	SiO2	Fe	Mn	F
	(km)							(mg/l)					
Be375	0	6.2	18	3	0.8	9.9	1.9	7.2	2.0	46	0.01	0.00	0.0
Be439	10	6.4	18	3.7	0.9	13	2.4	9	1.0	46	1.40	0.07	0.1
Be447	37	7.1	37	15	1.3	19	2.7	16	6.6	45	3.00	0.31	0.1
Cu829	64	7.1	65	22	4.6	28	3.1	24	3.4	57	0.33	0.34	0.3
Cu1040	88	7.4	98	37	8.6	37	2.8	31	3.6	44		0.29	0.0

sulfide with Iodometric method.

---Filter the water through 0.45 mm filter paper.

---Fill up two 125 ml plastic bottles with filtered water. One of them will be acidified with several drops of concentrated HCl to pH value of about 2 for cation analyses. The unacidified bottle will be used for anion analyses.

---Fill up two 50 ml glass bottles with filtered water. The one to be used for C isotope analysis, will have HgCl2 powder added for killing organisms. The other bottle is for O and H isotope analysis.

---Fill up a 500 ml plastic bottle with filtered water for Sr isotope analysis.

6.4.3 Results. (In preparation)

6.5 Spatial variations in water composition

Table 6.2 lists water compositions of samples along the selected flow path. As groundwater moves downdip the aquifer, pH, alkalinity, Ca, Mg, Na, K and Cl generally increase, and sulfate, Fe, and Mn increase initially then decrease while SiO_2 remains less varable. It is interesting that the peak value of Fe appears ahead of Mn peak value Figure 6.1, not the reversed order as given by Champ and others (1979). All these changes could partially be results of mineral dissolution, precipitation and/or redox reactions. For example, dissolution of minor amount of gypsum can increase of both sulfate and Ca concentrations of the groundwater, however, reduction of sulfate will result in decrease of sulfate in the groundwater. Reducing sulfate will produce sulfide, which can decrease Fe concentration in the water by precipitation of some kinds of iron sulfides, such as pyrite and marcasite. Indeed, mixing with downdip more saline water could also change groundwater chemistry. This possibility has not be tested in this study because this study mainly deals with fresh water.

(Rest of this section in preparation)

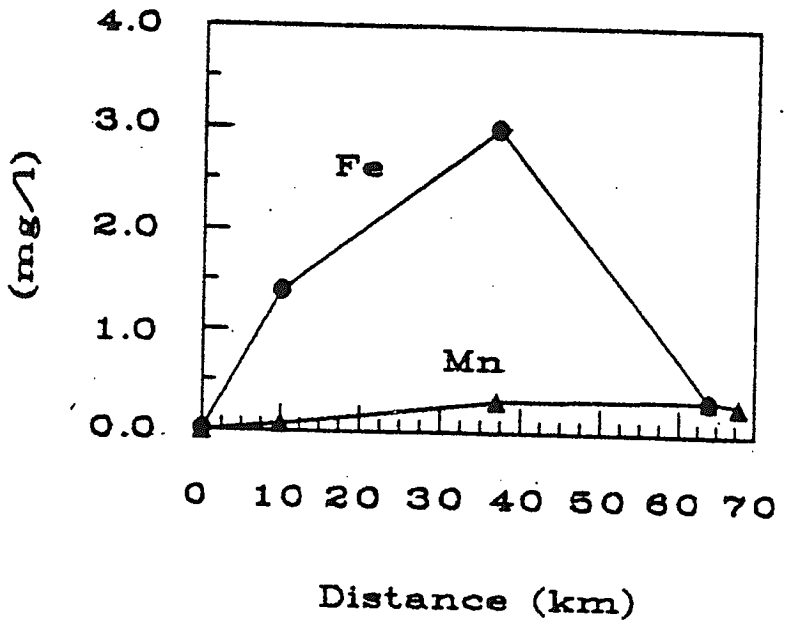

Figure 6.1 The concentrations of Fe and Mn in groundwater of the Chicot aquifer change downdip the aquifer. Both of them show peak values. The peak of Fe appeared earlier than that of Mn.

6.6 Comparison with other groundwater systems

The chemical compositions of groundwater in the Chicot aquifer are are very different with those of water in the underlying Evangeline aquifer. Figure 6.2 shows a series of diagrams of the chemical character plots for both the Chicot and the Evangeline aquifer. The HCO_3/Cl and Na/Cl ratios for samples from the Evangeline aquifer are much larger than those from the Chicot aquifer. Mg/Ca values of samples from the Evangeline aquifer are generally smaller than those from the Chicot aquifer. However, plots of HCO_3 versus Ca are interesting. Water in the Evangeline can be divided into two types based on HCO_3/Ca ratio, one is low, similar to the water in the Chicot aquifer, which may be result of mixing near the contact of these two aquifer which has not been tested, and the other is high. Similar results are also seen for Ca versus Na. Waters with high HCO_3/Ca ratio may be low in Ca/Na ratio. This may be the result of ion-exchange on the interdedded clay surface. As discussed previous, the Evangeline aquifer was marine in origin and contains many interbedded clays. These marine clays may have large amount of exchangeable Na (Chapter 5, Drever, 1988), which can be exchanged by Ca in groundwater. These diagrams may suggest that two types of reaction paths exist in the aquifer, which lead two types of water, even though the source waters are similar. Further study is needed to distinguish them.

Although there are no previous reports on the vertical variations of water chemistry in the Chicot aquifer, vertical variations of water compositions in the Evangeline aquifer have been found in this study. Vertical changes of water chemistry for some wells whose samples were obtained from different depths can be seen in Table 6.3. The pattern of variations is not clear. These variations may be caused by hydrological property differences among different layers separated by discontinued clay layers and/or the location of the aquifer, which can bring some advection and dispersion effects on the chemistry of water as well as reaction time. For example, the place or layer with coarse sands may have high flow velocity, therefore, the chemical composition of water there will be highly affected by advection and the reaction time between water and sediments is shorter than that with low flow velocity. Its chemical compositions will differ from adjacent places or layers where the flow velocities are lower. Variations in mineral composition could be another

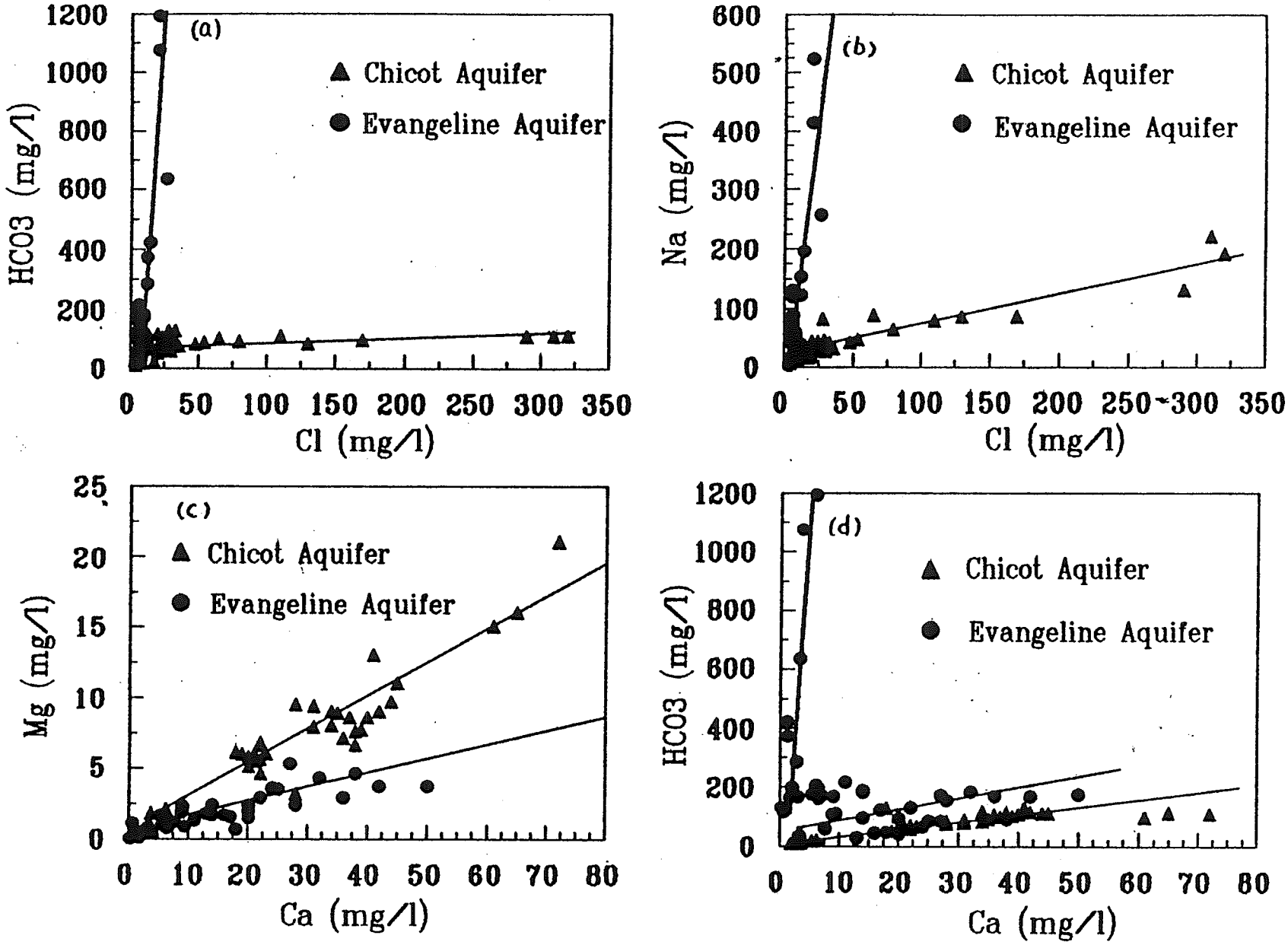

Figure 6.2 Chemical characters of groundwater plots for both the Evangeline aquifer and the Chicot aquifer.

Table 6.3 The chemical composition of water changes with depth in the Evangeline Aquifer

Well ID#	Depth(ft)	T (C)	pH	Cl	HCO3	SO4	Na	Ca	Fe
						(mg/l)			
Al-263A	484-494	21.5	8.3	13.0	127	2.4	54	1.3	0.24
Al-263B	839-849	23.5	8.4	5.4	179	2.2	75	0.6	0.36
Al-263C	1212-1222		8.5	5.2	230	8.2	97	0.4	0.06
Al-267A	575-585	22.0	7.8	4.9	152	7.2	56	4.0	0.87
Al-267B	700-710	22.0	7.5	5.9	145	5.6	43	13.0	0.37
Al-267C	1200-1210	25.0	7.8	8.2	167	7.2	60	7.8	0.25
Be-386A	375-386	22.0	7.3	12.0	106	4.4	37	8.8	1.20
Be-386B	590-600	23.5	7.1	8.1	166	3.6	60	3.0	0.26
Be-386C	1325-1335	27.0	8.2	7.9	181	6.6	54	14.0	0.36
Ev-682A	405-419	21.5	6.9	17.0	243	1.8	91	6.0	0.28
Ev-682B	765-780	24.0	7.6	98.0	786	2.2	360	1.9	0.87
Ev-695A	468-488	22.0	7.5	18.0	369	0.0	150	2.7	0.17
Ev-695B	658-678	23.5	7.9	62.0	500	0.0	228	2.0	0.11
Ev-698A	453-463		8.3	113.0	234	5.2	114	28.0	0.05
Ev-698B	996-1006	25.0	8.0	38.0	355	0.0	164	1.6	0.05
Ev-710A	525-535		7.8	128.0	493	0.0	242	15.0	0.17
Ev-710B	667-677	23.5	7.7	172.0	536	0.0	311	5.5	0.10
Ev-710C	774-784	24.0	8.6	223.0	648	0.2	399	2.5	0.35
Ev-716A	342-351	21.0	8.4	20.0	338	0.0	50	61.0	0.61
Ev-716B	448-457	22.0	8.3	23.0	314	0.2	50	50.0	1.10
Ev-716C	650-669	23.5	8.1	199.0	592	0.0	340	9.2	0.74

Table 6.4 The chemical compositions of samples for the selected flow path in the Evange line Aquifer

Well ID#	Danstance	pH	HCO3	Ca	Na	Mg	K	Cl	SO4	F	SiO2	Fe
	(km)						(mg/l)					
Be371	0.0	6.8	130.0	22.0	24	2.9	1.8	6.7	5.00	0.1	44	0.4
Be422A	17.5	6.9	46.3	16.0	18	1.7	2.1	5.5	2.60	0.2	39	0.4
Be386B	40.0	7.1	166.0	3.0	60	0.6	12.0	8.1	3.60	0.6	19	0.3
Be447B	50.0	7.6	165.0	1.8	120	0.1	1.8	6.0	0.40	1.6	13	0.2

possibility causing these variations. Study of sediment mineralogy will help to resolve these questions.

The change of chemical composition of groundwater in the Evangeline aquifer along any entire flow path, from recharge area to discharge area, is unknown because of present lack of data. However, such changes along a portion of flow path selected in this study can be seen in Table 6.4 which lists chemical analytical data for selected samples. It shows that pH, HCO_3^-, Na^+, and F^- generally increase as water moves downdip in the aquifer along the flow path while Ca^{2+}, Mg^{2+}, SO_4^{2-}, SiO_2 and Fe decrease. For HCO_3^- and SO_4^{2-}, the data for sample Be422A are suspicious because they appear to be too low, which may suggest that Be371 or Be422A is not on the flow path because of stratified properties in the Evangeline aquifer. Figure 4.2 has shown that Be 371 or Be422A may be relatively lower spatially in the aquifer than the others.

7. Thermodynamic Controls on Fluid Compositions

7.1 Introduction

The chemical composition of groundwater is largely the result of chemical and/or biochemical reactions between water and surrounding materials. These reactions include mineral hydrolysis reactions, isotope reequilibration reactions, and bacterial-mediated redox reactions.

7.2 Techniques

(Inpreparation)

7.3 Bacterial-mediated redox reactions

(In preparation)

7.4 Mineral hydrolysis reactions

Thermodynamic calculations in this study have been done by SOLMINEQ88, licensed to Dr. Hanor. This program has been used in this study for speciation and saturation index (SI) calculations. Because this is a shallow aquifer, pressure variations are small. Pressure has been assumed to be 105 Pa, the same as the surface pressure. Although this assumption is not true, however, the errors generated by such treatment are small enough to be neglected.

Figures 7.1a, 7.1b, 7.1c and 7.1d are plots of SI, saturation index, with respect to some common minerals, vs. distance. Figure 7.1a shows SI values of the groundwater with respect to calcite and dolomite. The groundwater is undersaturated with respect to both minerals in the entire segment of the flow path. As the groundwater is moving downdip, it is reaching the equilibrium state with respect to these carbonate minerals, which may be the results of calcite and/or some other Ca-containing mineral dissolution, and/or oxidation of organic materials, which will increase P_{CO_2} of water.

Figure 7.1b indicates the groundwater is supersaturated with respect to both quartz and

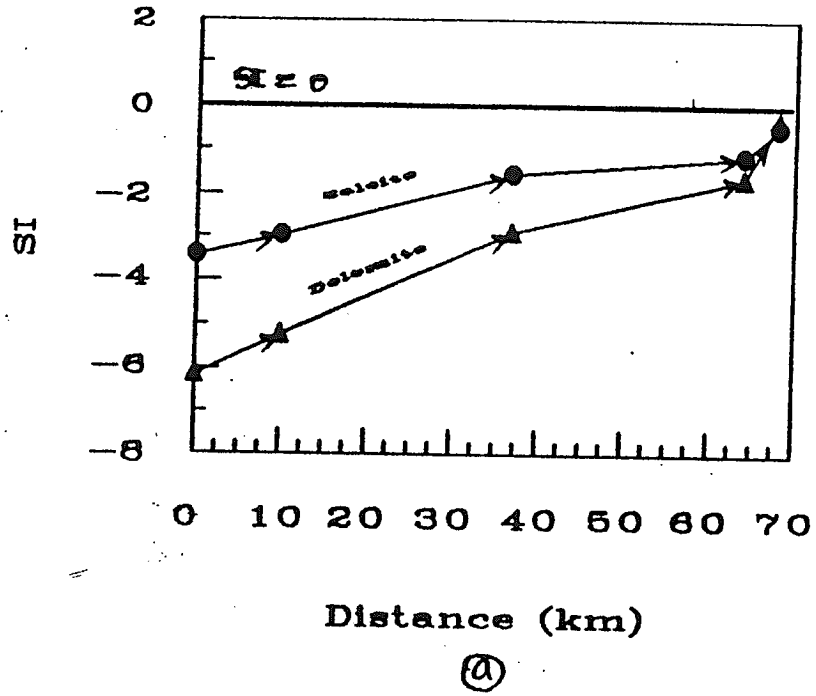

(a)

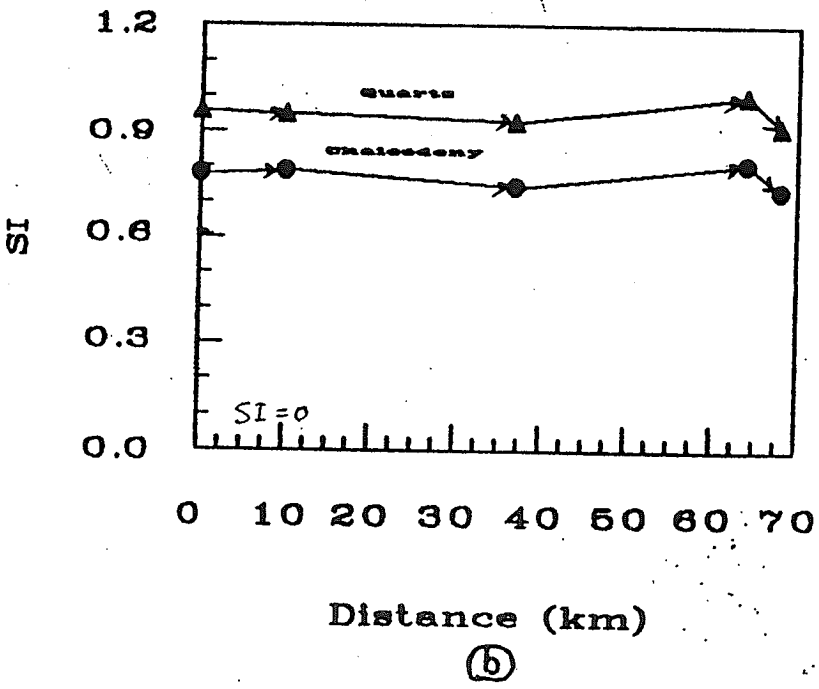

(b)

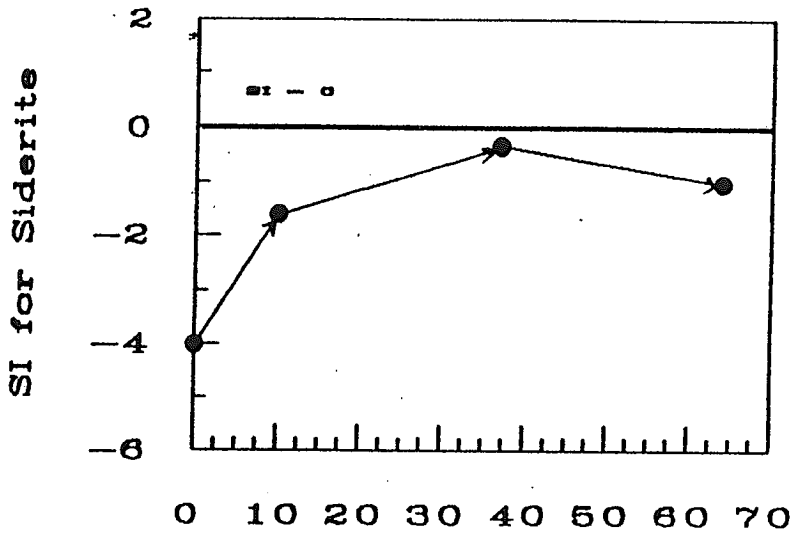

(c)

Figure 7.1 SI plots vs. distance for carbonate minerals (a), SiO_2 minerals (b) and siderite (c).

chalcedony, but undersaturated with respect to amorphous silica(Figure 7.2). Quartz and/or chalcedony can precipitate from the groundwater everywhere in this segment of the flow path. Quartz cements have been found in sediments of well A1157 (Jones, et al., 1956). The supersaturation of the groundwater with respect to quartz and chalcedony may be caused by kinetic factors. It suggests that these two minerals are not buffering minerals in the system. It is interesting why and how SiO_2 remains, more or less, constant in the system. Further investigation is needed to answer this question.

All selected samples are undersaturated with respect to siderite (Figure 7.1c). As groundwater moves downdip the aquifer, its SI value with respect to siderite increases initially, due to increase of HCO_3 and Fe concentrations, then decreases, due to removal of Fe by precipitation of pyrite. Figure 7.1c shows groundwater is approaching the equilibrium state with siderite even though none of samples is in apparently equilibrium with siderite. There are two possible cases concerning siderite. First, siderite has experienced precipitation at some place along the flow path. It may be at a point or a segment between Be439 and Be447 or between Be447 and Cu829, which has been missed for this study. The other possibility is that groundwater has never achieved equilibrium with siderite, therefore, no siderite has been precipitated from the groundwater. Field investigation (Jones, et al., 1956) supports the first possibility because secondary siderite has been found in sediments of the aquifer.

Figure 7.2a and 7.2b are activity-activity plots. These diagrams may suggest that groundwater reaches equilibrium with kaolinite as results of dissolution of K-spar and albite. As dissolution continues, groundwater reaches equilibrium with K-spar and Na-smectite. Then groundwater has been buffered by kaolinite-K-spar and kaolinite-smectite. Pyrite has also been precipitated in this stage as indicated by decrease of Fe on Figure 6.1.

Based on the above discussion, we may conclude the reaction sequence along this selected flow path can be divided into two zones:

Zone 1 (from Be375 to Be439, then to Be447)

Dissolution of K-spar, albite, calcite and gypsum;

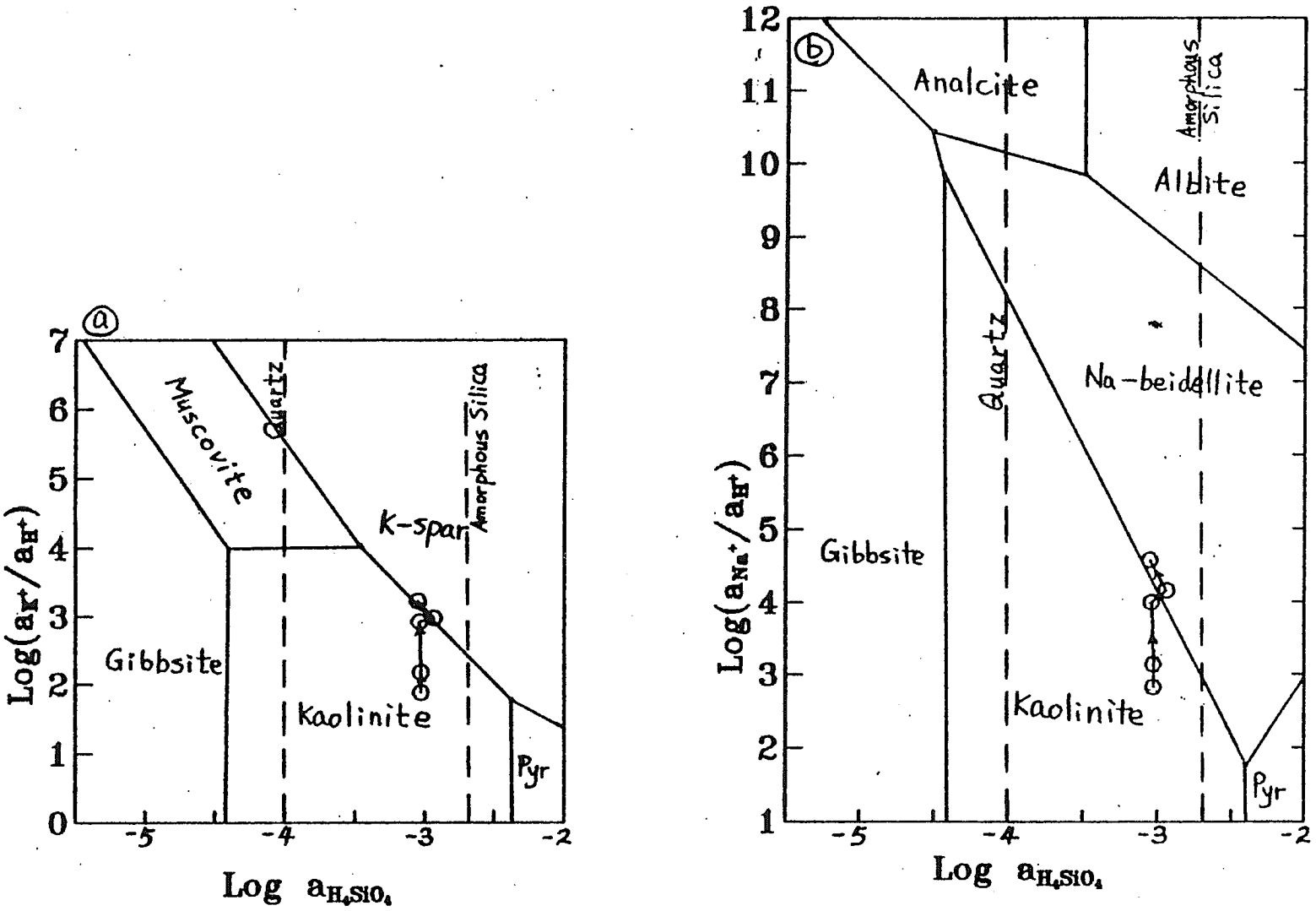

Figure 7.2 Activity-activity phase diagrams, and plots for samples of the selected flow path 1.

Precipitation of kaolinite;

Reduction of magnetite;

Possible precipitation of siderite, around Be447.

Zone 2 (from Be447 to Cu829, then to Cu1040)

Dissolution of albite and calcite;

Two buffering reactions:

$$K\text{-spar} + Al^{3+} + 2H_2O = Kaolinite + K^+ + SiO_2 + 2H^+$$

$$Smectite + 1.33H^+ + 0.33H_2O = Kaolinite + 0.33Na^+ + 0.33Al^{3+} + 1.67SiO_2$$

Reduction of sulfate;

Precipitation marcasite and/or pyrite.

Besides these reactions, some other minerals could also be involved in reactions, either precipitation or dissolution. For example, dissolution of biotite can used to explain progressive increase of K, Mg in the groundwater. Some of SiO_2 should also be precipitated out of the groundwater because of its supersaturation in the water. This reaction sequence may only be one of several possibilities which are responsible for chemical changes of the groundwater.

7.5 Kinetic factors

(In preparation)

7.6 Comparison with other groundwater systems

The thermodynamic calculations for samples from the Evangeline aquifer have also been done in the same way for samples from the Chicot aquifer. Results of the calculations have been plotted on figure 7.3a and 7.3b, which are SI plots vs. distance for SiO_2 minerals and carbonate minerals, respectively. Log Na^+/H^+, log K^+/H^+, and log Ca^{2+}/H^{+2} vs. log H_4SiO_4 have been plotted on figure 7.4a, 7.4b and 7.4c, respectively.

Figure 7.3a shows that the SI values with respect to all SiO_2 minerals are decreasing due to decreasing of SiO_2 concentration of the fluid that may be caused by precipitation of some kind of

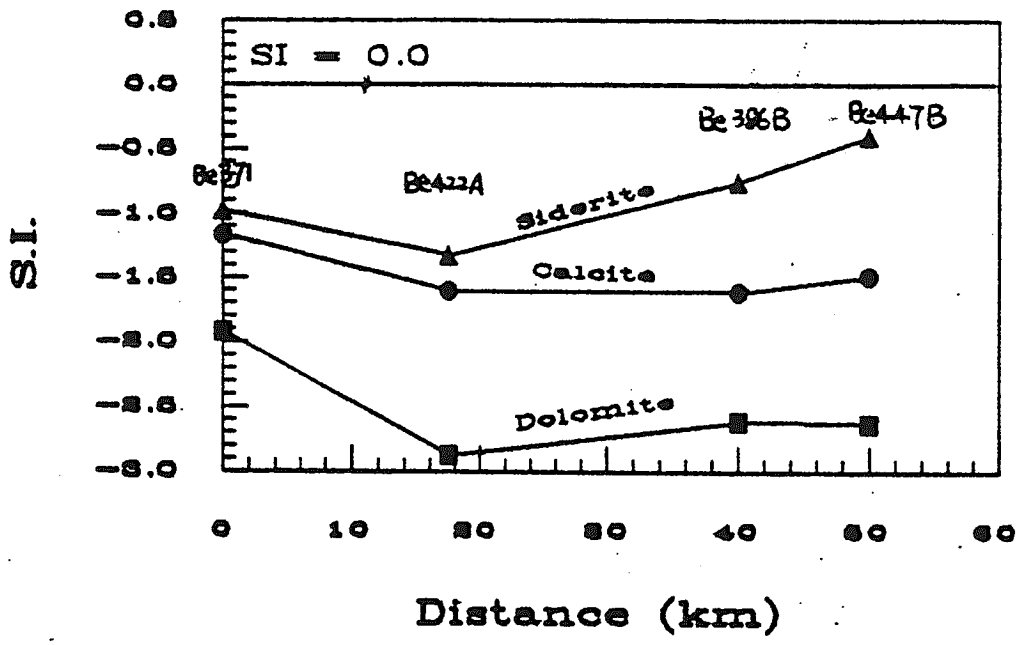

(b)

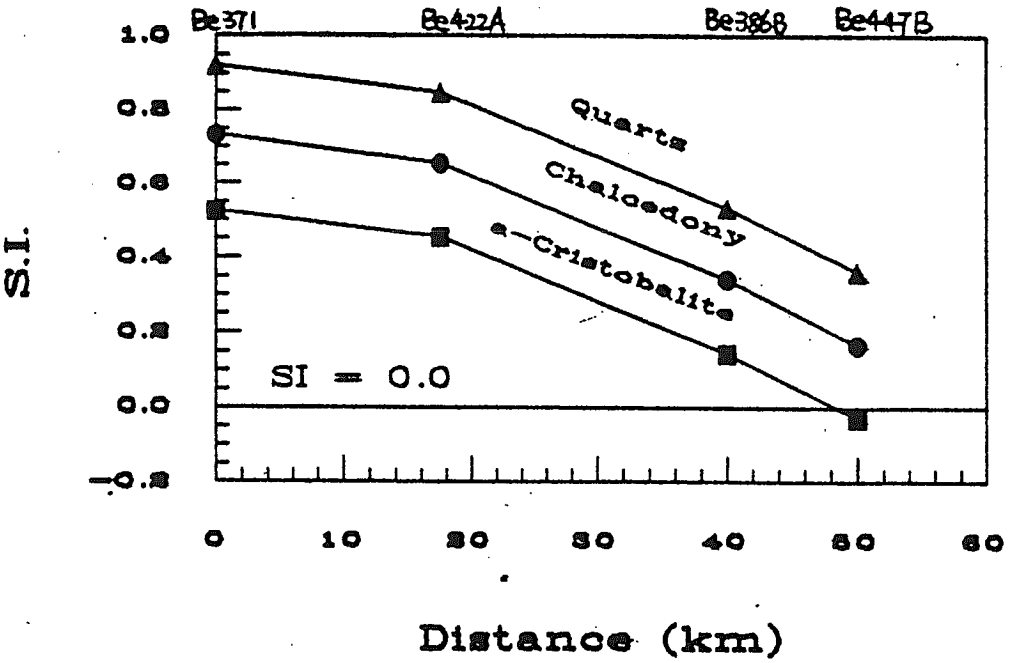

(a)

Figure 7.3 SI vs. Distance along the flow path 2
For Samples from the Evangeline Aquifer.

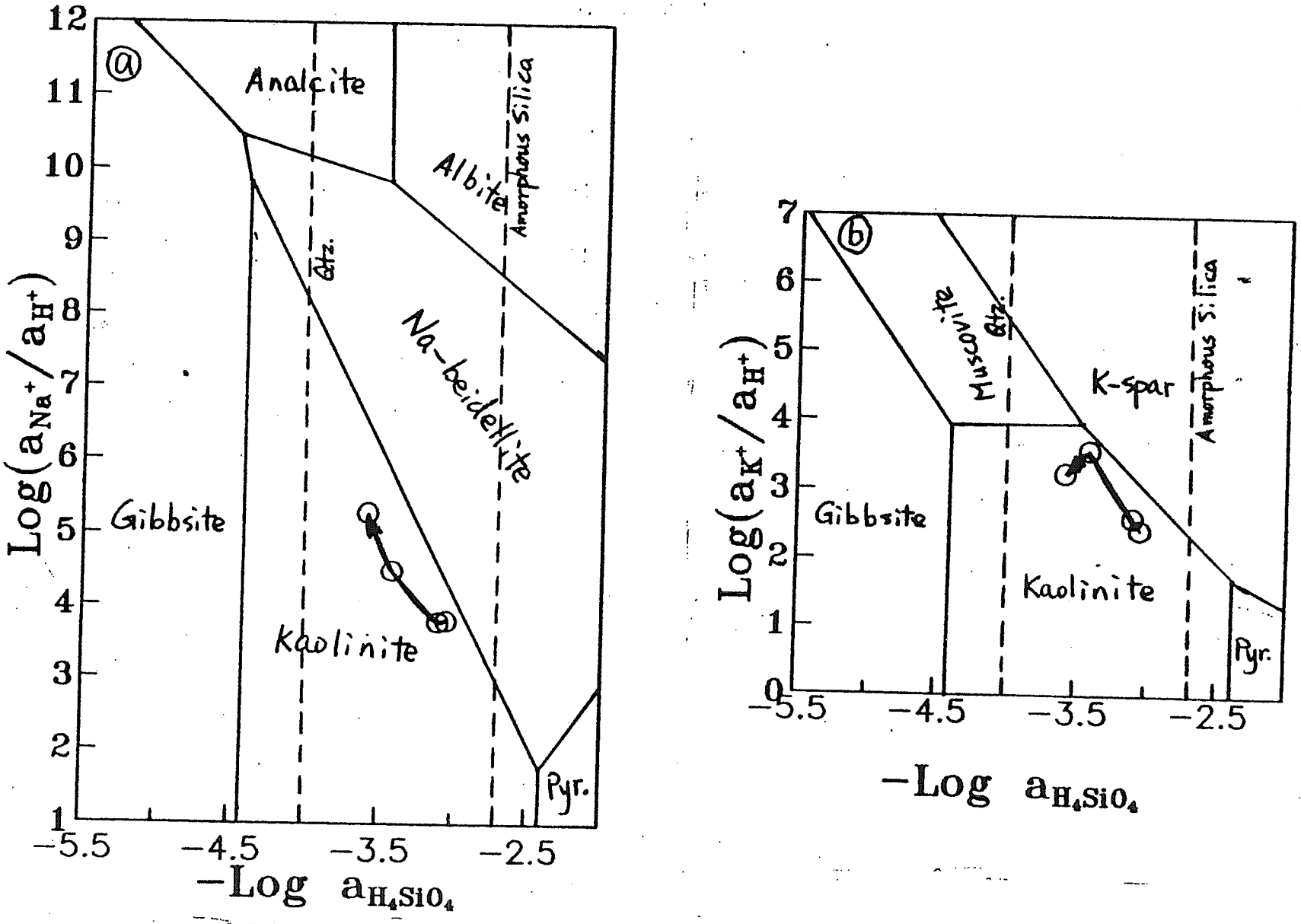

Figure 7.4 Activity - activity phase diagrams for Samples from the Evangeline Aquifer.

SiO_2 mineral or silicates. From Figure 6a, one could conclude that the fluid composition is not buffered by any of these SiO_2 minerals because their SI values with respect to these minerals are all continuously decreasing, not staying on the equilibrium line, as water moving down gradient.

Figure 7.3b suggests that the groundwater in this portion of flow path is undersaturated with respect to calcite, dolomite, and siderite. Therefore, precipitation of any one of these minerals is unlikely.

Activity-activity diagrams have been constructed as Figure 7.4a, 7.4b, and 7.4c. These figures indicate that kaolinite is one of important buffering minerals in the system. Most of plots are in the kaolinite field. Na-smectite and K-spar may also be buffering minerals (Figure 7.4a and 7.4b). These minerals should be included in the later mass-balance calculation.

7.7 Summary

(In preparation)

8. Solute Mass Balance Calculations

Mass-balance calculations have been done in this study with a spread-sheet program similar to the one of Hanor (1993). Several constraints were put on such calculations based on all above discussions. Table 8.1 lists all reactions included in the program.

The results are shown in table 8.2. These results generally agree with the above discussions. In the discussion which follows, the mineral names refer to minerals used in the mass balance model. Reactions which involve these phases are model reactions, which may be different from actual field reactions. Mass balance calculations support the model hypothesis that quartz or chalcedony is being precipitated out the system throughout the entire segment of the flow path. So are albite, calcite and biotite. In zone 2, smectite is being dissolved. As a buffering pair, kaolinite is, therefore, being precipitated. However, K-feldspar is being precipitated rather than dissolved as suggested by the other buffering mineral pair, kaolinite-Kspar. This may due to biotite dissolution, which produces K^+. Gypsum is continuously dissolving in the entire segment of the flow path except for only one sample, which may be due to data errors. Fluorite dissolves initially, then precipitates as Ca^{2+} continues to built up due to dissolution of calcite.

In terms of redox reactions, model magnetite has been reduced in zone 1. This reduction process is responsible for increase of aqueous iron ion (figure 6.1). However, reduction of sulfate in zone 2 produced sulfide, which has removed Fe^{2+} from the groundwater (Figure 6.1) by forming pyrite (or some kinds of iron sulfide) as indicated in the mass-balance calculation.

This mass-balance calculation is one of several possibilities. The accuracy of this calculation dependents on the selection of mineral assemblage and related reactions as well as on the accuracy of water analytical data. Because our current knowledge on the mineral composition of the sediments in this aquifer is very limited, results of the above mass-balance calculation should be used cautiously. Further investigation on the mineral composition of sediments in the aquifer will be done as part of this project.

Table 8.1 Minerals and Reactions used in the Mass-Balance Calculation:

Zone 1	(Be375 -> Be439 -> Be447)
Halite	$NaCl = Na^+ + Cl^-$
Calcite	$CaCO_3 + H^+ = Ca^{2+} + HCO_3^-$
Quartz	$SiO_2 = SiO_2^0$
K-spar	$KAlSi_3O_8 + 4H^+ = K^+ + Al^{3+} + 3SiO_2^0 + 2H_2O$
Albite	$NaAlSi_3O_8 + 4H^+ = Na^+ + Al^{3+} + 3SiO_2^0 + 2H_2O$
Biotite	$KMg_3AlSi_2O_{10}(OH)_2 + 10H^+ = K^+ + 2Mg^{2+} + Al^{3+} + 3SiO_2^0 + 6H_2O$
Kaolinite	$Al_2Si_2O_5(OH)_4 + 4H^+ = 2Al^{3+} + 2SiO_2^0 + 5H_2O$
Fluorite	$CaF_2 = Ca^{2+} + 2F^-$
Gypsum	$CaSO_4 \cdot 2H_2O = Ca^{2+} + SO_4^= + 2H_2O$
Magnetite	$2Fe_2O_3 + CH_2O + 7H^+ = 4Fe^{2+} HCO_3^- + 4H_2O$
Zone 2	(Be447 -> Cu829 -> Cu1040)
Halite	$NaCl = Na^+ + Cl^-$
Calcite	$CaCO_3 + H^+ = Ca^{2+} + HCO_3^-$
Quartz	$SiO_2 = SiO_2^0$
K-spar	$KAlSi_3O_8 + 4H^+ = K^+ + Al^{3+} + 3SiO_2^0 + 2H_2O$
Albite	$NaAlSi_3O_8 + 4H^+ = Na^+ + Al^{3+} + 3SiO_2^0 + 2H_2O$
Biotite	$KMg_3AlSi_2O_{10}(OH)_2 + 10H^+ = K^+ + 2Mg^{2+} + Al^{3+} + 3SiO_2^0 + 6H_2O$
Kaolinite	$Al_2Si_2O_5(OH)_4 + 4H^+ = 2Al^{3+} + 2SiO_2^0 + 5H_2O$
Na-Smectite	$Na_{0.33}Al_{2.33}Si_{3.67}O_{10}(OH)_2 + 7.33H^+ = 0.33Na^+ + 2.33Al^{3+} + 3.67SiO_2^0 + 4.67H_2O$
Fluorite	$CaF_2 = Ca^{2+} + 2F^-$
Gypsum	$CaSO_4 \cdot 2H_2O = Ca^{2+} + SO_4^= + 2H_2O$
Pyrite	$FeS_2 + 4H^+ + 4HCO_3^- = 4CH_2O + 2SO_4^= + Fe^{2+}$

Table 8.2 Results of Mass Balance for the Selected Flow Path1 in the Chicot Aquifer:

Minerals	Be375->Be439	Be439->Be447A	Be447A->Cu829	Cu829->Cu1040
	mole/kg H_2O			
Halite	-6.49E-5	-1.83E-4	-2.26E-4	-1.98E-4
Quartz	1.79E-4	1.38E-4	3.02E-4	6.96E-4
Kaolinite	3.46E-5	6.76E-5	3.08E-4	2.49E-4
Na-smectite			-2.20E-4	-1.55E-4
Albite	-7.00E-5	-7.77E-5	-9.33E-5	-1.43E-e
K-felfspar	-1.20E-5	-2.19E-6	3.50E-5	6.25E-5
Biotite	-8.23E-7	-5.48E-6	-4.52E-5	-5.49E-5
Calcite	-2.23E-5	-2.23E-4	-1.07E-4	-3.68E-4
Fluorite	-2.63E-6	0.00	-5.27E-6	7.90E-6
Gypsum	1.04E-5	-5.83E-5	-6.23E-5	-1.39E-5
Magnetite	-1.24E05	-1.43E-5		
Pyrite			4.78E-5	5.91E-6

Note: "+" sign means forming the mineral; "-" sign means destroying the mineral.

9. Integrated Numerical Modeling of Advection, Dispersion, and Reaction

(In preparation)

10. Summary and Conclusions

(In preparation)

11. Acknowledgments

(In preparation)

12. References

(Partial)

Champ, D.R., Gulens, J., and Jackson, R.E., 1979, Oxidation-reduction sequences in ground water flow systems: Canadian Journal of Earth Sciences, vol. 16, p.12 - 23.

Coleman, J.M., and Roberts, H.H., 1991, The Mississippi River Deposition System: A model for the Gulf Coast Tertiary, in An Introduction to Central Gulf Coast Geology, New Orleans Geological Society, 99 -122p.

Drever, J.I., 1988, The Geochemistry of Natural Waters. Prentice Hall, Englewood Cliffs, N.J., 437p.

Freeze, R.A., and Cherry, J.A., 1980, Groundwater. Prentice-Hall, Englewood Cliffs,N.J.,604 p.

Fisk, H.N., 1938, Geology of Grant and LaSalle Parishes: La. Dept. Conserv. Geol. Bulletin No.10, 246p.

Fisk, H.N., 1944, Geological Investigation of the Alluvial Valley of the Lower Mississippi River: U.S. Dept. Army, Mississippi River Comm., 78p.

Hanor, J.S. and McManus, 1988, Sediment alteration and clay mineral diagenesis in a regional ground water flow system, Mississippi gulf coastal plain: Transactions- Gulf Coastal Association of Geological Societies, Volume XXXVIII, p. 495 - 502.

Harder, A.H., 1960, The Geology and Ground-water Resources of Calcasieu Parish, Louisiana: U.S.G.S. Water-Supply Paper 1448, 102p.

Jones, P.H., Hendricks, E.L., and Irlan, B., 1956, Water Resources of Southwestern Louisiana: U.S.G.S. water-Supply Paper 1364, 460p.

Lee, R.W., 1985, Geochemistry of Groundwater in Cretaceous Sediments of the Southeastern Coastal Plain of Mississippi and Western Alabama: Water Resources Research, v. 21(10), p. 1545-1556.

Nyman, D.J., 1984, The Occurrence of High Concentrations of Chloride in the Chicot Aquifer System of Southwestern Louisiana: Louisiana Department of Transportation and Development, Office of Public Works Water Resources Technical Report 33. 75p.

Nyman, D. J., 1989, Quality of water in freshwater aquifers in Southeastern Louisiana: Louisiana Department of Transportation and Development Water Resources Technical Report No. 42. 22p.

Nyman, D.J., Halford, K.J., and Martin, Jr., A., 1990, Geohydrology and Simulation of Flow in the Chicot Aquifer System of Southeastern Louisiana: Louisiana Department of Transportation and Development Water Resources Technical Report No. 50. 58p.

Whitfield, M.S., 1975, Geohydrology of the Evangeline Aquifer and Jasper Aquifer of Southwestern Louisiana: Water Resources Bulletin, No. 20, 72p.

13. Appendices

(In preparation)

APPENDIX B

Hydrogeochemistry of a hazardous waste landfill, Southwestern Louisiana

Shaobing Su
Department of Geology and Geophysics
Louisiana State University
Baton Rouge, Louisiana 70803

Note: The research described in this appendix represents the results of the first year of an M.S. thesis research project being conducted by Ms. Su. The purpose of this report is to outline the long-term goals of this research and to document what has been completed during the 1992-93 period of funding by the Department of the Interior, U.S. Geological Survey, through the Louisiana Water Resources Research Institute. It should be understood that portions of the text which follows are preliminary in nature and some phases of the project are not yet complete. The figures referred to in the text are in the process of being drafted and will be included in the final thesis.

Hydrogeochemistry of a Hazardous Waste Landfill, Southwestern Louisiana

Shaobing Su

1.0 Introduction

The importance of groundwater resides in the fact that groundwater accounts for over 90 percent of the fresh water in the U.S., and more than 40 percent of the U.S. population use groundwater for drinking (McCarty et al., 1984). It is also estimated that between one and two percent of the shallow subsurface is contaminated. Today's challenges related to the protection of groundwater resources are of three kinds: (1) prevention of the introduction of contaminants into aquifers, (2) prediction of the behavior of contaminants once they have entered aquifer systems, (3) removal the contaminants from the aquifers so as to protect effectively the biosphere (U. S. National Academy of Sciences Geophysics Study Committee, 1984).

Since World War II, there has been a tremendous growth in the manufacture and use of synthetic chemicals. Many of these chemicals have contaminated water supplies. The most serious is the threat to groundwater from waste chemical dumps and landfills, storage lagoons, treating ponds, and other facilities. The primary environmental concern regarding hazardous wastes in the geosphere is the possible contamination of groundwater aquifers by waste leachates and leakage from wastes.

Figure 1. Sources, disposal, and movement of the hazardous in the geosphere.

There are a number of possible sources. The most obvious one is leachate from landfills containing hazardous wastes. In some cases, liquid hazardous material is placed in lagoons and can leak into aquifers.

The transport of contaminants in the groundwater depends largely upon hydrological factors governing the underground movement of water and the interactions of hazardous waste constituents with geological strata, particularly unconsolidated earth material.

Figure 2. Plug- flow of hazardous wastes in groundwater.

Groundwater contaminated with hazardous wastes tends to flow as a relatively undiluted plug or plume along with the ambient groundwater in an aquifer. The rate of flow is generally relatively slow, one meter per day would be considered fast.

1.1 Ground water contamination in the United States

Sources of ground water contamination vary throughout the United States. On a regional basis, the major sources of groundwater contamination are as follows (Pye and Kelley, 1984): (1) Northeast (New England, New York, New Jersey, Pennsylvania, Maryland, and Delaware): septic tanks, landfills, highway deicing, and abandoned oil wells. (2) Northwest (Colorado, Idaho, Montana, Oregon, Washington, and Wyoming): dry land farming, irrigation return flow, septic tanks, buried pipelines, and storage tanks. (3) Southeast (Alabama, Florida, Georgia, Mississippi, North Carolina, South Carolina): underground storage tanks, landfills, surface impoundments, and accidental spills. (4) Southcentral (Arkansas, Louisiana, New Mexico, Oklahoma, Texas): mineralization from the soluble components of the aquifer matrix, over-pumping, and disposal of oil field brines. (5) Remainder of States (Great lakes, North Central, Alaska, Hawaii): not known.

1.2 Hazardous waste disposal in the Louisiana Gulf Coast (LAGC)

Louisiana is one of the largest generators of hazardous waste per capita in the United States and is a recipient of large volumes of hazardous waste generated by other states and

countries (Reams et al., 1993). In 1987, Louisiana ranked number one in the nation in the per capita generation of hazardous waste (see appendix: Table 1.).

The quality of water in Louisiana's major aquifer systems on a regional basis remains excellent. As evidenced by the testing done by the U.S. Geological Survey and public water distribution systems, the deep aquifers, from which the majority of the State's drinking water is obtained, still remain free from contamination. Of specific concern in Louisiana, however, are the shallow aquifers and water-bearing zones. These strata, which have been shown to contribute significantly to the water recharge of deep aquifers, are becoming increasingly threatened (Nyman et al., 1989).

Sources of possible shallow ground water pollution in Louisiana include: active, inactive, and abandoned hazardous waste sites; waste impoundments of the petroleum industry; pipelines used for transmission of natural gas, crude oil, saltwater brine, and other fluids; leaking underground storage tanks and pipelines; injection wells and other underground control facilities; abandoned wells, solid waste sites; urban and suburban discharge (runoff, septic tanks); agricultural chemicals and animal wastes (Alan Plummer and Associates, Inc., 1984).

The State of Louisiana, under the DEQ (Department of Environment Quality), IASD (Inactive and Abandoned Sites Division), has identified 506 potential hazardous waste sites. 25 percent of these sites are oil waste sites, 19 percent are landfill sites, and 4 percent are hazardous waste disposal sites (DEQ, 1990) (see appendix, Table 2.).

Petrochemical manufacturing is the primary source of hazardous waste generated in Louisiana (Trudeau, in press). Landfills and impoundments constructed in clay have been typical places to dispose hazardous waste because clay has been regarded as an impermeable barrier to the migration of all fluids (Cramer,1988). The surficial clays should act as barriers to prevent contamination of ground water under such waste sites. However, of the 60 hazardous waste sites monitored by the State in 1985, at least half had

ground water contamination problems. The site that first confirmed this situation in Louisiana is located in Calcasieu Parish (Cramer, 1988) and is the subject of this project.

Overview contamination concerns in Calcasieu Parish include salt water intrusion; solid and hazardous waste sites, brine disposal sites, surface impoundments, and other sources, such as leaking underground storage tanks, improper well installation, and closure, improper liner placement, and agricultural sources such as improper use of pesticides, and septic tanks.

1.3 Importance of subsurface geology and hydrogeology in understanding contaminant transport.

Knowledge of subsurface geology, hydrology, and the chemistry of contaminants is essential for understanding the natural chemical and physical processes which control groundwater quality. And reliable and quantitative predictions of contaminant movement can be made only if we understand the physical processes controlling transport, and the chemical reactions that affect concentrations of contaminants in the subsurface.

1.4 Previous studies of contaminant transport in the Louisiana Gulf Coast

1.4.1 Previous studies at the Calcasieu facility

Several previous studies have been made at the Calcasieu site. Hanor and others (1986) studied the geochemistry and distribution of selected chemical contaminants, and sediment mineralogy. Trudeau (in press) developed a cross-sectional groundwater flow model to investigate the relation among the geohydrology, water levels, and groundwater flow. The flow model results showed that a groundwater time of travel through the surface clay comparable to the observed contaminant time of travel cannot be achieved without the use of unreasonably high recharge rates and groundwater flow. His study also described the use of a numerical simulation model to analyze the groundwater flow system. Cramer

(1988) studied the same site and indicated that both the depositional and post-depositional environment of a soil can greatly alter its in-situ permeability by providing preferential pathways for contaminants migration. BFI (Browning Ferris Industries) and their consultants have generated annual groundwater reports which include groundwater quality data, soil boring logs, field organic vapor and gas chromatographic analysis, hydrogeologic data, and descriptions of remedial activities.

1.4.2 Previous study at other hazardous waste sites in Louisiana

Recently, Hanor (in press) studied the effective hydraulic conductivity of fractured clay beds at a hazardous waste landfill in the southeastern Louisiana Gulf Coast. His study showed that intercalated sands and zones of pedogenic secondary porosity and fracturing developed during periods of subaerial weathering are apparently the dominant controls on vertical permeability, not the matrix properties of the clay.

1.5 Purposes of this study

The primary purposes of this study are as follows: (1) To understand the subsurface geology and hydrology of the waste site. By using available geotechnical and geohydrological data, several groundwater flow cross-sections can be made to characterize the site. (2) To understand the spatial variation in chemical composition of pore fluids at the site. Available water quality analysis are used to define two-dimensional variation of major cations, anions, redox sensitive metals, and several priority organics. (3) To understand the controls on the groundwater geochemistry. By evaluating the saturation states of the pore fluids with sedimentary mineral phases known to be present in the groundwater system, the extent to which the water compositions are being buffered by water-rock equilibria can be established. (4) To establish the redox and pH regime at this site and understand effects of variation in Eh and pH on water chemistry. (5) To predict

contaminant transportation patterns using numerical simulation, and compare the results with field data .

2.0 Description and history of the Willow Springs site

2.1 Location of Willow Springs site

The CEOS International, Inc. facility of lake Charles, also known as the Browning - Ferris Industries Willow Springs facility, is located 10 miles (16.1 km) northwest of Lake Charles (Meyer & Associates, Inc., 1988), and approximately 1500 feet (457.2 m) north of Willow Springs Road in Calcasieu Parish, Louisiana. Little River and the west Fork of the Calcasieu River are located to the north and northeast of the facility (Woodward-Clyde Consultants, 1982).

Figure 3. Map of the site.

2.2 Oil and gas production at site

(In preparation.)

2.3 Disposal of hazardous waste

Waste disposal activities at the site began in 1968 by Mud Movers, Inc.. Several large surface impoundments were constructed by excavating trenches to a depth of 8 feet (2.4 m).

Figure 4. Map showing location of lagoons.

Around each impoundment boundary, the excavated dirt was piled just outside the trench to build a dike which formed the lagoon (Woodward-Clyde Consultants, 1983). These large impoundments were used for the storage of a variety of industrial liquid wastes. These wastes included oils, sludge, and brines from oil field production waste, American Petroleum Institute (API) separator wastes, petrochemical and refinery waste, as

well as other inorganic and organic by-product materials. In this manner, liquid waste was ponded on the natural ground surface to a depth of about 6 to 8 feet (1.8 m to 2.4 m) (Hanor et al. 1986).

BFI acquired Mud Movers, Inc. this 80-acre (3.2×10^5 m^2) site, and site operations began in 1972. In 1976, BFI converted an abandoned oil well existing on site to a deep-injection disposal well. At that time, dewatering operations began on the existing waste lagoons, and the liquids were disposed of by deep-well injection (Woodward-Clyde Consultants, 1983). Upon completion of dewatering operation, sludges and oils remained on the lagoon bottoms.

Landfill operations began in 1977. The sludges and oils were solidified with kiln dust, and the solids were disposed. In chronological order, lagoons 5, 6, 4, 3 and 9 (see Figure 4.) were solidified in place and clay capped (Woodward-Clyde Consultants, 1983). In 1992, waste management activities conducted on this site included absorbent solidification (using fly ash) of industrial liquid and semi-solid waste, secure landfill disposal of bulk and containerized industrial solid wastes, and deep well injection disposal of predominately aqueous industrial liquid wastes.

2.4 Waste characterization

(1) Leachate from the leachate collection system of landfill cell 3 (at the west of the site) was collected in May 1980 and February 1982 and analyzed for a total of 32 chemical constituents (Woodward-Clyde Consultants, 1983). This leachate is nearly neutral with respect to pH and has relatively low concentration of heavy metals. Chloride concentration and conductivity are relatively high as is concentration of certain other constituents such as calcium, sulfates, sodium, and magnesium.

(2) Equalization basin (at north of the site) liquids are acidic with pHs ranging from 2.6 to 3.4. Chloride concentrations are in the range of 3,000 to 7,000 ppm. Concentrations of metal ions are relatively high as compared to the landfill cell 3 leachate. Also, the

variability of the chemical character of the equilization basin liquid is less than that of liquids from cell 3 leachate.

No organic chemical analyses of these wastes are available for this site. The suspected and potential sources of organic priority pollutants include the following. Waste oils disposed of in the lagoons are presumably generated from crude oil, which contains monocyclic aromatics such as benzene, and polycyclic aromatic hydrocarbons such as naphthalene (Murray and others, 1984). The API separator sludge is denser than water and contains monocyclic aromatics such as phenol and benzene, and polycyclic aromatic hydrocarbons such as naphthalene (Brown and others, 1983). Petroleum refinery waste contains a broad range of organic priority pollutants including monocyclic aromatics, halogenated aliphatic hydrocarbons, pesticides, phthalate esters, polycyclic aromatic hydrocarbons, and nitrosamine and others (Hanor et al, 1986).

2.5 Monitoring and remediation

Since early 1982, more than twenty monitor wells have been installed in "50-foot pervious zone" as well as in "200-foot zone" (Figure 5.). By 1988, operations at the site were limited to use of the receiving basins, the equilization basins, and the injection well. Recovered contaminants were separated into solids and liquids. The liquids were placed in the injection well, and the solids were transported to the CECOS Livingston site for disposal (Meyer & Associates, Inc., 1988).

Figure 5. Map showing location of monitor wells.

These monitor wells were also used as hydraulic control for developing potentionmetric maps and cross sections across the site. Two areas of contamination have previously been identified at the site: (1) shallow contamination in the northeast corner area, and (2) the

latent contamination beneath the original lagoon areas extending into the "50-foot pervious zone." (Woodward-Clyde Consultants, 1983).

The overall remedial action is to prevent contaminant movement by minimizing infiltration and other driving forces such as heavy meteoric precipitation. Since late 1983, several remedial actions were undertaken at the site. These have included improved capping and drainage, elimination of surface water ponding and reduction of surface water infiltration. At the northeast corner, trenches were excavated in both east-west and north-south directions to characterize the areal distribution of the contamination. Later remedial action includes: continued ground water monitoring and data evaluation, and a health risk assessment (Woodward-Clyde consultants, 1983).

The overall effectiveness of the recovery activities were summarized in a 1992 annual report (Triegel & Associates, Inc., 1992). It claims that the recovery system in the northeast corner and in the vicinity of the closed impoundments has been effective in retrieving both dissolved and oily phase volatiles. The pumping wells have produced an inward gradient which covers the area of known contamination, and is intended to prevent organics from leaving the site. Improved cap over the former impoundments and the existing recovery well system are intended to prevent contaminants from reaching the 200-foot sand in the future.

2.6 Present Status

The present status of the site presented here are based on information collected from Triegel & Associates, Inc., 1992 annual report. Contaminants at this site are in several forms: (1) oily contaminants in soils presented to a depth of 30 feet (9.1 m) below the ground surface; (2) solidified wastes residing in the closed lagoons; (3) dissolved contaminants present in the shallow and 50-foot zones, and in one well in the 200-foot zone. In the northeast corner of the site, contaminants are in groundwater and occasionally, as a dense immiscible oil which is confined to the bottom of the silt layer due

to density differences with the groundwater. In addition, contaminants in the northeast corner will not migrate toward and discharge to the Little River (GeoTrans report, 1989). As discussed previously, the recovery system in the site is claimed to be effective in retrieving both dissolved and oily phase volatiles.

3. Subsurface Geology

3.1.1 Regional geology

Southwestern Louisiana is underlain in large part by deltaic plain deposits of late Pleistocene and Recent or Holocene age. They were either deposited on land as a part of river deltas, or they were deposited close to the shore around the margins of the deltas on the continental shelf. These deposits comprise a thick sequence of southerly and southeasterly dipping interbedded gravels, sands, silts, clays. However, these unconsolidated deposits constitute only a thin upper veneer overlying the many thousands of feet of older strata which fill the Gulf Coast Geosyncline.

Figure 6. Generalized geological map of Southwestern Louisiana.

Table 3. Stratigraphic column for the area.

3.1.2 Local geology

Most of the 80-acre (3.2×10^5 m^2) site is immediately underlain by 35 to 50 feet (10.7 to 15.2 m) of Pleistocene age silty clays and clays with occasional discontinuous thin sand or silt lenses prior to encountering the "50-foot pervious zone" below.

In the northeast corner of the site, at a lower elevation adjacent to the Little River, the near surface soils consist of more recent Holocene deposits which vary from clays and silty clays to clayey silts and sandy silts. The more silty and sandy soils are not encountered over the entire area but are often observed at depths of about 14 to 25 feet (4.3 to 7.6 m) below the ground surface.

The thin "50-foot pervious zone" generally consists of sandy silts and clayey silts with occasional layers of silty sands and sands and may be continuous across the site. This "50-foot pervious zone" is typically underlain by clays, silty clays and sandy clays extending to a depth of 75 to 80 feet (22.9 to 24.4 m) below ground surface, below which the "200-

foot" sand is encountered and extends to about 150 to 160 feet (45.7 to 48.8 m) below the ground surface. A clay or silty clay underlies the "200-foot" sand.

3.2 Sources of data and techniques

Knowledge of the subsurface geology and hydrology is essential for understanding the natural chemical and physical processes which control the groundwater quality. Information from soil borings have been used here to determine the subsurface geology.

Over 250 subsurface borings have been drilled at the site. Wells with L-prefix are BFI Master boring wells. Wells with MW-prefix are BFI monitor wells. Wells with Cu-prefix are USGS wells. Correlation of the USGS numbering system with BFI site numbering is presented in the appendix (Table 4.).

Figure 7. Map showing location of log boring.

About 117 subsurface boring logs are available for this site. They are: well L-78 to L-175, L-93 to L-196, L-208, L-217, and L-219 of BFI master borings; MW-35 to MW-47 (except MW-37 and MW-40) of BFI monitor wells; Cu-939, Cu-941, and Cu-1220 of USGS wells.

Three major groups of sediment have been used in this study to represent the subsurface lithology. They are sand, silt and clay. For each well, the subsurface lithology was recorded form the log information available. Other important information was also noted at the corresponding depth. This includes joints, slickensides, roots and wood, organic matter, oil spots and pockets, oily sheen, and calcareous and ferrous nodules. The subsurface distribution of sediment types was made by correlating similar lithologies.

3.3 Cross-sections and maps

By reviewing the hydrogeological and geochemical information available at the site, two cross-sections were chosen to represent the subsurface geology of the site. Cross-section AA' is from north-northwest off the site to south-southeast off the site (which later on will be referred to cross-section AA' from south to north), Cross-section BB' extends southwest of the site to northeast of the site. The choice of specific wells on the cross sections is based on the availability of log information, water level information, and geochemical information.

Cross-section AA' includes the following wells: L-148, L-142, L-37, L-124, L-125, L-38, L-207, Cu-908, L-209, L-96, Cu-881, Cu-907, Cu-906, L-153, L-218, Cu-874 and Cu-1220 from north to south. This cross section is parallel to the ground water flow direction.

Cross-section BB' extends southwest of the site to northeast of the site. Cross-section BB' includes the following wells: L-103, MW-45, MW-31, L-195, L-108, L-169, MW-18, L-82, MW-41, Cu-936, L-211, MW-35, MW-36 and L-87 from southwest to northeast. Cross-section BB' is perpendicular to the ground water flow direction.

Figure 8. Map showing locations of cross-sections through the site.

Figure 9(a). Map of simplified geologic cross-section AA' through the site.

Figure 9(b). Map of simplified geologic cross-section BB' through the site.

On the basis of these cross-sections, most of the site is underlain by 25 to 50 feet (7.6 to 15.2 m) of clays and silty clay with occasional discontinuous thin sand and silt lenses. The average clay thickness is about 40 feet (12.2 m). In the northeast corner of the site, because of the low surface elevation adjacent to the Little River, the clay layer is as thin as 5 feet (1.5 m) below ground surface. The more silty and sandy layers are observed at depths of about 10 to 25 feet (3.0 to 7.6 m) below ground surface, but these layers are not encountered over the entire area, and the thickness of these layers varies. In the northeast

corner of the site, there is a shallow zone, consisting of silt layers, with a thickness of about 10 feet (3.05 m). The 50-foot zone is encountered about 35 feet (10.7 m) below the ground surface, with a thickness varying from a few feet to more than 30 feet (9.4 m). This thin "50-foot pervious zone" generally consists of silt with occasional layers of sand and is continuous across the site. Under this pervious zone are alternating layers of clay, silt, and sand. The "200-foot" sand is encountered approximately 80 to 145 feet (24.4 to 44.2 m) below the ground surface. A clay or silty clay underlies the "200-foot" sand (see cross-sections AA' and BB').

It is important to note that at depths of about 5 to 20 feet (1.5 to 6.1 m) below the mean sea level, there are post-deposition structural fractures such as joints, slickensides over the entire site. This may represent preferential pathways for groundwater and contaminants to move downward.

Figure 10(a). Important subsurface characters at cross-section AA'.

Figure 10(b). Important subsurface characters at cross-section BB'.

3.4 Comparison with previous studies

3.4.1 This site

Trudeau (unpublished) made two cross-sections at this site in his 1986 studies. Cross section AA' of this study has the same location as Trudeau's cross-section AA'. Comparing these two cross-sections, the majorities of the subsurface geology of the site under cross-section AA' are similar with difference in detail. In Trudeau's cross-section, only two types of lithologies are noted, one was clay, another was silt and sand. Also, this study has noted more detailed subsurface geological characteristics, especially the important subsurface structures which implied important information about the migration of fluid as well as contaminants.

The west section of cross-section BB' of this study is similar to west section of cross-section DD' of TAI's study (Triegel & Associates, Inc., 1993), while east part of cross-section BB' of this study was more north oriented than east part of cross section DD' of TAI's. The choice of cross-section is dependent on the information (logs boring, water level, and geochemistry) available. Thus, most of western part of these two cross-sections are similar, with differences in detail. The eastern part of these two cross-sections are also similar. The contribution of this study is the more detailed subsurface structural characterization.

3.4.2 Other sites in the Louisiana Gulf Coast

Recently, Hanor (in press) completed a geological research at a hazardous waste landfill in southeastern Louisiana. Comparing the subsurface geology of his study to this study, similarities and differences are noted.

Table 5. Similarities and differences of Hanor's study and this study.

It is important to point out that both Hanor's and this study showed that an important type of heterogeneity consists of laterally-correlational pedogenic features (Retallack, 1988) within the clay section of both sites.

3.4.3 Other study in the United States

(In preparation)

3.5 Summary

The Calcasieu Facility contains closed secure landfill cells, closed surface impoundments, existing surface basins, storage tanks, and a deep injection disposal well. (Triegel & Associates, 1992). Most of the 80-acre (3.2×10^5 m^2) site is underlain by 25 to

50 feet (7.6 to15.2 m) of Pleistocene age clays and silty clay with occasional discontinuous thin sand and silt lenses. The average clay thickness is about 40 feet (12.2 m). In the northeast corner of the site, due to the low surface elevation adjacent to the Little River, the clay layer is as thin as 5 feet (1.5 m) below ground surface. The more silty and sandy layers are observed at depths of about 10 to 25 feet (3.0 to 7.6 m) below ground surface, but these layers are not encountered over the entire area, and the thickness of this layer varies. In the northeast corner of the site, there is a shallow zone consisting of silt layers, with thickness about 10 feet (3.0 m). The 50-foot zone is encountered about 35 feet (10.7 m) below the ground surface. Its thickness varies from few feet to more than 30 feet (9.1 m). This thin "50-foot pervious zone" generally consists of silt with occasional layers of sand and is continuous across the site. Under this pervious zone are alternating layers of clay, silt, and sand. The "200-foot" sand is encountered approximately 80 to 145 feet (24.4 to 44.2 m) below the ground surface. A clay or silty clay underlies the "200-foot" sand.

It is important to note that at depths about 5 to 20 feet (1.5 to 6.0 m) below the mean sea level, there are post depositional structural fractures such as joints, slickensides over the entire site. These may provide preferential pathways for groundwater and contaminants to move downward.

4. Hydrology

4.1 Introduction

Using available water level information, the potentiometric field was made and the general direction of groundwater flow in "50-foot pervious" zone was determined to be from northwest to southeast. Conditions in the eastern part of the site are more complex, with groundwater flow from north, northeast to the south. Figure 11(a) and 11(b) show the position of the water table in the two study cross sections

Figure 11(a). Water table under cross-section AA'.

Figure 11(b). Water table under cross-section BB'.

Laboratory and field permeability test results from previous investigations at the site are available. The results range widely. Using Darcy's law, the lateral and vertical groundwater velocities can be calculated, as will be shown.

4.2 Climatology

Because of its location in the southern half of Louisiana, the study area is influenced by a humid subtropical climate, characterized by long, hot summers and short, mild winters. The climate is affected by the proximity of the Gulf of Mexico, the land mass to the north, and the Bermuda high and the Mexican heatflow (Sancier, 1963; Stone, 1972).

Data from the climate station at Lake Charles Airport south of the study site show that the average monthly temperature varies from 11°C in January to 28°C in July, and the yearly average is about 20°C . Monthly average rainfall varies from a low of 3.0 inches (76.2 mm) in March to 5.6 inches (142.2 mm) in July, and the yearly average is 53.0 inches (1346.2 mm). The summer months are a period of seasonal precipitation, while the fall (September, October, November) is the driest period.

Evaporation data reported by Jones and others ranged from 2.2 inches (55.9 mm) in January to 6.2 inches (157.5 mm) in June with an annual total of 52.0 inches (1320.8 mm). Highest evaporation rates occur during the summer months. In December, January, and February, evaporation rates are at a minimum.

4.3.1 Regional hydrology

The freshwater aquifers in southwestern Louisiana are the Alluvial aquifer of the Atchafalaya River and Terrace aquifers, both of Quaternary age, the Chicot aquifer of Pleistocene age, the Evangeline of Pliocene age, and the Miocene aquifers of Tertiary age. All of the aquifers generally dip to the southeast. The major aquifers are often overlain by terrace deposits or covered by alluvial deposits. Regional ground water flow is controlled by the permeability of the sediments, geologic structure, topography, and pumping (Ground Water Protection Division, LADEQ, 1989).

4.3.2 Local hydrology

The most important near surface fresh water used to obtain water for public consumption in the area is designated as the Chicot Aquifer (TAI, 1993). The Chicot Aquifer is a regional aquifer composed of three distinct hydraulic units throughout Calcasieu Parish. These units are the "200-foot" sand, "500-foot" sand, and "700-foot" sand. The depth implied in their names refers to the depth below land surface of the base of the individual units at Lake Charles. The Chicot Aquifer beds gently dip to the south at the rate of 5 to 15 feet per mile (0.9 to 2.8 m per km) (Woodward-Clyde Consultants, 1983).

Beneath the BFI Calcasieu site, the top of the "200-foot" sand is about 80 to 100 feet (24.4 to30.5 m) below land surface. The top of the "500-foot" sand is about 250 feet (76.2 m) below the land surface, and the top of the "700-foot" sand is about 600 feet (182.9 m) below the land surface (Woodward-Clyde Consultants, 1983). There exists

beneath the existing 80-acre site a pervious zone above the "200-foot" sand which is normally found at a depth of 40 to 50 feet (12.2 to 15.2 m) below land surface and is generally separated from the "200-foot"sand by a clay aquiclude which is typically 5 to 20 feet (1.5 to 6.1 m) thick. This zone, is termed the "50-foot pervious zone"(Woodward-Clyde Consultants, 1983).

4.4 Water level measurements

Water levels from January 1983 to 1992 are available for some wells. In order to understand the groundwater conditions before pumping, earlier water level information of March 1985 (maximum), and September 1985(minimum) were recorded (see appendix: Table 6.). The choice of 1985 water level data is also considered in accordance with USGS geochemical samples which were also collected in 1985.

4.5 Effects of pumping

Total of 18 recovery wells (wells with RW-prefix and MW-prefix) were installed at the site (maps showing location of wells) from period 1982 to 1992. Among them, three recovery wells were installed within the shallow zone in northeast corner of the site (MW-30, MW-35, and MW-36); six were installed in the 50-foot zone along the south boundary of the site (MW-32, MW-46, MW-47, RW-2, RW-6, and RW-13); and nine were installed in the 50 foot zone in the center to eastern part of the site (RW-1, RW-3, RW-5, RW-8, RW-9, RW-10, RW-11, RW-12, and MW-27).

In March, 1989 Geotrans asserted with regard to the potential off-site migration of contaminants to the south of the 50-foot zone that recovery pumpage is effective in preventing migration to the south in this area. Most areas where contamination has been detected are within the capture area of the recovery well system.

4.6 Potentiometric field

4.6.1 Pre-remediation

Using September 1985 water level data, the potentiometric surface of 50-foot zone was constructed. For the shallow and 200-foot zone, there is not enough water level information available, thus no potentiometric maps can be made for these zones.

Figure 12. Potentiometric surface of the 50-foot zone.

From the potentiometric field, the general direction of groundwater flow in "50-foot pervious" zone is determined to be from northwest to southeast. The conditions at the east of the site are more complex, with groundwater flow from north-northeast to the south. The ground water hydraulic gradient (dH / dL) ranges from 0.0061 to 0.0197 as determined from the slope of the potentiometric surface.

4.6.2 1992 potentiometric surface

Fourth-quarter 1992 potentiometric surface for pumping condition are available from 1992 Triegel & Associates, Inc. annual report.

Figure 13. Potentiometric map of the 50-foot zone (pumping condition, 4th quarter, 1992).

Comparing this with 1985 potentiometric map (Figure 12.), it is obvious that at the west part of the site, the groundwater flow direction is still from southwest to northeast because no recovery wells were installed in this part. However, at the east part and south boundary of the site, groundwater flow is now toward the recovery well.

4.7 Hydraulic conductivity

Hydraulic conductivity and permeability information are available from several sources.

Table 7. Summary of hydraulic conductivity and permeability information

4.8 Flow fields

4.8.1 USGS study

(In preparation)

4.8.2 Contractor's study

(In preparation)

4.8.3 This study

(in preparation)

5. Ground water geochemistry- 1985

5.1 Introduction

(In preparation)

5.2 Sources of data and techniques

5.2.1 Water quality analyses

1985 USGS Willow Springs data for each of USGS wells have been used. This data base has over 60 items including major cations, anions, organic contaminants, temperature, pressure, and other parameters.

5.2.2 Sediment mineralogy

(In preparation)

5.2.3 Computer program SOLMINEQ.88

The main computer program used to analyze the thermodynamic aspects of ground water geochemistry of the site is SOLMINEQ.88 (Kharaka et al, 1988), an advanced version of SOLMINEQ (Aggarwak et ak, 1986; Kharaka & Barnes, 1973). SOLMINEQ.88 is a geochemical modelling program, which reduces water analyses and allows the user to simulate many processes which occur between waters, minerals and gases. The program allows these processes to be monitored from data on the chemical composition of waters and can be used as a predictive tool. Some of the many possible applications would include: the monitoring of water-water and water-mineral incompatibility; the identification of scale forming phases and the calculation of their scaling potential at elevated temperatures and pressures; the calculation of condensate pH and water chemistry in boilers; various geothermometers in the code; ion exchange;

calculating activity of separation of an annulus gas on water composition in oil production; and calculation of the partitioning of volatiles between oil, water and gas in oil reservoirs. A large volume of information is output and examination of it is the key to the interpretation of the water chemistry and associated processes.

5.3 Spatial variations in ground water composition

(In preparation)

5.4 Physical controls on ground water composition

(In preparation)

5.5 Chemical controls

5.5.1 Mineral -fluid equilibria

Program SOLMINEQ. 88 has been used to compute the saturation index of some common minerals. The saturation state for a mineral is expressed as saturation index:

$$S.I. = \text{Log}\,(Q / K)$$

where Q is the ionic activity product, K is the mineral equilibrium constant at in situ pressures and temperatures.

For: S.I. > 0, mineral is supersaturated

S.I. = 0, mineral is saturated

S.I. < 0, mineral is undersaturated

Table 9. Saturation Index of several minerals calculated using SOLMINEQ.88.

Mineral-fluid equilibrium calculations indicate that shallow groundwaters at the site are saturated with respect to some minerals. The shallow groundwaters are all saturated with

respect to quartz. Waters from wells Cu-875, Cu-881, Cu-904, Cu-907, Cu-914, Cu-936, Cu-939, Cu-941, Cu-942, Cu-945, Cu-1217, and Cu-1219 are saturated with respect to barite, reflecting a high concentration of Ba-present. Waters from wells Cu-874, Cu-881, Cu-936, Cu-940, Cu-1217, and Cu-1219 are saturated with respect to calcite. Waters from wells Cu-872, Cu-874, Cu-875, Cu-907, Cu-908, Cu-914, Cu-936, Cu-939, Cu-940, Cu-941, Cu-945, Cu-1217, and Cu-1219 are saturated with respect to dolomite. Waters from wells Cu-893, Cu-899, Cu-904, Cu-907, Cu-908, Cu-939, Cu-940, Cu-941, Cu-942, Cu-943, and Cu-1221 are saturated with respect to Cu_2O, indicating a prevailing reducing environment.

Evaluation of saturation with respect to aluminosilicate phases present problems because of lack of Al analyses, and the lack of some suitable Gibbs Free Energy data, especially for the smectite clays. Thus aluminosilicate phases are analyzed using phase diagrams which are reproduced from Drever (1988). In the phase diagram of system CaO-Al_2O_3-SiO_2-H_2O, most waters fall in Ca-beidellite stable area, except waters from cu-899 and cu-1220 are in kaolinite stability field. In the phase diagram for the system of K_2O-Al_2O_3-SiO_2-H_2O, waters from these wells are in kaolinite or k-feldspar stability field, and have a trend to parallel this phase boundary, indicating these waters are buffered by these two minerals. In the phase diagram for the system Na_2O-Al_2O_3-SiO_2-H_2O, these waters are apparently saturated with respect to kaolinite or Na-beidellite, and also plot parallel to their phase boundary, indicating these waters may buffered by these two minerals.

Figure 15(a). Phase diagram in system Na_2O - Al_2O_3-SiO_2-H_2O at 25°C.

Figure 15(b). Phase diagram in system K_2O-Al_2O_3-SiO_2-H_2O at 25°C.

Figure 15(c). Phase diagram in system CaO-Al_2O_3-SiO_2-H_2O at 25°C.

5.5.2 Redox reactions

(In preparation)

6. Contaminant transport and reaction - organic

6.1 Introduction

(In preparation)

6.2. Sources of data and techniques

(In preparation)

6.3 Organic contaminants

(In preparation)

6.4 Spatial distribution

(In preparation)

6.5 Temporal distribution

(In preparation)

6.6 Transport mechanisms

(In preparation)

6.7 Chemical reactions

(In preparation)

6.8 Summary

(In preparation)

7. Contaminant transport and reaction - inorganic

7.1 Introduction

(In preparation)

7.2 Sources of data and techniques

(In preparation)

7.3 Inorganic contaminants

(In preparation)

7.4 Spatial distribution

(In preparation)

7.5 Temporal distribution

(In preparation)

7.6 Transport mechanisms

(In preparation)

7.7 Chemical reactions

(In preparation)

7.8 Summary

(In preparation)

8. Discussion and conclusions

(In preparation)

APPENDIX C

An experimental invesitgation of the effects of variable salinity on water-rock chemical interaction

Lee Esch
Department of Geology and Geophysics
Louisiana State University
Baton Rouge, Louisiana 70803

Note: The research described in this appendix represents the results of the first year of a dissertation research project being conducted by Mr. Esch. The purpose of this report is to outline the long-term goals of this research and to document what has been completed during the 1992-93 period of funding by the Department of the Interior, U.S. Geological Survey, through the Louisiana Water Resources Research Institute. It should be understood that portions of the text, figures, and tables which follow are preliminary in nature and subject to revision and that some phases of the project will not be completed for another year or more.

An experimental investigation of the effects of variable salinity on water-rock chemical interaction

Lee Esch

1. Introduction

Fluid migration in sedimentary basins can expose sediments to variable salinity conditions during burial diagenesis. In particular, sediments near evaporites may be exposed to saline fluids that are migrating away from dissolving evaporites. Brine disposal by deep-well injection and leakage from waste ponds containing brines also subjects sediments to variable salinity conditions. In the Louisiana Gulf Coast, shallow, fresh groundwaters, such as those in the Chicot Aquifer, are locally being contaminated by deeper brines.

Experimental investigations of variable salinity effects in diagenetic environments are sparse, so laboratory experiments are being conducted to investigate the influence of variable salinity on water- rock interaction and its control of fluid compositions.

2. Experimental Procedures and Results

Experimental conditions in a set of closed system experiments were set at 90° C, 1 bar; and 25° C, 1 bar. Ten artificial NaCl solutions were prepared with concentrations ranging from 1 mg/l NaCl to halite saturation at the two experimental temperatures. These solutions were reacted for 90 days with clay-rich silts. The dominant minerals in the starting sediments were quartz, kaolinite, smectite, and detrital muscovite. Albite and potassium feldspar were also present in minor amounts. Reacted fluids and sediments were analyzed by X-Ray diffractometry, scanning electron microscopy, and inductively coupled plasma-atomic emission spectrometry (ICP-AES).

Ca, K, and Mg attain concentrations in solution of 100 to 1000 mg/l in the experiments where initial salinities were above 35000 mg/l. These cations are obtained by exchange with Na on smectite exchange sites. Ba, Sr, and Mn are also introduced into solution by surface exchange, but in lesser amounts. Bulk sediment exchange capacity of the original sediments is 70 meq/100 g of dry sediment. Si concentrations, reported as dissolved silica, approach 310 mg/l in the halite saturated experiments, suggesting substantial dissolution of quartz and aluminosilicates. Al concentrations remain near detectable limits by ICP-AES, indicating that aluminosilicate dissolution is incongruent. It is likely that aluminum initially is precipitated in kaolinite. Ca and Si drop in concentration in the halite saturated 90°C experiment at 90 days. These components may be precipitating in an amorphous silicate or aluminosilicate phase.

XRD work on the reacted sediments is inconclusive because the method is not sensitive enough to detect the small amounts of reaction product in the sediments, or amorphous phases. However, a decrease in the 26.6° 2Θ peak for quartz in the < 2μm fraction as a function of increasing salinity in the 90° experiments suggests that quartz dissolution is enhanced in the high salinity solutions. SEM imaging also reveals increased dissolution of

detrital quartz with increasing salinity. Heavily corroded quartz grains were observed in the highest salinity experiments.

3. Evaluation of controls on fluid compositions

Brine experiment data were processed in SOLMINEQ.88 (Kharaka et al., 1988), which is a thermodynamic modeling program. Data from the 60 and 90 day 90°C, and 30, 60, and 90 day 25°C experiments numbers 2, 4, 6, 8, and 10 were processed in SOLMINEQ.88. Experiments 2, 4, 6, 8, and 10 represent initial NaCl salinities of 10 mg/l, 1000 mg/l, 35000 mg/l, 165000 mg/l, and halite saturation (ca. 350,000 mg/l) respectively.

Aluminum data are presented in Appendix 1 for some of the experiments, but they are unreliable because concentrations in sample aliquots were very close to aluminum's ideal detection limit by ICP- AES. Consequently, aluminum was not included in the SOLMINEQ.88 runs.

4. Mineral Saturation State

SOLMINEQ.88 was primarily used to evaluate log activity of H4SiO4 and log activity ratios for Ca/H2, Na/H, and K/H. The Pitzer option for calculating activity coefficients was utilized when initial salinities equaled or exceeded that of seawater. These values were plotted on published 25° C, 1 bar activity diagrams from Drever (1988) for the 25° C experiments, and on 150° C, Psat activity diagrams from Bowers et al. (1984). One diagram for 100° C, Psat was taken from McManus (1991) dissertation. Published activity diagrams for 90° C, 1 bar apparently do not exist. An additional problem was encountered in attempting to apply the Pitzer option in SOLMINEQ.88 for modeling activity coefficients at temperatures above 75° C. Apparently there is some problem within the original SOLMINEQ.88 program with missing or unopenable data files that are required for Pitzer calculations of activity coefficients.

4.1. 25° C Experiments

The activity plots for experiments at 25° C, 1 bar, 30 days (Appendix pg. 20) show that the solutions are in equilibrium with smectite. Experiments with initial NaCl concentrations of 165000 mg/l and halite saturation, respectively, plot close to the amorphous silica line which suggests Si buffering by amorphous silica or some disordered silica phase. At 60 and 90 days (Appendix pgs. 21 and 22), Si concentrations drop precipitously in experiments with the 165000 mg/l and saturated starting solutions to levels below Si detection limits by ICP-AES. Obviously, this prohibits plotting of the results at 60 and 90 days. At the same time, carbonate alkalinity substantially increases in all of the solutions. It appears that if the experiments ran long enough, calcite might eventually buffer solution compositions also. Note that experiments at 10 mg/l, 1000 mg/l, and 35000 mg/l initial NaCl concentration) move toward the calcite (PCO2=10-2) stability boundary and quartz stability boundary (see

Appendix pg. 22). These data also plot within the kaolinite stability field at 90 days. Ultimately, this system at 25° C and 1 bar apparently would be buffered by quartz, kaolinite, and calcite, as long as exchanged calcium is available.

4.2. 90° C Experiments

Appropriate phase diagrams for the 90° C experiments were not available. Instead, phase diagrams were adapted from Bowers et al. (1984) for 150° C, p sat.. Field data published by Land et al. (1988) from offshore Louisiana oil fields in Miocene sediments (Appendix pgs. 23-26) were also evaluated. The Land et al. data are plotted as polygonal figures to allow differentiation from the experimental data. These formation waters have TDS values in the 10000 to 35000 mg/l range and allow comparison of the experimental data to actual formation water analyses. In most cases, the experiments with similar and higher salinities to the Land et al. data compositionally plot close to the Land et al. data. This probably occurs because the high salinity fluids exchange substantial amounts of Ca, K, and Mg along with dissolving substantial amounts of quartz. The effect of these two processes is to quickly generate a fluid that resembles an oil-field brine. It would be worthwhile to run the same experiment again, except to pre-saturate the sediments with seawater to evaluate the difference this would cause in the exchangeable cations and final solution compositions. This might illustrate the difference between similar sediments deposited with fresh connate water as opposed to those deposited with seawater. Calculations with the cation exchange capacity suggest that less than 30% of the exchangeable cations are exchanged even in the highest initial Na solution concentrations. This suggests that even more Ca, Mg, and K (and other minor cations such as Ba, Sr, Mn, and Pb) may be released if we deal with an open system rather than a closed system.

The apparent compositional trend shown on the activity plots on Appendix page 26)

show that the linear trend of the oil-field brine data is continued by all of the experimental data. This suggests that the experimental conditions have at least been partially successful in duplicating chemical conditions in the subsurface where fluids with variable salinity are present.

The principal difference between the experimental brines and real oil-field brines is the lower Ca concentration of the former. This is not surprising since calcite was not included in the sediments used in the experiments. This fact shows up clearly on Appendix pg. 25) where the oil-field brine activity ratios for calcium plot in a range 1 magnitude higher than the experimental points do. In the other activity diagrams for the 90° C experiments, where Ca is not considered, experiments with starting salinities of 35000 mg/l, 150000 mg/l and halite saturation plot remarkably near the real oil-field brines. This fact suggests that the combination of exchange and mineral dissolution-precipitation reactions in the presence of high salinity NaCl fluids can quickly generate a solution with the compositional characteristics of an oil-field brine.

REFERENCES

Bowers T. S., Jackson K. J. and Helgeson H. C. (1984) Equilibrium activity diagrams for coexisting minerals and aqueous solutions at pressures and temperatures to 5kb and 600 °C. Springer-Verlag, New York, 397p.

Drever J.I. (1988) The Geochemistry of Natural Waters. Second Ed. Prentice-Hall, New Jersey, 437p.

Land L.S., Macpherson G.L. and Mack L.E. (1988) The geochemistry of saline formation waters, Miocene, offshore Louisiana. Transactions-Gulf Coast Association of Geological Societies 38, 503-511.

APPENDIX

Table of Contents

Experiment	92-1-1			92-2-1		
Temp. °C	90			25		
Days	30	60	90	30	60	90
pH	-	5.90	5.85	7.00	6.95	7.20
(following values in mg/L)						
Al	0.63	0.42	-	-	-	-
Ba	0.	0.1	0.	0.	0.5	0.
Ca	20	29	38	5	10	9
Clat t=0: 0.61						
K	16	11	17	0.	11	3.7
Fe	0.	0.	1.0	3.0	0.	0.
Mg	6	6	6	0.	0.	0.
Mn	1	1	1	0.	0.	0.
Na	8	47	32	0.	84	0.
Naat t=0: 0.39						
Pb	0.	0.	1.2	4.3	0.	0.
$SiO2^-$	107	107	128	77	11	17
Sr	0.	0.	0.	0.	0.1	0.
Zn	0.	0.	0.	0.	0.1	0.
Total Alk. as HCO3-	-	30.5	28.7	62.2	60.4	73.2
Hardness as CaCO3	-	25.0	23.5	51.0	49.5	60.0

Note; 0. indicates values below detection limit; - indicates no analysis or data currently not tabulated from existing analyses.

Experiment	92-1-2			92-2-2		
Temp. °C	90			25		
Days	30	60	90	30	60	90
pH	-	6.10	5.80	6.75	6.90	7.05
(following values in mg/L)						
Al	0.94	-	-	-	-	-
Ba	0.1	0.2	0.2	0.	0.1	0.
Ca	15	28	39	4	6	8
Clat t=0: 5.45						
K	11	15	14	6	0	4
Fe	0.	2.0	1.0	1.0	0.	0.
Mg	3	6	8	0.	0.	0.
Mn	0.	1	1	0.	0.	0.
Na	21	38	33	11	101	4
Naat t=0: 3.54						
Pb	2.3	1.2	2.2	0.	0.	0.
$SiO2^{-}$	94	126	126	58	17	15
Sr	0.	0.	0.	0.	0.	0.
Zn	0.	0.	0.1	0.	0.	0.
Total Alk. as HCO3-	-	27.5	25.6	56.0	73.8	75.6
Hardness as CaCO3	-	22.5	21.0	46.0	60.5	62.0

Note; 0. indicates values below detection limit; - indicates no analysis or data currently not tabulated from existing analyses.

Experiment	92-1-3			92-2-3		
Temp. °C	90			25		
Days	30	60	90	30	60	90
pH	-	5.98	5.65	6.50	7.05	7.03
(following values in mg/L)						
Al	1.09	-	-	-	-	-
Ba	0.1	0.2	0.1	0.	0.1	0.
Ca	25	36	49	13	14	17
Clat t=0: 59.7						
K	21	17	14	2	0.	8
Fe	0.	0.	0.	0.	0.	0.
Mg	5	8	11	1	0.	1
Mn	1	1	2	0.	0.	0.
Na	51	79	67	38	114	23
Naat t=0: 38.7						
Pb	4.5	2.5	8.4	0.	0.	2.6
$SiO2^-$	107	105	120	51	11	13
Sr	0.1	0.1	0.1	0.	0.	0.
Zn	0.	0.	0.	0.	0.1	0.
Total Alk. as HCO3-	-	25.6	23.2	53.7	69.5	53.7
Hardness as CaCO3	-	21.0	19.0	44.0	57.0	44.0

Note; 0. indicates values below detection limit; - indicates no analysis or data currently not tabulated from existing analyses.

Experiment	92-1-4			92-2-4		
Temp. °C	90			25		
Days	30	60	90	30	60	90
pH	-	5.80	5.55	6.50	6.95	6.91
(following values in mg/L)						
Al	1.61	0.52	-	-	-	-
Ba	0.4	0.5	2.19	0.1	0.3	0.1
Ca	70	82	97	75	69	75
Clat t=0: 607.0						
K	22	20	21	6	14	13
Fe	1.0	0.	0.	0.	0.	0.
Mg	12	11	15	14	11	13
Mn	2	3	3	0.	0.	0.
Na	310	322	333	329	409	309
Naat t=0: 393.5						
Pb	0.2	0.2	2.2	0.8	0.	0.
$SiO2^-$	98	94	105	49	11	13
Sr	0.2	0.3	0.3	0.3	0.2	0.2
Zn	0.	0.	0.	0.	0.	0.
Total Alk. as HCO3-	-	19.0	13.4	43.3	54.0	53.1
Hardness as CaCO3	-	15.5	11.0	35.5	44.0	43.5

Note; 0. indicates values below detection limit; - indicates no analysis or data currently not tabulated from existing analyses.

Experiment	92-1-5			92-2-5		
Temp. °C	90			25		
Days	30	60	90	30	60	90
pH	-	5.65	5.48	6.35	6.65	6.75
	(following values in mg/L)					
Al	1.06	0.8	-	-	-	-
Ba	2.4	3.0	3.2	1.5	1.6	1.3
Ca	322	342	361	373	366	363
Clat t=0: 6099						
K	28	29	32	25	17	17
Fe	0.	0.	0.	0.	0.	0.
Mg	56	59	64	74	74	72
Mn	11	13	15	0.	0.	0.
Na	3476	3580	3684	3767	3402	3580
Naat t=0: 3955						
Pb	5	0.	1	4.0	2.1	0.
$SiO2^-$	92	90	105	43	9	9
Sr	1.3	1.5	1.6	1.5	1.4	1.3
Zn	0.	0.	0.	0.	0.	0.
Total Alk. as HCO3-	-	18.3	17.1	34.2	40.3	37.8
Hardness as CaCO3	-	15.0	14.0	28.0	33.0	31.0

Note; 0. indicates values below detection limit; - indicates no nalysis or data currently not tabulated from existing analyses.

Experiment	92-1-6			92-2-6		
Temp. °C	90			25		
Days	30	60	90	30	60	90
pH	-	5.45	5.41	6.25	6.57	6.75
(following values in mg/L)						
Al	1.3	2.1	-	-	-	-
Ba	7.5	8.5	9.8	4.8	4.9	4.9
Ca	593	572	610	622	671	704
Clat t=0: 21720						
K	42	33	38	36	52	57
Fe	0.	0.	0.	0.	0.	0.
Mg	99	102	109	123	128	135
Mn	22	26	29	0.	0.	0.
Na	12757	13130	13534	14184	13981	14628
Naat t=0: 14085						
Pb	2.8	0.5	0.8	11	4.5	0.
$SiO2^{-}$	98	81	90	41	2	4
Sr	2.7	2.9	3.2	2.7	2.7	2.9
Zn	0.	0.1	0.1	0.	0.1	0.
Total Alk. as HCO3-	-	14.6	16.5	33.0	25.6	29.3
Hardness as CaCO3	-	12.0	13.5	27.0	21.0	24.0

Note; 0. indicates values below detection limit; - indicates no analysis or data currently not tabulated from existing analyses.

Experiment	92-1-7			92-2-7		
Temp. °C	90			25		
Days	30	60	90	30	60	90
pH	-	5.40	5.35	6.15	6.35	6.45
(following values in mg/L)						
Al	2.13	3.23	-	-	-	-
Ba	13	14	16	7.4	6.9	8.8
Ca	687	755	768	626	717	882
Clat t=0: 44524						
K	45	37	52	45	85	72
Fe	0.	0.	0.	0.	0.	0.
Mg	106	132	138	109	126	150
Mn	28	37	43	0.	0.	0.
Na	26695	28517	28210	29467	25417	27518
Naat t=0: 28872						
Pb	0.	3	0.	29	29	0.
$SiO2^-$	116	83	96	45	0.	2
Sr	3.4	3.8	4.0	3.1	2.8	3.7
Zn	0.1	0.	0.2	0.	0.3	0.
Total Alk. as HCO3-	-	11.0	15.9	26.8	17.7	15.3
Hardness as CaCO3	-	9.0	13.0	22.0	14.5	12.5

Note; 0. indicates values below detection limit; - indicates no alysis or data currently not tabulated from existing analyses.

Experiment	92-1-8			92-2-8		
Temp. °C	90			25		
Days	30	60	90	30	60	90
pH	-	5.20	5.19	5.70	5.95	6.08
	(following values in mg/L)					
Al	3.1	13.4	-	-	-	-
Ba	18	20	23	11	9	11
Ca	766	789	826	717	938	855
Clat t=0: 100000						
K	88	117	112	65	164	47
Fe	0.	0.	0.	2.0	0.	0.
Mg	126	135	136	132	181	149
Mn	41	49	54	0.	0.	0.
Na	59044	58641	52529	63206	58417	61204
Naat t=0: 65000						
Pb	5.3	25	12	4.0	26	0.
$SiO2^-$	135	86	90	47	0.	0.
Sr	4.0	4.0	4.0	3.0	2.0	3.0
Zn	0.	1.0	1.0	0.	0.	0.
Total Alk. as HCO3-	-	2.4	12.8	20.1	9.2	11.6
Hardness as CaCO3	-	2.0	10.5	16.5	7.5	9.5

Note; 0. indicates values below detection limit; - indicates no nalysis or data currently not tabulated from existing analyses.

Experiment	92-1-9			92-2-9		
Temp. °C	90			25		
Days	30	60	90	30	60	90
pH	-	5.05	5.01	5.25	5.50	5.58
(following values in mg/L)						
Al	4.7	19.4	-	-	-	-
Ba	22	21	20	11	8	11
Ca	800	792	777	842	967	846
Clat t=0: 180341						
K	181	205	246	131	226	136
Fe	1.0	0.	0.	1.0	1.0	1.0
Mg	119	125	128	154	196	136
Mn	55	59	61	1	1	0.
Na	98011	98438	99925	108042	116105	102808
Naat t=0: 116944						
Pb	7	8	44	21	17	1
$SiO2^-$	263	94	94	62	0.	0.
Sr	4.	4.0	3.0	3.0	2.0	3.0
Zn	1	1	2	0.	2	0.
Total Alk. as HCO3-	-	1.2	1.8	20.7	4.0	1.8
Hardness as CaCO3	-	1.0	1.5	17.0	3.3	1.5

Note; 0. indicates values below detection limit; - indicates noanalysis or data currently not tabulated from existing analyses.

Experiment	92-1-10			92-2-10		
Temp. °C	90			25		
Days	30	60	90	30	60	90
pH	-	4.95	4.98	5.00	5.48	5.32
(following values in mg/L)						
Al	3.9	11.9	-	-	-	-
Ba	21	23	18	12	9	11
Ca	792	763	722	947	967	846
Clat t=0: -						
K	268	287	306	134	290	261
Fe	0.	0.	1.0	0.	3.0	3.0
Mg	115	113	111	176	196	124
Mn	56	63	63	0.	1	0.
Na	115619	125674	122209	109938	109359	113287
Naat t=0: -						
Pb	2.8	51.6	77	51	5	14
$SiO2^-$	310	107	118	49	0.	0.
Sr	4.0	4.	3.	4.	3.	4.
Zn	1	2	2	0.	0.	0.
Total Alk. as HCO3-	-	38.4	6.1	10.4	6.7	0.6
Hardness as CaCO3	-	31.5	5.0	8.5	5.5	0.5

Note; 0. indicates values below detection limit; - indicates no analysis or data currently not tabulated from existing analyses.

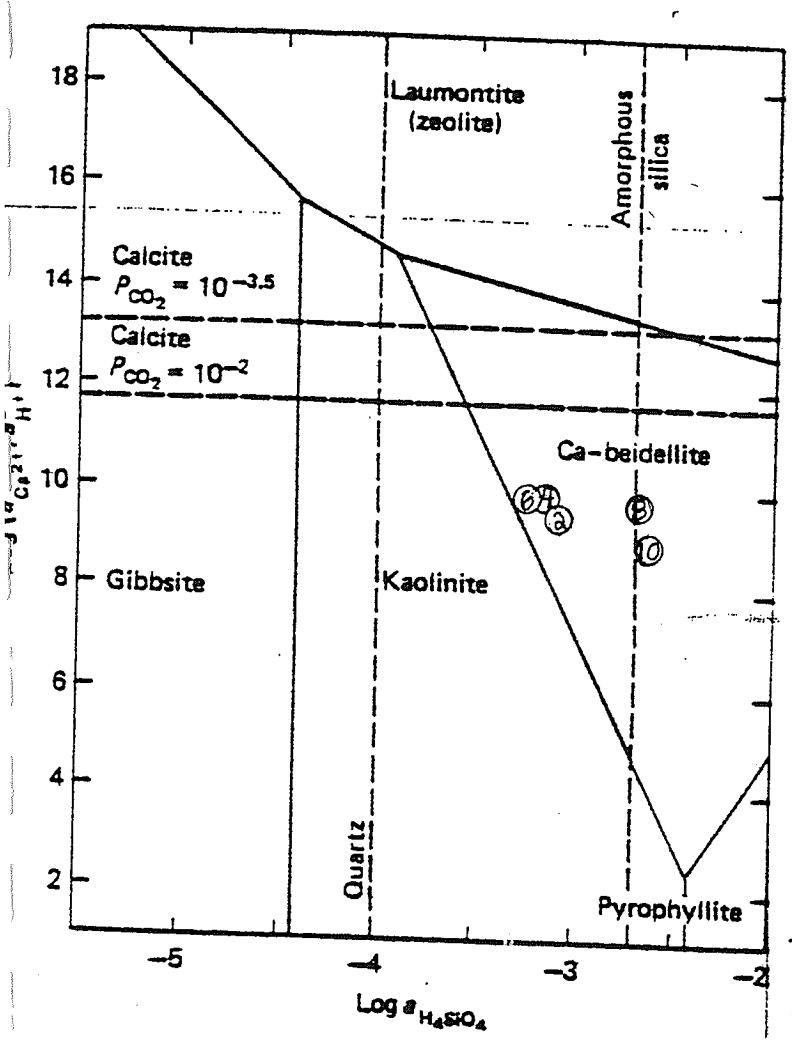
Laumontite
(zeolite)
Amorphous
silica
Calcite
$P_{CO_2} = 10^{-3.5}$
Calcite
$P_{CO_2} = 10^{-2}$
Ca-beidellite
Gibbsite
Kaolinite
Quartz
Pyrophyllite
Log $a_{H_4SiO_4}$

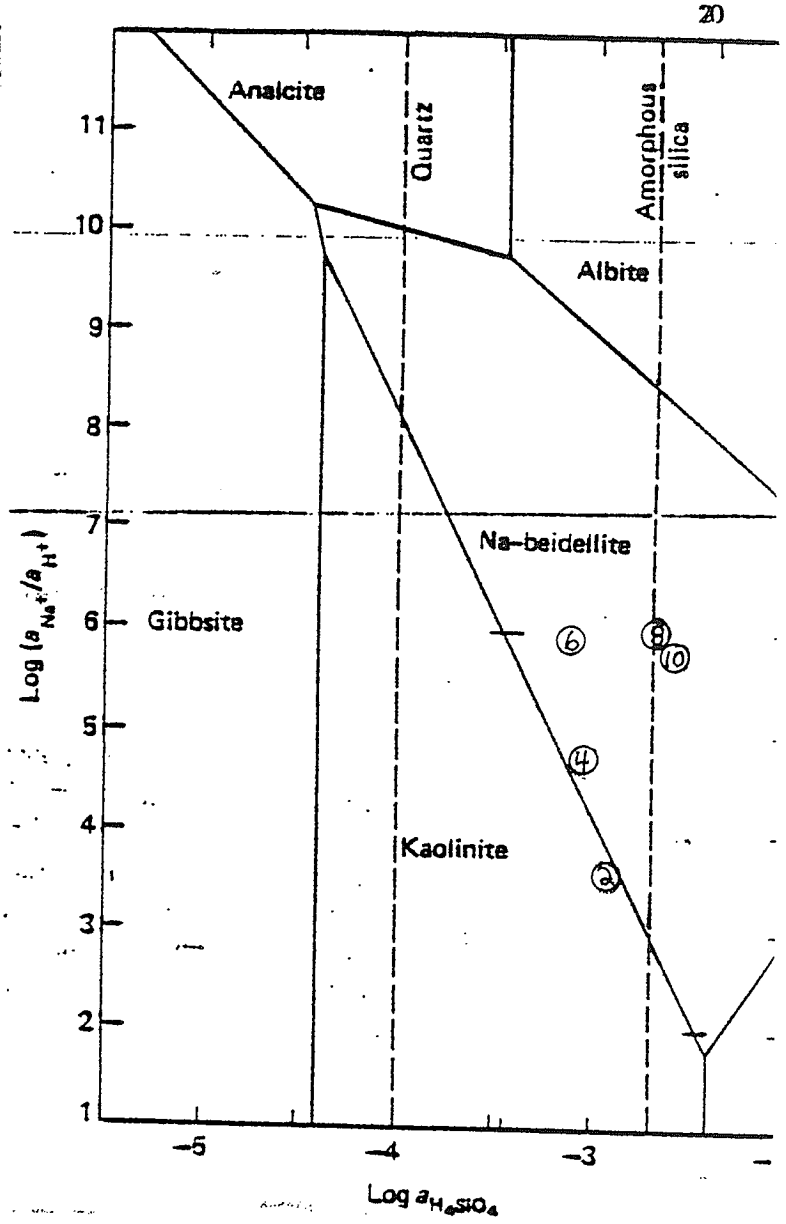
Analcite
Quartz
Amorphous
silica
Albite
Na-beidellite
Gibbsite
Kaolinite
Log (a_{Na^+}/a_{H^+})
Log $a_{H_4SiO_4}$

30 days

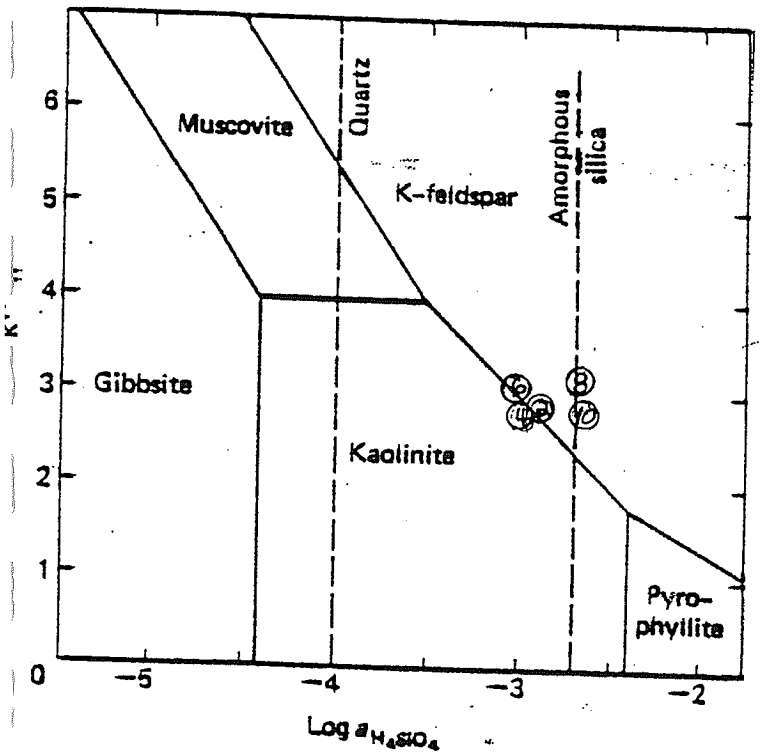
Muscovite
Quartz
K-feldspar
Amorphous
silica
Gibbsite
Kaolinite
Pyro-
phyllite
Log $a_{H_4SiO_4}$

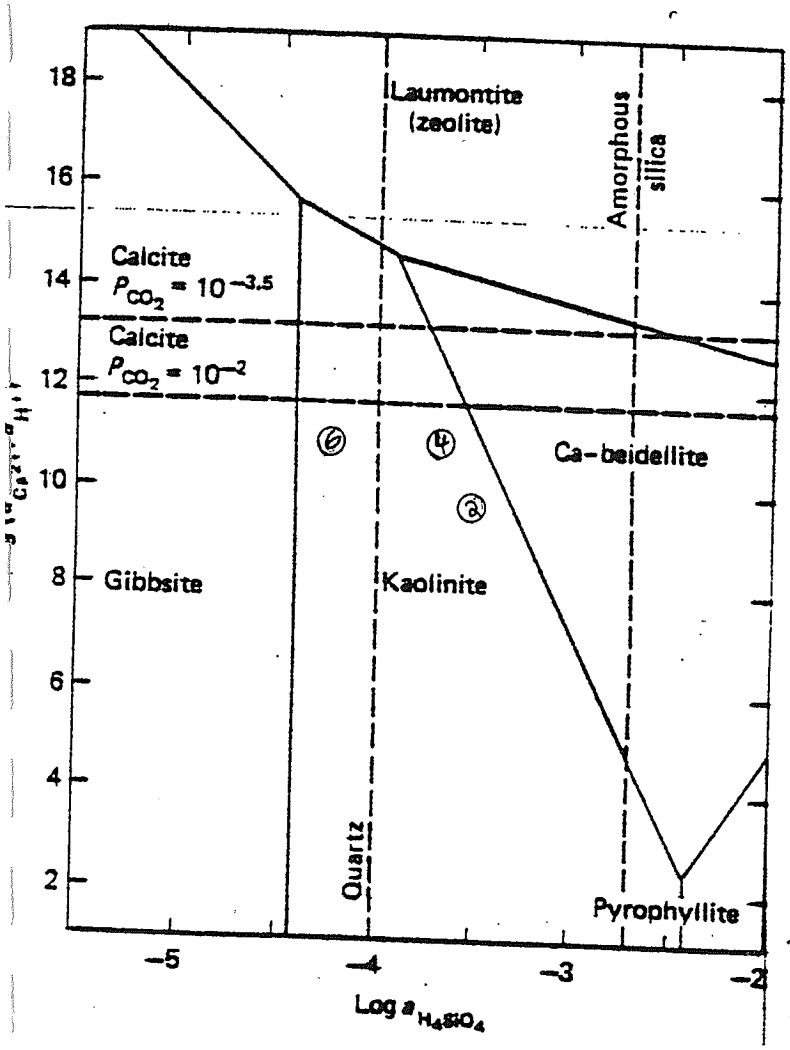
Laumontite
(zeolite)
Amorphous
silica
Calcite
$P_{CO_2} = 10^{-3.5}$
Calcite
$P_{CO_2} = 10^{-2}$
Ca-beidellite
Gibbsite
Kaolinite
Quartz
Pyrophyllite
Log $a_{H_4SiO_4}$

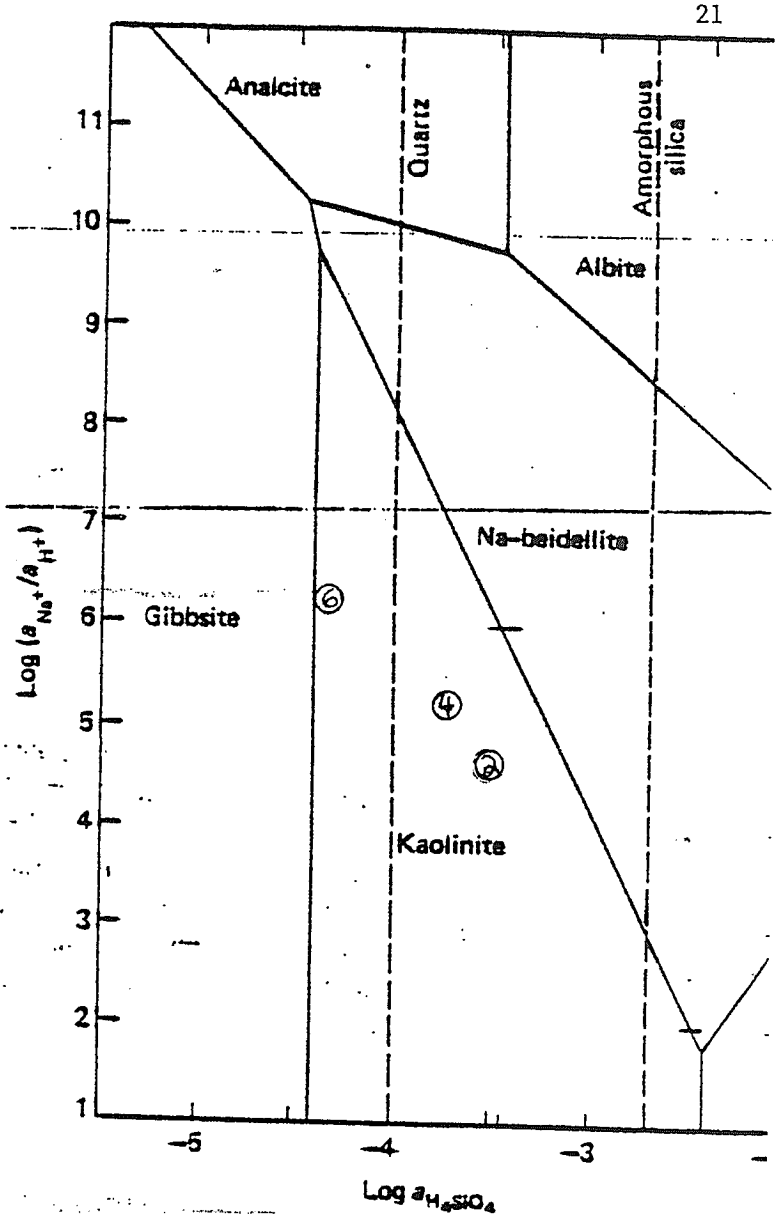
Analcite
Quartz
Amorphous
silica
Albite
Na-beidellite
Gibbsite
Kaolinite
Log (a_{Na^+}/a_{H^+})
Log $a_{H_4SiO_4}$

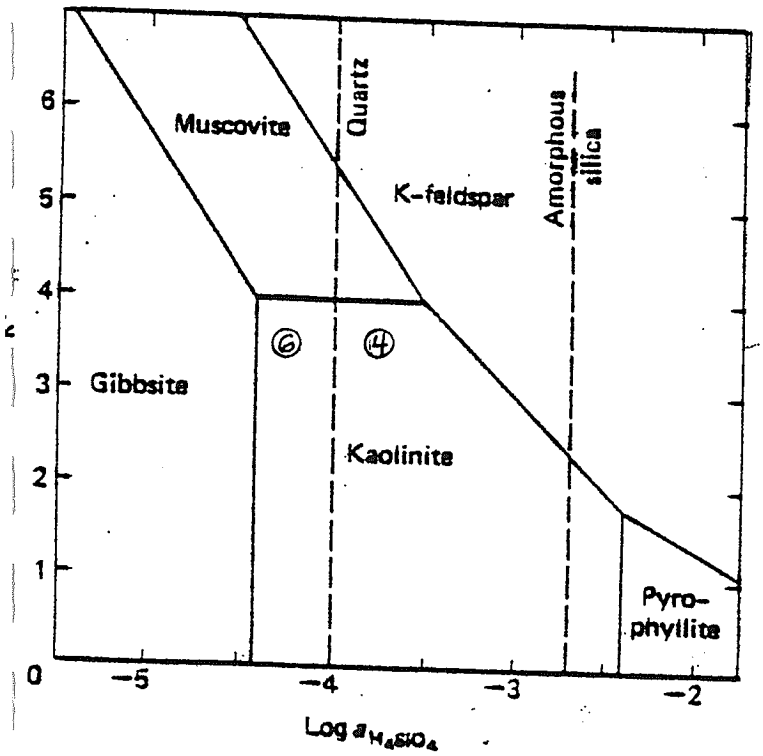
Muscovite
Quartz
K-feldspar
Amorphous
silica
Gibbsite
Kaolinite
Pyro-
phyllite
Log $a_{H_4SiO_4}$

60 days

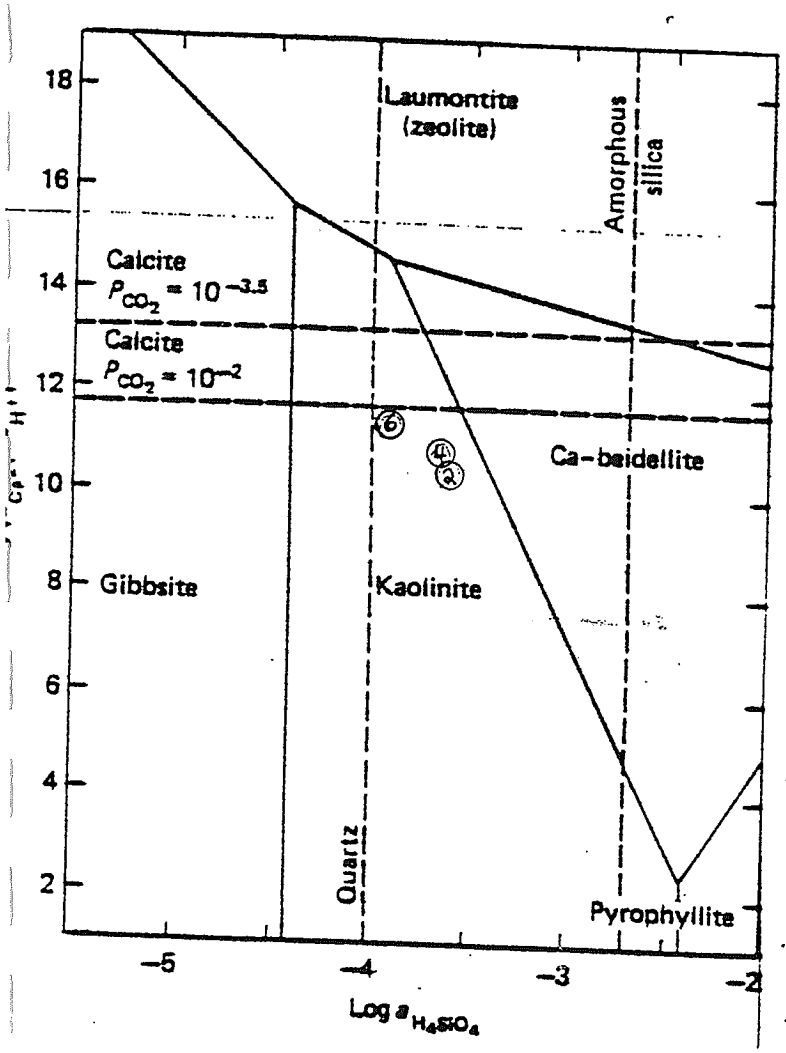
Laumontite
(zeolite)
Amorphous
silica
Calcite
$P_{CO_2} = 10^{-3.5}$
Calcite
$P_{CO_2} = 10^{-2}$
Ca-beidellite
Gibbsite
Kaolinite
Quartz
Pyrophyllite
Log $a_{H_4SiO_4}$

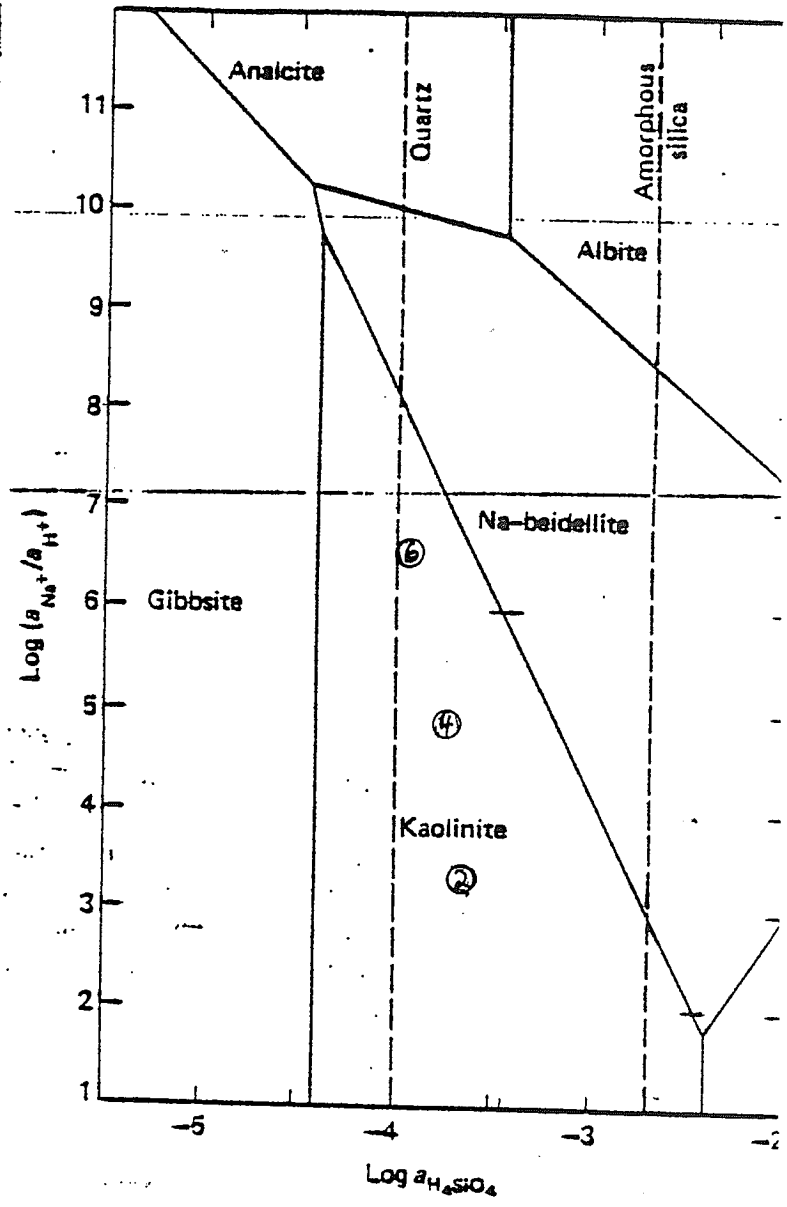
Analcite
Quartz
Amorphous
silica
Albite
Na-beidellite
Gibbsite
Kaolinite
Log (a_{Na^+}/a_{H^+})
Log $a_{H_4SiO_4}$

90 days

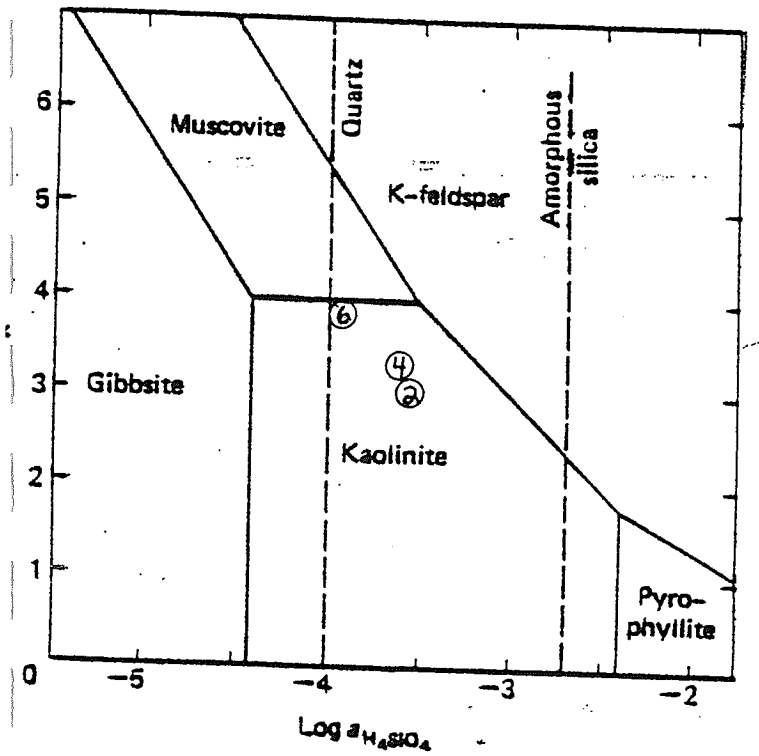
Muscovite
Quartz
K-feldspar
Amorphous
silica
Gibbsite
Kaolinite
Pyro-
phyllite
Log $a_{H_4SiO_4}$

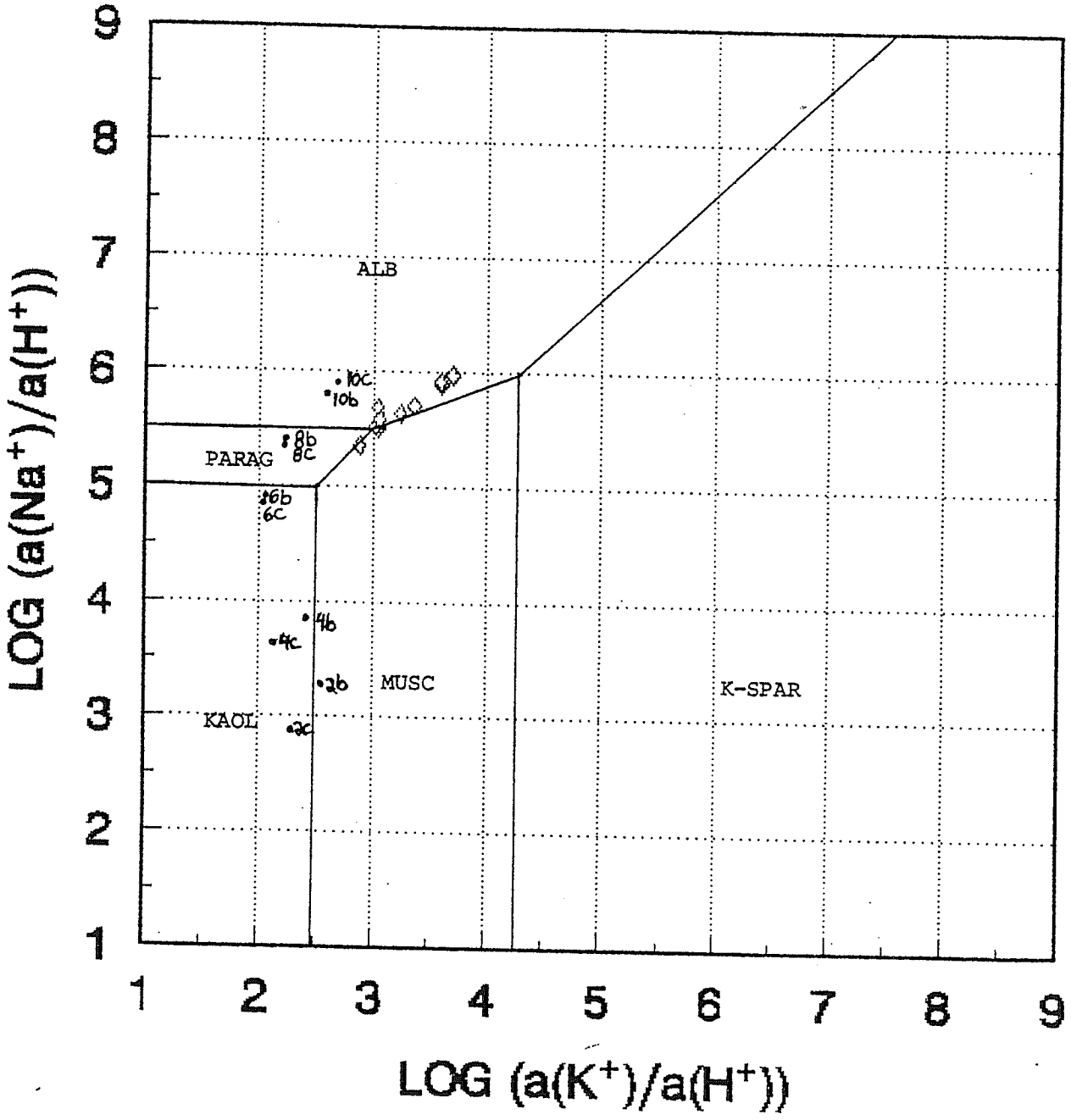

Figure 4) $\log(a_{Na+}/a_{H+})$ vs. $\log(a_{K+}/a_{H+})$. ALB=Albite, PARAG=Paragonite, KAOL=Kaolinite, MUSC=Muscovite, K-SPAR=Potassium Feldspar, T=150° C, P=P_{sat}, Adapted from Bowers et al., (1984)

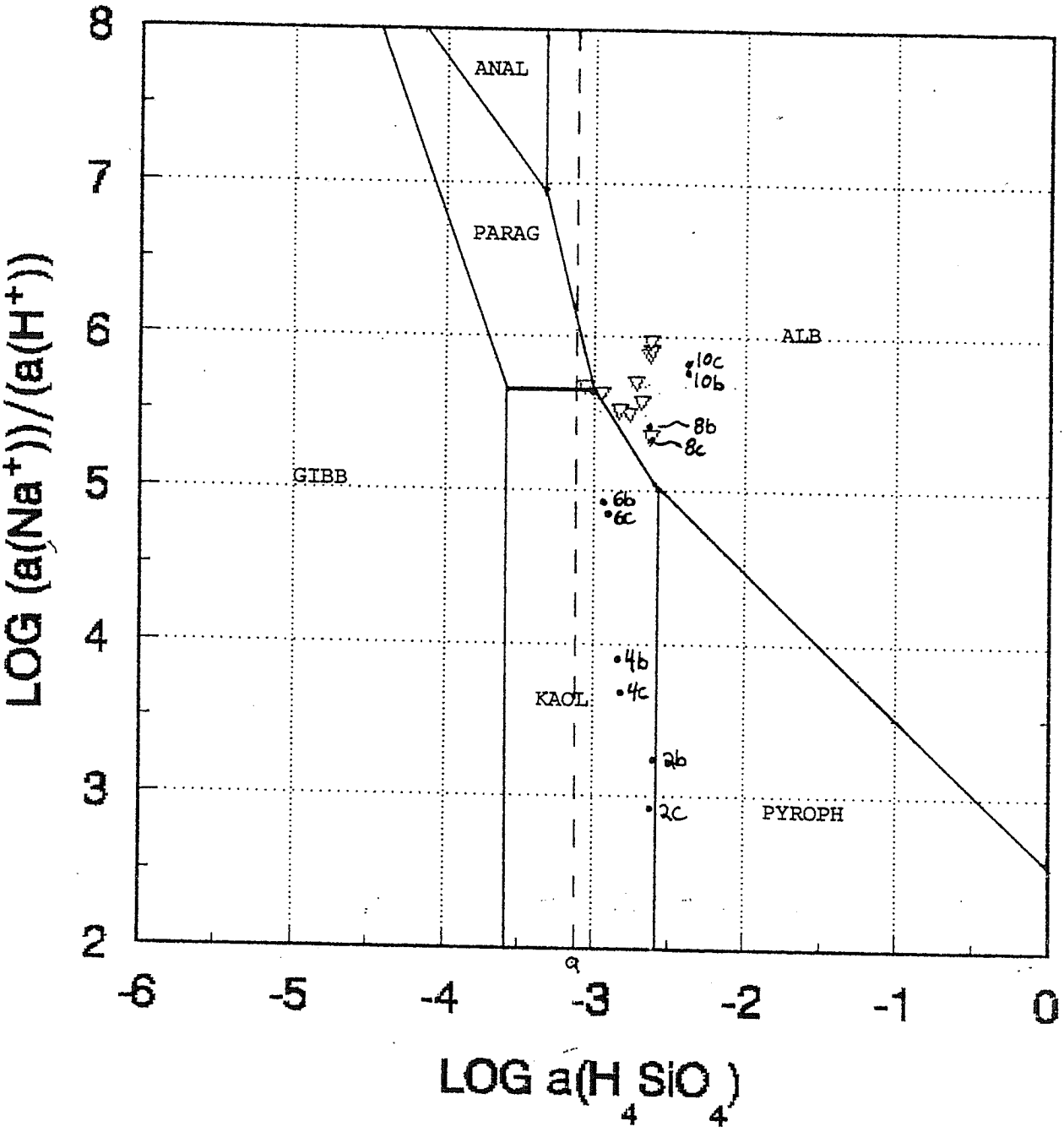

Figure 1b) $\log(a_{Na+}/a_{H+})$ vs. $\log(a_{H4SiO4})$. ANAL=Analcime, ALB=Albite, KAOL=Kaolinite, PARAG=Paragonite, PYROPH=Pyrophillite, GIBB=Gibbsite, T=100° C, P=P_{sat}, Adapted from McManus, (1991)

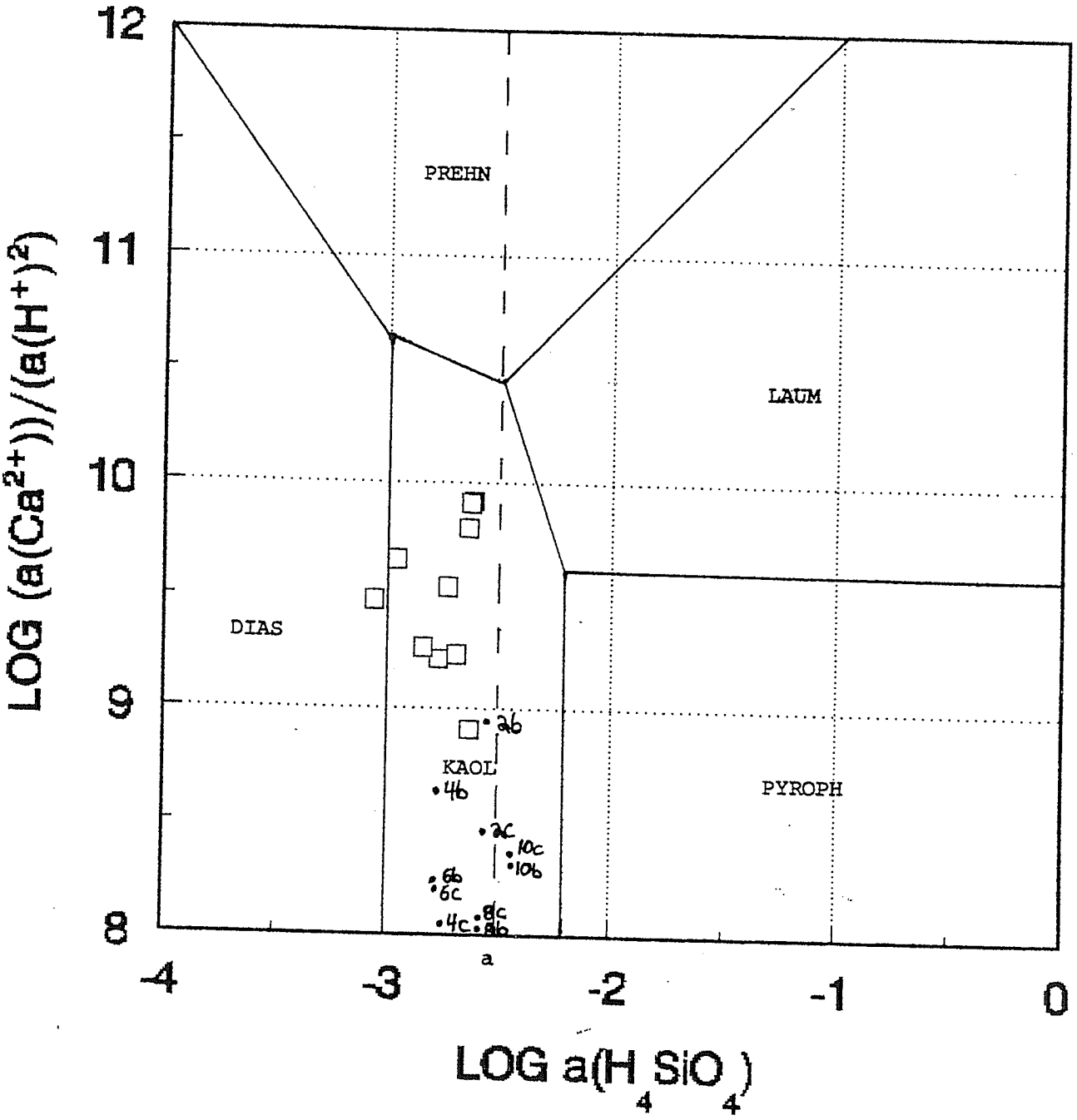

Figure 2) $\log(a_{Ca^{2+}}/a_{H^+}{}^2)$ vs. $\log(a_{H_4SiO_4})$. PREHN=Prehnite, LAUM=Laumontite, KAOL=Kaolinite, PYROPH=Pyrophyllite, DIAS=Diaspore, T=150° C, P=P_{sat}, Adapted from Bowers et al., (1984)

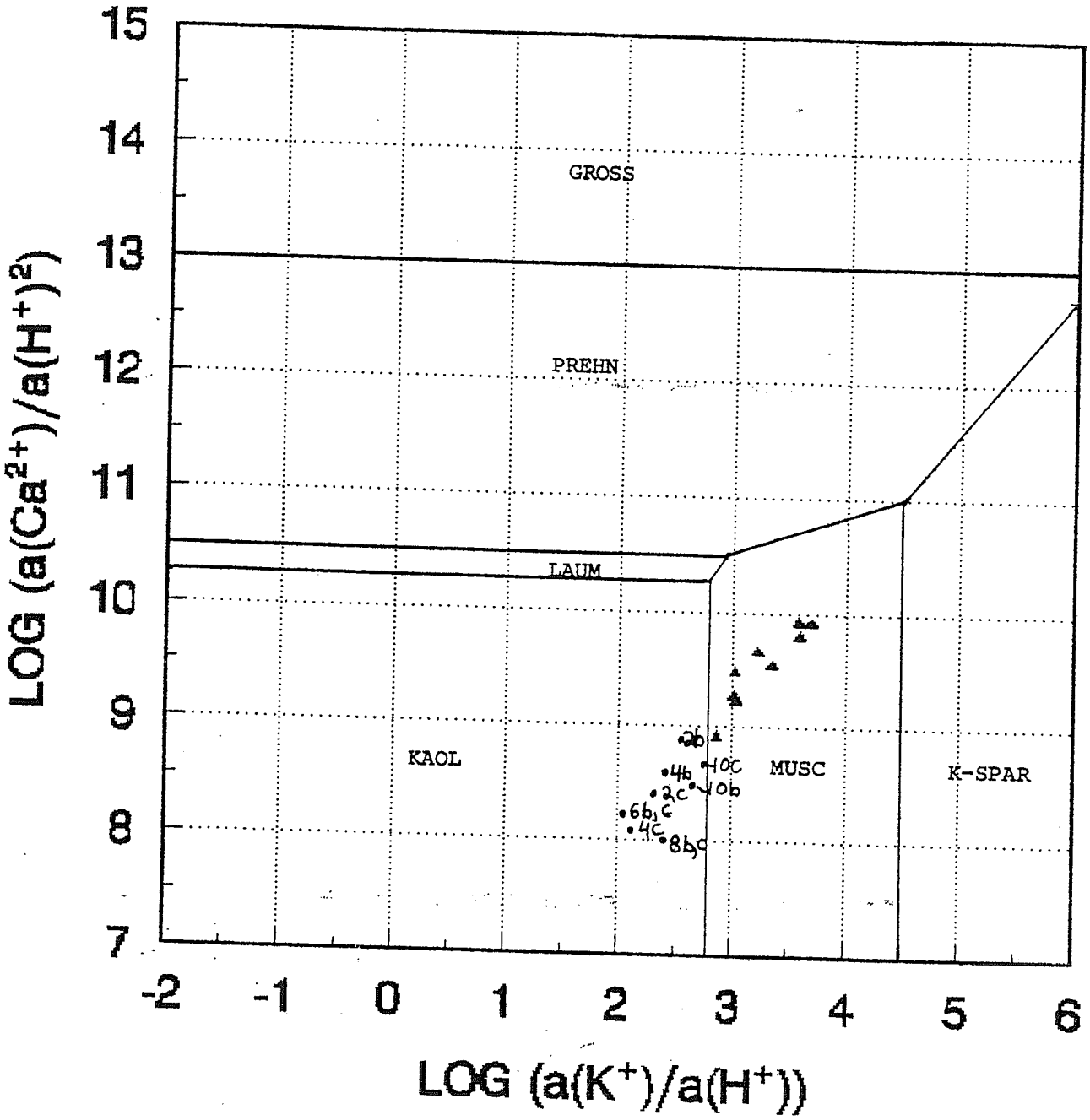

Figure 3) $\log(a_{Ca^{2+}}/a_{H^+}^2)$ vs. $\log(a_{K^+}/a_{H^+})$. GROSS=Grossular, PREHN=Prehnite, LAUM=Laumontite, KAOL=Kaolinite, MUSC=Muscovite, K-SPAR=Potassium Feldspar, T=150° C, P=P_{sat}, Adapted from Bowers et al., (1984)